

AD-A017 097

DEVELOPMENT OF DEICING TECHNIQUES FOR DIELECTRIC  
WINDOWS

Edward A. Strouse

Perkin-Elmer Corporation

Prepared for:

Air Force Materials Laboratory

August 1975

DISTRIBUTED BY:

**NTIS**

National Technical Information Service  
U. S. DEPARTMENT OF COMMERCE

322067

AFML-TR-75-99

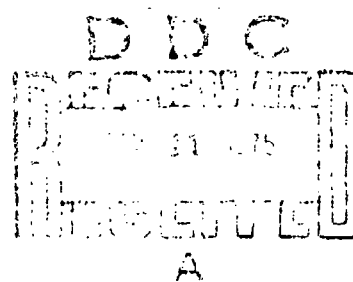
AD A017092

## DEVELOPMENT OF DEICING TECHNIQUES FOR DIELECTRIC WINDOWS

THE PERKIN-ELMER CORPORATION  
NORWALK, CONNECTICUT 06856

AUGUST 1975

FINAL REPORT FOR PERIOD APRIL 1973-APRIL 1975



Approved for public release; distribution unlimited

Prepared for  
AIR FORCE MATERIALS LABORATORY  
Air Force Systems Command  
Wright-Patterson Air Force Base, Ohio 45433

Reproduced by  
NATIONAL TECHNICAL  
INFORMATION SERVICE  
U.S. Department of Commerce  
Springfield, VA 22151

UNCLASSIFIED

SECURITY CLASSIFICATION OF THIS PAGE (When Data Entered)

REPORT DOCUMENTATION PAGE		READ INSTRUCTIONS BEFORE COMPLETING FORM
1 REPORT NUMBER AFML-TR-75-99	2 GOVT ACCESSION NO.	3 RECIPIENT'S CATALOG NUMBER
4 TITLE (and Subtitle)  DEVELOPMENT OF DETICING TECHNIQUES FOR DIELECTRIC WINDOWS		5 TYPE OF REPORT & PERIOD COVERED Final Report April 1973 - April 1975
		6 PERFORMING ORG. REPORT NUMBER 12464
7 AUTHOR(s)  Edward A. Strouse		8 CONTRACT OR GRANT NUMBER(s)  F33615-73-C-1080
9 PERFORMING ORGANIZATION NAME AND ADDRESS  The Perkin-Elmer Corporation Norwalk, Connecticut 06856		10 PROGRAM ELEMENT, PROJECT, TASK AREA & WORK UNIT NUMBERS Task 7371 Project 737101 Work Unit 73710145
11 CONTROLLING OFFICE NAME AND ADDRESS  Air Force Materials Laboratory (LPO) Air Force Systems Command Wright-Patterson Air Force Base, Ohio 45433		12 REPORT DATE August 1975
		13 NUMBER OF PAGES 145
14 MONITORING AGENCY NAME & ADDRESS (If different from Controlling Office)		15 SECURITY CLASS. (of this report)  Unclassified
		15a DECLASSIFICATION DOWNGRADING SCHEDULE
16 DISTRIBUTION STATEMENT (of this Report)  Approved for public release; distribution unlimited		
17 DISTRIBUTION STATEMENT (of the abstract entered in Block 20, if different from Report)		
18 SUPPLEMENTARY NOTES		
19 KEY WORDS (Continue on reverse side if necessary and identify by block number)  Conductive Coatings  FLIR Windows (ZnS, ZnSe, ZnSSe)		
20 ABSTRACT (Continue on reverse side if necessary and identify by block number)  This report covers measurements and techniques that have led to the development of the first prototype windows coated with a continuous thin-film heater transparent in the 8 to 12 micron spectral region. The effort involved the measurement of the complex optical constants of indium-tin-oxide and the dependence of these values on both process parameters and the conductivity of the films. The performance of a full coated window has a transmission greater than 70%, and a sheet resistance of 160 $\Omega$ /square is described. Also included is a thermo-optical		

DD FORM 1 JAN 73 1473 EDITION OF 1 NOV 65 IS OBSOLETE

UNCLASSIFIED

SECURITY CLASSIFICATION OF THIS PAGE (When Data Entered)

UNCLASSIFIED

SECURITY CLASSIFICATION OF THIS PAGE(When Data Entered)

analysis of conductive films and patterns for zinc sulfide, zinc selenide, and zinc sulfo-selenide windows.

UNCLASSIFIED

SECURITY CLASSIFICATION OF THIS PAGE(When Data Entered)

## FOREWORD

This report was prepared by The Perkin-Elmer Corporation, Norwalk, Conn., under Contract No. F33615-73-C-1080, Project 7371, Task 737101, entitled "Development of Deicing Techniques for Dielectric Windows". The work was administered under the direction of the Air Force Materials Laboratory, Wright-Patterson Air Force Base, Ohio. Mr. D.W. Fischer was project engineer and E.A. Strouse was the principal investigator.

This is the Final Technical Report for Contract F33615-73-C-1080. It covers the period April 1973 to April 1975.

The report was submitted by the author in May 1975.

## TABLE OF CONTENTS

<u>Section</u>	<u>Title</u>	<u>Page</u>
1	INTRODUCTION	1
	1.1 Conductive Multilayer Films	1
	1.2 Background	1
	1.3 Program Objectives	3
2	OPTICAL CHARACTERISTICS OF INDIUM-TIN-OXIDE FILMS AT IR WAVELENGTHS	4
	2.1 Experimental Results	4
	2.2 Optical Constants of Indium-Tin-Oxide on ZnS and ZnSe	8
	2.3 Dependence of n and k on Film Conductivity	10
3	DESIGN OF CONDUCTIVE ANTIREFLECTION COATINGS FOR IR WAVELENGTHS	12
	3.1 Induced Transmission Filter Technique	12
	3.2 Technique Applied to Indium-Tin-Oxide Films in the 8 to 11.5 Micron Spectral Region (Theory)	12
	3.3 Experimental Effort	19
4	ANTIREFLECTION COATINGS	24
	4.1 Theoretical Design	24
	4.1.1 Single Layer Designs	24
	4.1.2 Double-Layer Designs	28
	4.2 Experimental Effort	28
5	USE OF CONDUCTIVE COATINGS IN NONPARALLEL BUS BAR CONFIGURATIONS	38
	5.1 Nonuniform Coating Techniques	38
	5.2 Glacier Process Description	39
	5.2.1 Definition Phase	39
	5.2.2 Mask Preparation	39
	5.2.3 Deposition Phase	40
	5.3 Experimental Effort	40
	5.4 Conclusions	41
6	THERMO-OPTICAL ANALYSIS OF CONDUCTIVE FILMS AND PATTERNS	47
	6.1 Assumed Conditions	48
	6.2 Basic Analytical Procedure	49
	6.3 Power Density and Temperature Control Requirements	49
	6.4 Steady State Thermal Stresses	52

# TABLE OF CONTENTS (Continued)

<u>Section</u>	<u>Title</u>	<u>Page</u>
	6.5 Combined Steady-State Stresses (at Exterior Surface)	55
	6.6 Transient Thermal Stresses	60
	6.7 Temperature Control Circuit Malfunction	60
	6.8 Wavefront Degradation (Uniform EC Coating on Interior Surface)	61
	6.9 Lateral Temperature Gradients	61
	6.10 Increasing Coated Window Transmission with Conductive Patterns	64
	6.11 Wavefront Distortion of Heater Patterns	75
7	FABRICATION AND EVALUATION OF COATED ZINC SULFIDE WINDOWS	88
	7.1 Fabrication of Test Fixtures	88
	7.2 Fabrication of Windows	88
	7.3 Evaluation of ZnS Windows	91
	7.3.1 MTF Measurements	91
	7.3.2 Optical Performance of Coated Witness Pieces	91
	7.3.3 Coating Durability	92
	7.3.4 Measurement of the Thermal Profile Across a Heated Window	92
8	CONCLUSIONS AND RECOMMENDATIONS	106
	8.1 Transmission Values	106
	8.2 Coatings for Irregular Shaped Windows	106
	8.3 Follow-On Investigations	107
	REFERENCES	108
<u>Appendix</u>		
A	OPTICAL TEST DATA FOR UNCOATED ZINC SULFIDE WINDOWS	109
B	OPTICAL TEST DATA FOR COATED ZINC SULFIDE WINDOWS	121

# LIST OF ILLUSTRATIONS

<u>Figure</u>	<u>Title</u>	<u>Page</u>
1	Reflection and Transmission Through a Tin-Doped Indium Oxide Film	5
2	Reflection and Transmission Input Data for ZnS Window Study	6
3	Typical Computer Output	7
4	k Versus Sheet Resistance for an Indium-Tin-Oxide Film 0.16 $\mu$ Thick	11
5	Transmission for Nonabsorbing Substrate	14
6	Transmission for Three-Film System	15
7	Herpin Equivalent Index Value for Three-Film System	16
8	Three-Film System with Antireflection Coating of Thorium Fluoride	17
9	Indium-Tin-Oxide Three-Film System with Antireflection Coating of Thorium Fluoride	18
10	Three-Film Herpin Sections	20
11	Spectral Performance of Coating Design Deposited on ZnS	21
12	Spectral Response for ZnS	25
13	Spectral Response for ZnSe	26
14	Herpin Equivalent Index Film System	27
15	Herpin System for ZnS	29
16	Herpin System for ZnSe	30
17	Spectral Response for ZnS Double-Layer Design	31
18	Spectral Response for ZnSe Double-Layer Design	32
19	Spectral Response for ZnS Coated with ZnSe and ThF <sub>4</sub>	33
20	Spectral Response for ZnSe Coated with ZnSe and ThF <sub>4</sub>	34
21	Spectral Performance of ZnS with Protective Film of CeF <sub>3</sub>	36
22	Spectral Performance of ZnSe with Protective Film of CeF <sub>3</sub>	37
23	Overcoating of Graded Film	39
24	Variable Resistance Coating	42
25	Transmission Wavefront Interferograms	43
26	Trapezoidal Window Layout	44



# LIST OF ILLUSTRATIONS (Continued)

<u>Figure</u>	<u>Title</u>	<u>Page</u>
27	Temperature Control Schematic, IR Window Defogger/ Deicer with Guard Heater	53
28	Thermal Schematic of Heated 8.8" x 10" x 0.75" ZnSe Window with EC Coating on Exterior Surface	56
29	Thermal Schematic of Heated 8.8" x 10" x 0.75" ZnSe Window with EC Coating on Interior Surface	57
30	Loss of Performance Due to Window with Axial Tempera- ture Gradient and Pressure Differential	62
31	Window Mount Concept	63
32	Temperature Gradients in Quarter Window	65
33	Loss of Performance Due to Window with Radial Tempera- ture Gradient	66
34	Loss of Performance Due to Window with Radial Tempera- ture Gradient	67
35	Loss of Performance Due to Window with Radial Tempera- ture Gradient	68
36	Insulating Window Mount Concept	69
37	Nodal Temperature Diagram	73
38	Nodal Temperature Diagram	77
39	Nodal Temperature Diagram	78
40	Nodal Temperature Diagram	79
41	Distribution of Optical Path Difference Around Each Heater Stripe	83
42	Affect of Thermally-Induced Optical Path Differences	84
43	Thermally-Induced Point Spread Function	85
44	Striped Pattern Window Heater with Central Bus Bar	87
45	Thermal Vacuum Chamber	89
46	Insulated Chamber Housing	90
47	Spectral Performance at 70.8°F	94
48	Spectral Performance at Ambient	95
49	Spectral Performance at 0°F and 120°F	96
50	Spectral Performance at 70.0°F	97
51	Spectral Performance at Ambient	98
52	Spectral Performance at 0°F and 120°F	99
53	Spectral Performance at 69.0°F	100

LIST OF ILLUSTRATIONS (Continued)

<u>Figure</u>	<u>Title</u>	<u>Page</u>
54	Spectral Performance at Ambient	101
55	Spectral Performance at 0°F and 120°F	102
56	Positions and Recorded Temperatures of Thermocouples	103
57	Positions and Recorded Temperatures of Thermocouples	104

# LIST OF TABLES

<u>Number</u>	<u>Title</u>	<u>Page</u>
1	n and k for $\text{In}_2\text{O}_3/\text{SnO}_2$ on ZnS	9
2	n and k for $\text{In}_2\text{O}_3/\text{SnO}_2$ on ZnSe	9
3a	Coating Design	22
3b	Durability Evaluation	22
4	Window Characterization	45
5	Recorded Temperatures of Nonuniformly Coated Window	46
6	Recorded Temperatures of Uniformly Coated Window	46
7	CVD Material Properties	50
8	Summary of EC-Coated ZnSe and ZnSSe Window	54
9	Steady-State Thermal Stresses	58
10	Effect of Window Support Conditions on Steady-State Window Stresses	59
11	Diffraction Image Intensity	71
12	Temperature Distribution Comparison	74
13	Temperature Distribution Comparison	80
14	Average Transmission of Striped Window Heater Patterns	81
15	Optical Path Difference Distribution Around Each Stripe	82
16	MTF Measurements	91
17	Optical Performance	93
18	Coating Durability	93

## SECTION 1

### INTRODUCTION

#### 1.1 CONDUCTIVE MULTILAYER FILMS

Continuous thin-film heaters transparent in the visible spectrum have been in use for some time now as deicing and defogging elements on aircraft transparencies. The heaters are generally made from either gold or semiconductor films based on indium oxide or tin oxide. The oxide films for pilot windshield defogging are generally deposited by a chemical pyrolytic decomposition technique; temperatures in excess of 500°C are involved in this process. For high quality optical windows such as those used in aircraft camera bays, the oxide films are deposited by RF sputtering or thermal evaporation techniques. Perkin-Elmer employs a proprietary process that combines conductive films with dielectric films in the form of interference multilayers, which can actually improve the transmission through a glass surface as well as provide deicing and defogging capabilities.

A characteristic of all highly conductive thin films, whether gold or oxide based, is a strong attenuation of wavelengths longer than 2  $\mu$ . The absorption edge begins in the region of 1  $\mu$  and, for oxide semiconductor materials, reaches a steady level in the 2-3  $\mu$  region. The attenuation in gold films increases progressively with wavelength. This report describes more fully the nature of the attenuation in indium-tin-oxide films and how the understanding of the complex optical constants enable these films to be combined with dielectric films to produce conductive multilayers with relatively high transmission values in the 8-12  $\mu$  spectral region.

#### 1.2 BACKGROUND

In the region of transparency, a conductive film can be designed into a multilayer system in the same way as any other transparent dielectric film. Perkin-Elmer has already employed this technique in the production of a variety of devices requiring high transparency conductive film systems based on the indium-tin-oxide films. The indium-tin-oxide films have a refractive index of

2.0 at visible wavelengths, and there are a number of well known antireflection coating designs for glass surfaces that can be adapted to accommodate films of this index.

In the regions where the conductive films are nontransparent, it is necessary to use those design techniques that are used for metallic films. To illustrate this, it is convenient to consider designs used for gold-based coatings that are transparent at visible wavelengths. 150 Å thick gold films show a transmission of approximately 65% in the visible spectrum yet still have a high conductivity. By placing suitable thickness and refractive index dielectric films on either side of the gold film, one can increase the transmission to approximately 85% in the same spectral region. This program was designed to apply similar techniques to the existing Perkin-Elmer indium-tin-oxide conductive film for use in the 8 to 12 micron region and to fabricate a demonstration ZnS window.

The multilayer designs are very similar to the induced transmission through gold films. The oxide semiconductor films are treated essentially as metallic films, the thickness of the films being substantially less than interference thickness in the 8 to 12 micron range.

The thermo-optical analysis examines deicing techniques as applicable to infrared windows. These techniques will be limited to uniform, transparent, electrically conductive coatings. Analysis determined the image spoiling or wavefront degrading effects due to each material investigated.

The thermal analysis was not restricted to the optical effects but included an investigation of the thermal stress/shock imposed by heating and cooling rates. Furthermore, the deicing techniques that were developed include a study of the safety aspects in the event of potential thermal runaway. The danger of a catastrophic failure due to heating was eliminated by designing a fail-safe thermal system to preclude overly rapid heating rates or absolute overheating in the event of a failure of the thermal controller.

After the most promising deicing and antireflective coating techniques were established and fully developed through the coating experimental work, a test demonstration was conducted to demonstrate the achievement of the thermal

and optical goals. A demonstration ZnS optic has been fabricated consisting of a customer-supplied plano-parallel window to which the deicing technique has been applied.

### 1.3 PROGRAM OBJECTIVES

A study and experiments were conducted to investigate various methods for deicing zinc sulfide, zinc selenide, and zinc sulfo-selenide windows. The goal was to develop a deicing method that will not significantly degrade the performance of a sensor receiving radiation through the window. The projected flight envelope of the B-1 was to be used as the anticipated window environment, and the deicing technique developed was to be consistent with FLIR window configurations for the B-1 and with B-1's FLIR window performance requirement.

The work performed under Contract F33615-73-C-1090 for Wright-Patterson Air Force Base is presented as follows:

- Optical characteristics of indium-tin-oxide films at IR wavelengths
- Conductive antireflection coatings for IR wavelengths
- Antireflection coatings
- Use of conductive coatings in nonparallel bus bar configurations
- Thermo-optical analysis of conductive films and patterns
- Fabrication and evaluation of coated zinc sulfide windows
- Conclusions

## SECTION 2

### OPTICAL CHARACTERISTICS OF INDIUM-TIN-OXIDE FILMS AT IR WAVELENGTHS

The transmission and reflection characteristics of a 0.15 micron thick film are shown in Figure 1. It can be seen that whereas the transmission value stays approximately level in the region from 2.5 to 14.0 microns, the reflection value rises steadily with increasing wavelength. This is indicative of a complex index behavior in which the real part ( $n$ ) remains essentially constant whereas the imaginary part ( $k$ ) increases with increasing wavelength. In the first phase of this program, a detailed examination of these optical constants in the 8 to 14 micron region was made. The relationship between the values of  $n$  and  $k$  for various process parameters was evaluated. The first optical constant measurements were made on films of identical thickness processed by exactly the same techniques as the films used in the low-light-level TV window conductive transparent coatings. Process parameters were then varied to produce films with a range of conductivity values in order to assess the dependence of the optical constants on this parameter.

#### 2.1 EXPERIMENTAL RESULTS

The optical constants of the films were calculated from spectral measurements made through the plate ( $T$ ), double surface reflection from the plate measured from the coated side ( $R$ ), and double surface reflection measured from the uncoated side ( $R'$ ). Figure 2 shows a diagram of these measurements. The optical constants of the plate itself were determined by separate experiments. The measured data is computer-reduced to yield the optical constants of the film in the spectral range of interest. The input data and a typical computer output are shown in Figures 2 and 3. Spectral measurements were made on a Perkin-Elmer Model 180 spectrophotometer, and film thickness measurements were made on a Sloan angstrometer.

The  $n$  and  $k$  program takes the normalized transmission and reflection data (shown in Figure 2) and converts this data to single surface values.

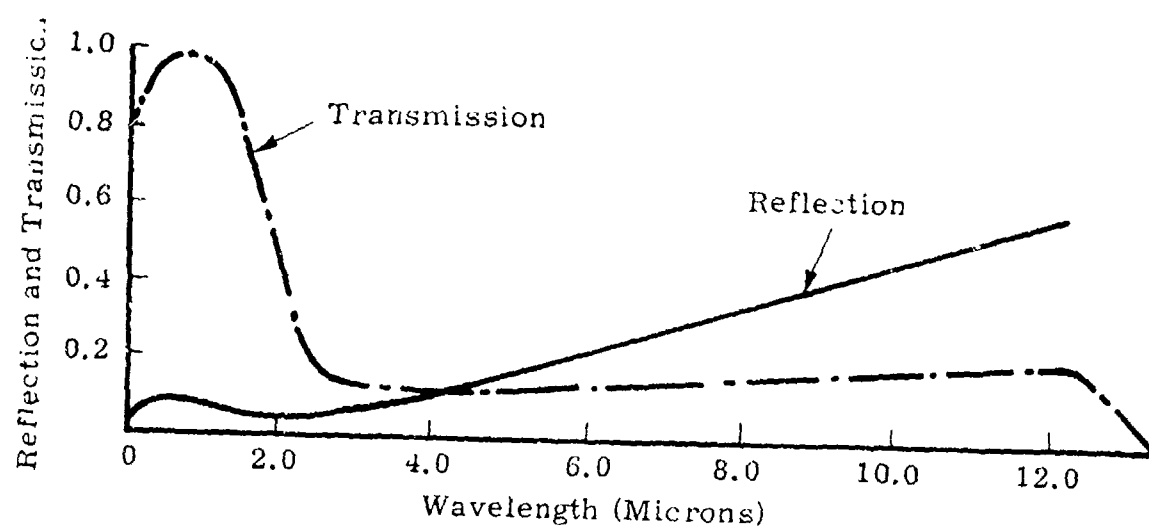


Figure 1. Reflection and Transmission Through a Tin-Doped Indium Oxide Film  
0.15  $\mu\text{m}$  Thick and 85  $\Omega/\text{Square}$  Sheet Resistance



$N_s = \text{ZnSe}$

$N_s \text{ Thk} = 1.32 \text{ mm}$

$N_s = 2.40$

Wavelength  
(Microns)

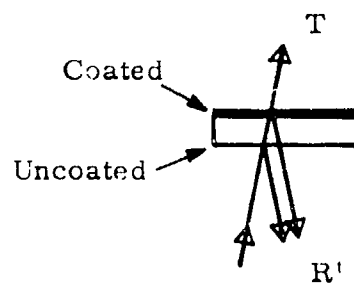
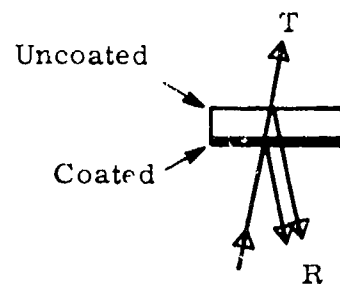
% T

% R

% R'

Remarks

8.0	30.82	37.24	18.44
8.5	30.61	37.43	18.27
9.0	30.51	27.41	18.23
9.5	30.44	37.34	18.12
10.0	30.86	37.09	18.04
10.5	30.81	37.72	17.89
11.0	30.94	37.67	17.83
11.5	31.11	37.97	18.02
12.0	31.31	37.98	17.78
12.5	31.28	38.06	17.92
13.0	31.15	38.39	17.95
13.5	31.08	38.06	17.70
14.0	30.71	38.75	17.75
14.5	30.43	39.60	17.82
15.0	30.17	38.90	17.95



Coated Substrate

In and Sn (87.5: 12.5)

MT = 1602Å

(measurements taken after  
vacuum baking)

Figure 2. Reflection and Transmission Input Data for ZnS Window Study

33105-91100  
 TZNS4B COND. FILM ON ZIS. RUN NO. ZNS4B

11.23.04 05/16/73

AMPEN = 1.500  
 AMPAX = 2.500

AKMIN = 3.000  
 AKMAX = 6.000

WFR = 1.0  
 WFT = 1.0  
 WFA = 1.0  
 BEN = 1.000

FILM THICKNESS = 0.1602 MICRONS  
 NO. OF DATA POINTS = 15

\$\$\$\$\$\$\$\$\$\$\$\$\$\$\$\$

WVL	RC-RM	TC-TM	AC-AM	N	K	SEC
8.000000	-0.17	0.00	0.16	1.830	4.020000	6.5
8.500000	-0.15	-0.01	0.16	1.830	4.220000	6.2
9.000000	-0.11	0.02	0.09	1.850	4.419999	6.2
9.500000	-0.04	0.02	0.02	1.956	4.599999	6.2
10.000000	0.06	-0.02	-0.04	1.940	4.779999	6.2
10.500000	0.05	-0.03	-0.02	1.782	4.999999	6.2
11.000000	0.02	-0.11	0.09	1.920	5.139999	6.2
11.500000	0.03	-0.04	0.01	1.940	5.319999	6.1
12.000000	0.06	-0.03	-0.02	1.880	5.399999	6.2
12.500000	-0.02	0.05	-0.04	1.712	5.559999	6.1
13.000000	0.06	-0.04	-0.03	1.714	5.719999	6.2
13.500000	-0.07	0.04	0.03	1.622	5.879999	6.2
14.000000	-1.31	-2.11	3.43	1.490	5.919999	6.1
14.500000	-13.58	-11.93	25.51	1.490	4.759999	6.1
15.000000	-1.48	24.87	-23.39	2.522	6.219999	6.2

TOTAL TIME = 92.9

\$\$\$\$\$\$\$\$\$\$\$\$\$\$\$\$

Figure 3. Typical Computer Output

The film constants are then calculated. Figure 3 shows the output of a typical calculation. The symbols used are as follows:

WVL = Wavelength  
 RM = Single surface reflection at air boundary obtained from data  
 RC = Calculated single surface reflection using film n and k  
 TM = Single surface transmission obtained from data  
 TC = Calculated single surface transmission using film n and k  
 AM = Single surface reflection at substrate boundary obtained from data  
 AC = Calculated single surface reflection using film n and k  
 N = The real part of the film index  
 K = The imaginary part of the film index  
 RC-RM = Deviation of measured and calculated film reflectance  
 TC-TM = Deviation of measured and calculated film transmission  
 AC-AM = Deviation of measured and calculated film absorption

The deviation values give an estimate of the validity of the calculation. It can be seen that the dispersion of the imaginary part (k) of the complex refractive index ( $\tilde{N}$ ) is approximately linear with wavelength ( $\lambda$ ). The complex index can then be defined by the expression

$$\tilde{N} = n - jk = 1.9 - j(1 + 3/8\lambda) \text{ for ZnS}$$

in the region in which n is essentially constant.

## 2.2 OPTICAL CONSTANTS OF INDIUM-TIN-OXIDE ON ZnS AND ZnSe

Table 1 lists the optical constants of 1600 Å thick 85% indium oxide/15% tin oxide after a 250°C vacuum bake. The results shown are the average of four coating runs. Table 2 lists the optical constants of the same thickness and process parameters when deposited onto ZnSe.

Because of the oxidation of ZnSe during film processing, it was impossible to achieve good reproducibility of the optical constants. One can observe by comparing Tables 1 and 2 that the optical properties of the conductive film vary with the substrate being coated.

TABLE 1. n AND k FOR  $\text{In}_2\text{O}_3/\text{SnO}_2$  ON ZnS

$\lambda(\mu)$	<u>n</u>	<u>k</u>
8.0	1.85	4.35
8.5	1.85	4.57
9.0	1.95	4.78
9.5	2.00	4.99
10.0	2.12	5.14
10.5	2.13	5.37
11.0	2.25	5.58
11.5	2.35	5.82
12.0	2.28	6.00
12.5	2.12	6.20
13.0	2.02	6.38
13.5	1.98	6.59
14.0	1.72	6.62

TABLE 2. n AND k FOR  $\text{In}_2\text{O}_3/\text{SnO}_2$  ON ZnSe

$\lambda(\mu)$	<u>n</u>	<u>k</u>
8.0	2.05	5.41
8.5	1.98	5.76
9.0	2.05	6.00
9.5	2.06	6.28
10.0	2.11	6.52
10.5	2.22	6.78
11.0	2.11	7.06
11.5	2.13	7.33
12.0	2.04	7.57
12.5	2.01	7.84
13.0	1.99	8.08
13.5	2.01	8.32
14.0	1.97	8.64

### 2.3 DEPENDENCE OF $n$ AND $k$ ON FILM CONDUCTIVITY

Figure 4 shows the variation of the imaginary refractive index  $k$  (at 10 microns) with sheet resistance for a 0.16  $\mu\text{m}$  thickness indium-tin-oxide film. The film composition is 85% indium oxide, 15% tin oxide. The sheet resistance values were varied by subjecting the films to a number of different vacuum bake regimes. The plot points are the average values from three films of the same thickness and composition.

The value of 75 $\Omega$ /sq. represents the lowest value to which the film resistance can be reduced by vacuum baking without the liberation of free metal particles. These free metal particles drastically change the absorption properties of the film at long wavelengths making it very difficult to achieve reproducible values of  $n$  and  $k$  for the film. For sheet resistances greater than 200 $\Omega$ /square, the variation in  $k$  is approximately linear, inversely proportional to the sheet resistance, and  $k$  is reducing at a rate of -0.12 per 100 $\Omega$ /square.

The corresponding variation in  $n$  with sheet resistance was impossible to evaluate from the set of data that yielded the variation in  $n$  for each of the three films tested; following each of the process adjustments, these variations could not be correlated with conductivity values for the films. It is more likely that the variations were attributable to differences in the free metal content of the films. Generally, the range of values for  $n$  that were recorded fell in a fairly tight range and could not be anticipated as strong an influencing factor in the multilayer design considerations as the much larger variations in  $k$ .

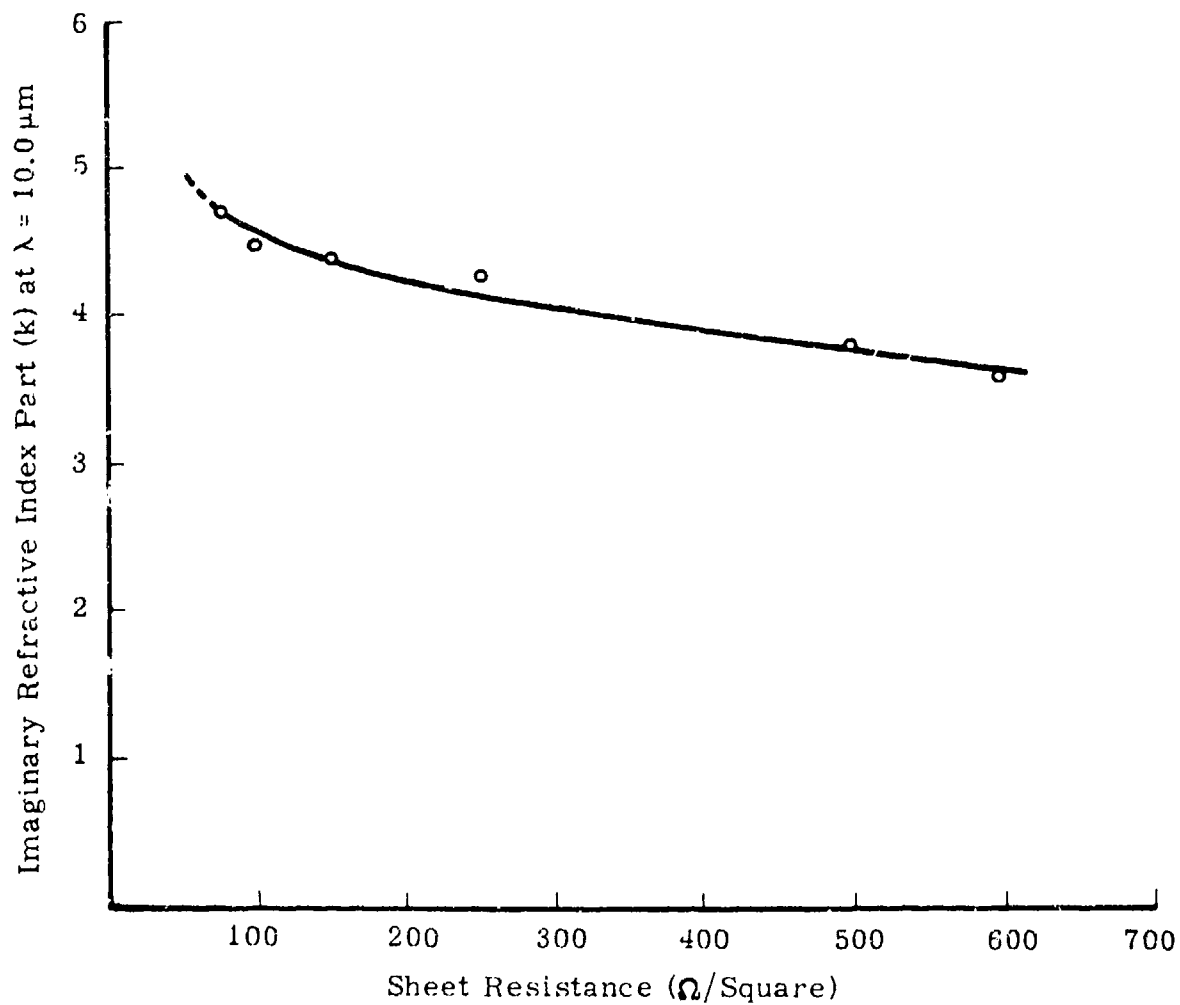


Figure 4.  $k$  Versus Sheet Resistance for an Indium-Tin-Oxide Film 0.16  $\mu$  Thick

## SECTION 3

### DESIGN OF CONDUCTIVE ANTIREFLECTION COATINGS FOR IR WAVELENGTHS

In this program phase, the  $n$  and  $k$  information gathered in the previous phase was used to generate transparent conductive coating designs using the induced transmission filter technique.

#### 3.1 INDUCED TRANSMISSION FILTER TECHNIQUE

The technique of augmenting the transmission through metal films by the use of additional dielectric films is referred to by thin-film filter designers as the induced transmission filter technique. The technique involves reducing the reflection contribution of the imaginary part ( $k$ ) of the complex index of the film by matching it to the real index of a dielectric film or the effective real index of a dielectric film stack. These matching films are disposed symmetrically on either side of the metallic film. The symmetrical grouping of metal and dielectric films has an effective  $k$  value that is significantly lower than the value for the metal film and, for the purpose of impedance matching into the substrate and the surrounding medium, the grouping can be treated as though it had a real index only.

The multilayer groupings of dielectric films are required when the  $k$  value of the metallic film exceeds the highest real value that can be obtained using a single material. In systems such as these, the index value is strongly dispersive and the high transmission is obtained only over a narrow spectral region. The technique is in fact employed in the fabrication of narrow-band spectral filters. In the following section, we will trace step by step the development of an induced transmission design for a ZnS window based on a conductive film.

#### 3.2 TECHNIQUE APPLIED TO INDIUM-TIN-OXIDE FILMS IN THE 8 TO 11.5 MICRON SPECTRAL REGION (THEORY)

Using the optical constants shown in Table 1, the transmission was computed through the uncoated side of a zinc sulfide plate (coated on the other

side with the indium-tin-oxide film) and is shown in Figure 5. The transmission value in the range is approximately 24%, a value far too low for the film to be useful as a heater element.

Figure 6 shows the transmission through a three-film system of germanium/indium-tin-oxide/germanium. The thickness of the films is chosen such that the sum of the phase retardation introduced by the germanium film and the phase retardation suffered on reflection at the germanium-indium-tin-oxide boundary is  $\pi/2$ . The index of germanium in the 8 to 12 micron region is equal to 4.0, which is the closest approximation of the  $k$  value for the indium-tin-oxide that we can achieve with a single discrete material. The transmission peaks at 10.0 microns at a value of 72% but falls off rapidly at both larger and shorter wavelengths. Figure 7 shows the behavior of the complex Herpin equivalent index value for the three-film system. It can be seen that the equivalent  $k$  value for the system has been reduced to less than 1.0 over most of the spectral range while the equivalent real index value at wavelengths longer than 10.0 microns is on the order of 2.2.

The next stage in the design formulation is to provide films for the reduction of the reflections from the three-film system and the air and substrate values. The simplest of these approaches is based on the assumption that the real index of the system is 2.2. In this case, the system is already a good index match to the substrate, so no films are necessary at the substrate/system boundary. The problem then reduces to one of providing an antireflection coating for a medium of index 2.2. The simplest such coating would be a single quarter-wave optical thickness (at  $\lambda = 10.0$  microns) of material with a refractive index equal to 1.47. A close approximation to this in practice would be a film of thorium fluoride ( $n \sim 1.40$ ). Figure 8 shows the computed performance of such a system. It can be seen that the transmission gain over the three-film group at the peak transmission wavelength is not spectacular. Reasonable gains are recorded at the off peak wavelengths giving the four-film system a fairly flat transmission characteristic.

Using the same design approach, a coating design was calculated using an 800 Å indium-tin-oxide conductive film. The anticipated resistance would be 200 ohms per square and would have approximately 86% transmission as shown in Figure 9.



33105-91100  
COND-IR CONDUCTIVE FILM ONLY ON IPT-2 SUBSTRATE

11.31.32 04/27/73

DESIGN FOR SIDE 1

FILM SATCK PARAMETERS WR = 9.500000 MICRONS  
NO. MATERIAL THK (MU) OPT.THK. (WR UNITS)

SUB 2.2200  
1 COND-IR 0.16020 0.03204  
ENN 1.0000

TOTAL THICK. 0.16020 MICRONS.

\*\*\*\*\*

33105-91100  
COND-IR CONDUCTIVE FILM ONLY ON IPT-2 SUBSTRATE

11.32.08 04/27/73

DESIGN FOR SIDE 2

FILM SATCK PARAMETERS WR = 9.500000 MICRONS  
NO. MATERIAL THK (MU) OPT.THK. (WR UNITS)

SUB 2.2200  
ENN 1.0000

TOTAL THICK. 0.0 MICRONS.

\*\*\*\*\*

\*\*\*\*\*

33105-91100  
COND-IR CONDUCTIVE FILM ONLY ON IPT-2 SUBSTRATE

11.32.49 04/27/73

WR = 9.500000 MICRONS 1/WR = 0.10526

DATA FOR BOTH SIDES COMBINED :  $T = T1 * T2 / (1.0 - R_{SUB1} * R_{SUB2})$

PERCENT ENN-SIDE TRANSMITTANCE AT NORMAL INCIDENCE

PCT.	WAVE	0	20	40	60	80	100
TRANS	LENGTH	I+++++	I+++++	I+++++	I+++++	I+++++	I+++++
24.5376	8.000000	+	+ @				
24.6114	8.500000	+	+ @				
24.6462	9.000000	+	+ @				
24.6473	9.500000	+	+ @				
24.6188	10.000000	+	+ @				
24.5642	10.500000	+	+ @				
24.4867	11.000000	+	+ @				
24.3823	11.500000	+	+ @				
\$\$\$\$\$\$\$\$\$\$\$\$\$\$\$\$							

Figure 5. Transmission For Nonabsorbing Substrate

33105-91300  
CC ON ZNS

14.43.51 06/14/73

FILM STACK PARAMETERS WR = 8.000000 MICRONS  
NO. MATERIAL THK(MU) OPT.THK.(WR UNITS)

SUB 2.2200  
1 Ge 0.49610 0.25363  
2 ALPHA-1 0.16020 0.03805  
3 Ge 0.49610 0.25363  
ENN 1.0000

TOTAL THICK. 1.15240 MICRONS.  
\*\*\*\*\*

33105-91300  
CC ON ZNS

14.45.34 06/14/73

WR = 8.000000 MICRONS  $1/WR = 0.12500$

PERCENT EN.-SIDE TRANSMITTANCE AT NORMAL INCIDENCE

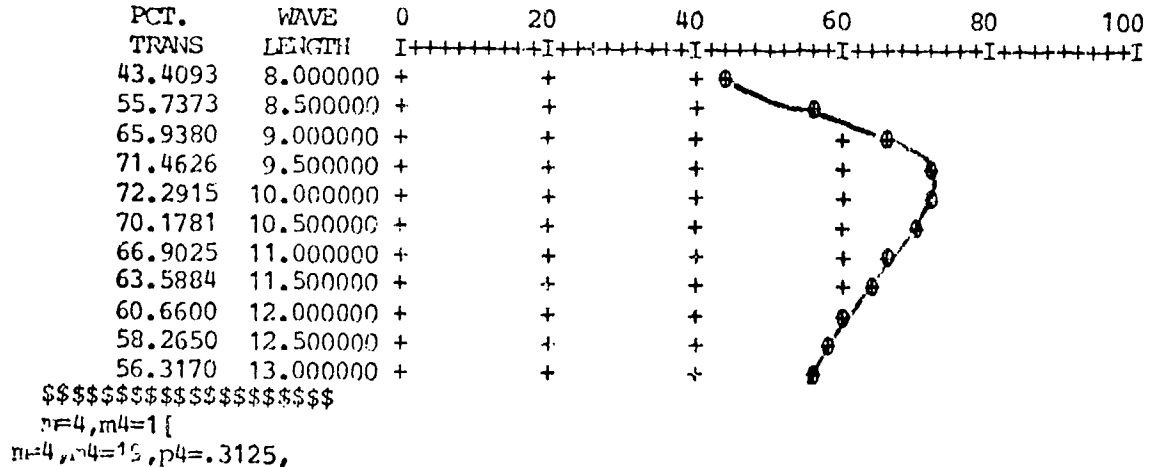


Figure 6. Transmission for Three-Film System

33:05-91100

06.23.33

04/27/73

COND-IR1 CONDUCTIVE FILM .1602 MU. THICK ON IRT-2(ZNS)

FILM STACK PARAMETERS WR = 10.000000 MICRONS

NO. MATERIAL THK (MU) OPT.THK. (WR UNITS)

SUB 2.2200

2 Ge 0.52109 0.21000

3 COND-IR 0.16020 0.03044

4 Ge 0.52109 0.21000

ENN 1.0000

TOTAL THICK. 1.20238 MICRONS.

33105-91100

06.23.33

04/27/73

COND-IR1 CONDUCTIVE FILM .1602 MU. THICK ON IRT-2(ZNS)

WR = 10.000000 MICRONS 1/WR = 0.10000

COMPLEX H E R P I N I N D E X AT  
0.0 DEGREES ANGLE OF INCIDENCE.

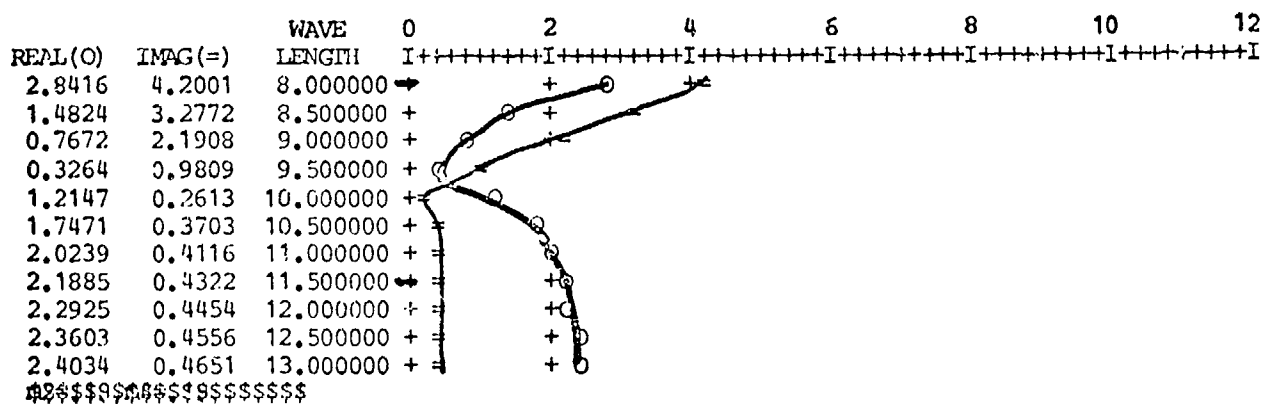


Figure 7. Herpin Equivalent Index Value for Three-Film System

33105-91300  
CC ON ZNS

14.48.44 06/14/73

FILM STACK PARAMETERS WR = 8.000000 MICRONS  
NO. MATERIAL THK (MU) OPT. THK. (WR UNITS)

NO.	MATERIAL	THK (MU)	OPT. THK. (WR UNITS)
SUB	2.2200		
1	Ge	0.49610	0.25363
2	ALPHA-1	0.16020	0.03805
3	Ge	0.49610	0.25363
4	ThF <sub>4</sub>	1.62637	0.31250
ENN	1.0000		

TOTAL THICK. 2.77877 MICRONS.

\*\*\*\*\*

33105-91300  
CC ON ZNS

14.49.39 06/14/73

WR = 8.000000 MICRONS 1/WR = 0.12500

PERCENT ENN-SIDE TRANSMITTANCE AT NORMAL INCIDENCE

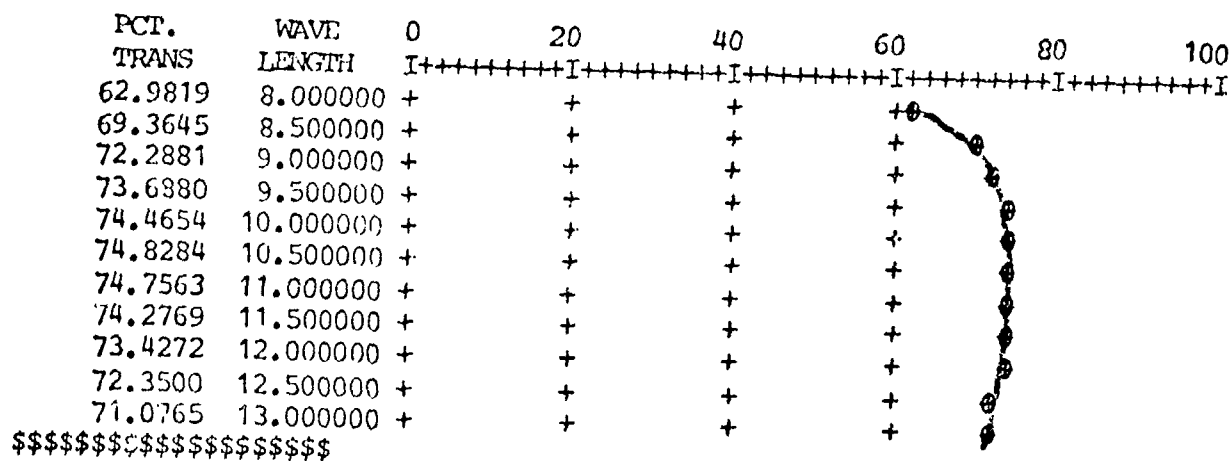


Figure 8. Three-Film System with Antireflection Coating of Thorium Fluoride

33105-91100

11.11.54

04/27/73

COND-IR2 CONDUCTIVE FILM STACK ON IRT-2 (ZNS) SUBSTRATE

FILM STACK PARAMETERS WR = 9.500000 MICRONS

NO. MATERIAL THK(MU) OPT.THK.(WR UNITS)

SUB 2.2200

1 Ge 0.50494 0.21500

2 COND-IR 0.08000 0.01600

3 Ge 0.50494 0.21500

4 ThF4 1.54761 0.25000

ENN 1.0000

TOTAL THICK. 2.63750 MICRONS.

\*\*\*\*\*

33105-91100

11.13.24

04/27/73

COND-IR2 CONDUCTIVE FILM STACK ON IRT-2 (ZNS) SUBSTRATE

WR = 9.500000 MICRONS 1/WR = 0.10526

PERCENT ENN-SIDE TRANSMITTANCE AT NORMAL INCIDENCE

PCT.	WAVE	0	20	40	60	80	100
TRANS	LENGTH	I++++++I	I++++++I	I++++++I	I++++++I	I++++++I	I++++++I
83.4769	8.000000	+	+	+	+	+ ⊕	
86.5780	8.500000	+	+	+	+	+ ⊕	
87.4465	9.000000	+	+	+	+	+ ⊕	
87.5176	9.500000	+	+	+	+	+ ⊕	
87.1023	10.000000	+	+	+	+	+ ⊕	
86.1393	10.500000	+	+	+	+	+ ⊕	
84.5900	11.000000	+	+	+	+	+ ⊕	
82.5731	11.500000	+	+	+	+	+ ⊕	
\$\$\$\$\$\$\$\$\$\$\$\$\$\$\$\$							

Figure 9. Indium-Tin-Oxide Three-Film System with  
Antireflection Coating of Thorium Fluoride

Other more complicated designs are, of course, possible, but the real limiting factor for the transmission that can be induced through the indium-tin-oxide film is the absorption in this film. More complex multilayers could not be expected to yield, even in theory, more than 2 or 3% more transmission than the design used in the foregoing example. In practice, the reproducibility of these complex designs will be limited by the reproducibility of the  $n$  and  $k$  values for the indium-tin-oxide film.

Figure 10 shows the use of three-film Herpin sections to obtain a higher real index for impedance matching purposes. This technique yields a higher maximum transmission (86%) but has a much narrower bandwidth ( $\sim 1.0$  micron) due to the dispersive properties of the Herpin sections.

### 3.3 EXPERIMENTAL EFFORT

The initial prototype coatings using the theoretical design shown in Figure 8 exhibited extremely poor durability and low transmission. Thin films of  $\text{ZnS}$  and  $\text{ThF}_4$  were inserted into the film system. During this study the following was observed:

- a. The optical constants of the conductive films are influenced by the substrate and previously deposited films.
- b. The sticking coefficient of the conductive film is a function of the surface being coated.
- c. The  $n$  and  $k$  values of the indium-tin-oxide may be varied by post deposition processes such as air or vacuum bake cycles.
- d. Diffusion between the germanium film and conductive film occurs at temperatures  $< 250^\circ\text{C}$ .

The final coating design and durability is shown in Table 3. Figure 11 shows the spectral performance of the coating design when deposited onto  $\text{ZnS}$ . All attempts to increase the transmission by the use of  $800 \text{ \AA}$  conductive films resulted in marginal increase in transmission and a tenfold increase in resistance.

By comparing Figures 8 and 11, it can be seen that at the peak transmission wavelength, the agreement between measured and computed data is excellent, the difference of approximately 2% containing the contributions

33105-91300  
NARROW BAND CONDUCTIVE COATING

13:19:20 02/21/75

FILM STACK PARAMETERS NR = 9.500000 MICRONS  
NO. MATERIAL THK(MU) OPT.THR.(GR UNITS)

NO.	MATERIAL	THK(MU)	OPT.THR.(GR UNITS)
608	2.2105		
1	Ge	0.54017	0.23000
2	ZnS	0.99183	0.23000
3	Ge	0.54017	0.23000
4	ALPHA-I	0.15998	0.03368
5	Ge	0.54017	0.23000
6	ZnS	0.99183	0.23000
7	Ge	0.54017	0.23000
8	1.4000	1.69643	0.25000
ERR.	1.0000		

TOTAL THICK. 6.00076 MICRONS.  
\*\*\*\*\*

33105-91300  
NARROW BAND CONDUCTIVE COATING

13:20:02 02/21/75

NR = 9.500000 MICRONS 1/2NR = 0.19526

PERCENT PER-ODGE TRANSMITTANCE AT NORMAL INCIDENCE

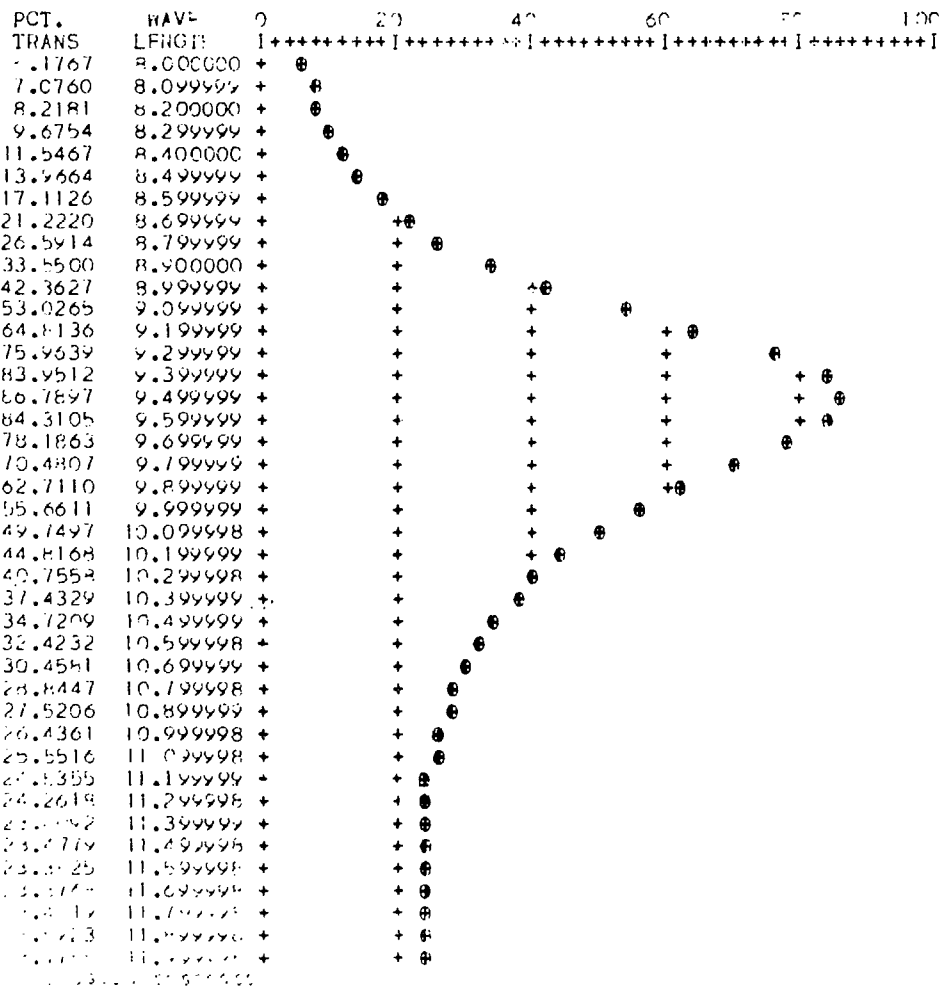


Figure 10. Three-Film Herpin Sections

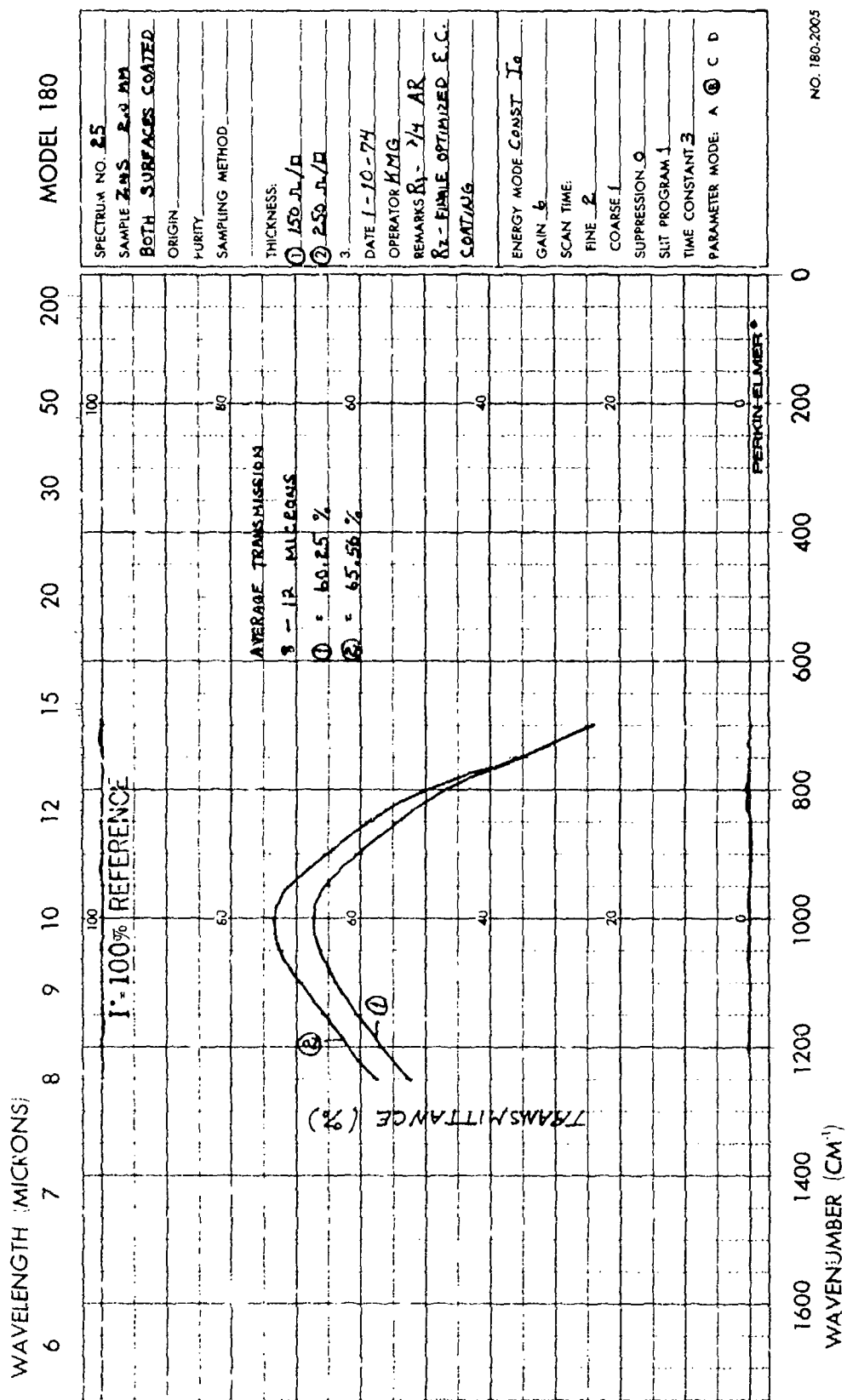


Figure 11. Spectral Performance of Coating Design Deposited on ZnS



TABLE 3a. COATING DESIGN

Step	Film Material	Thickness	Substrate Temperature (°C)	Notes
1	ZnS	$1/2\lambda \pm 0.441 \mu$	120°	Binder Film
2	Ge	$\lambda \pm 1.690 \mu$	120°	Impedance Matching Film
3	ZnS	$1/2\lambda \pm 0.441 \mu$	120°	Diffusion Barrier Film
4	Indium-Tin-Oxide	$1600 \text{ \AA}$		
5				Post Deposition Processes
6	$\text{ThF}_4$	$1/4\lambda \pm 0.473 \mu$	250°	Diffusion Barrier and Binder Film
7	Ge	$\lambda \pm 1.690 \mu$	250°	Impedance Matching Film
8	$\text{ThF}_4$	$\lambda \pm 1.920 \mu$	250°	Matching Film System Into Air

TABLE 3b. DURABILITY EVALUATION

Test	Results
Washing	Passed
Adherence per MIL-M-13508E	Passed
Abrasion per MIL-M-13508B	Passed
Abrasion per MIL-C-675A	Failed
Humidity per MIL-C-675A	Passed

from the uncertainty in the  $k$  values for the indium-tin-oxide film, absorption in the dielectric films, and absorption at film interfaces.

The coating design then clearly demonstrates the viability of the induced transmission technique as a means of providing conductive thin-film coatings with high infrared transmission. The work directed towards the understanding of the optical constants of the indium-tin-oxide films has enabled us to obtain an idea of some of the practical limits of the technique for considerations such as film durability and the spectral coverage that can be obtained.

## SECTION 4

### ANTIREFLECTION COATINGS

The design types that can be used most effectively for high index substrates such as zinc sulfide and zinc selenide comprise one or more films, each being one-quarter wavelength optical thickness at a wavelength centered in the frequency range of interest.

#### 4.1 THEORETICAL DESIGN

##### 4.1.1 Single Layer Designs

The simplest design is the well known single quarter-wave design, which provides for a minimum reflectivity value at or close to zero when

$$n_1 = (n_o n_s)^{\frac{1}{2}}$$

where

- $n_1$  is the refractive index of the film
- $n_o$  is the refractive index of the medium
- $n_s$  is the refractive index of the substrate

For zinc sulfide ( $n = 2.2$ ),  $n_1 = 1.48$  and for zinc selenide ( $n = 2.4$ ),  $n_1 = 1.55$ ; the spectral response of these film systems are shown in Figures 12 and 13. Since no known nonabsorbing material having the above indices in the 8 to 12 micron region exists, it will be necessary to simulate this index.

One method of realizing films having refractive indices not available in any practical material is the use of the Herpin equivalent index film system technique. This technique basically involves the use of a symmetrical system of 3, 5 or some other odd multilayer stack of film to simulate a single film with some index intermediate between the values for the two films. Figure 14a illustrates the single film design for ZnSe and Figure 14b illustrates the simplest equivalent stack, a three-film equivalent of a single quarter-wave optical thickness. The solution can be affected with either two high index

12:12:21

SUB	2.2000		
1	1.4800	1.00473	0.25000
END	1.0000		

331 05-71500  
A. P. COALING

12:12:40

$$\mu_{\text{H}} = 9.50070 \text{ m/eV} \quad 1/\mu_{\text{H}} = 0.10526$$

PERCENT END-SIDE REFLECTANCE AT NORMAL INCIDENCE

REFL.	LENGTH	1	2	4	8	10
2.5301	1.50000	+	+	+	+	+
1.9350	1.15000	+	+	+	+	+
1.3505	3.00000	+	+	+	+	+
0.9318	3.25000	+	+	+	+	+
0.5499	6.50000	+	+	+	+	+
0.2744	3.15000	+	+	+	+	+
0.1240	9.00000	+	+	+	+	+
0.0799	2.25000	+	+	+	+	+
0.0335	2.50000	+	+	+	+	+
0.0210	2.15000	+	+	+	+	+
0.1111	10.00000	+	+	+	+	+
0.2152	10.25000	+	+	+	+	+
0.3527	10.50000	+	+	+	+	+
0.5374	10.75000	+	+	+	+	+
0.7344	11.00000	+	+	+	+	+
0.9491	11.25000	+	+	+	+	+
1.1775	11.50000	+	+	+	+	+
1.4105	11.75000	+	+	+	+	+
1.6531	12.00000	+	+	+	+	+
1.9149	12.25000	+	+	+	+	+
2.1993	12.50000	+	+	+	+	+
2.4995	12.75000	+	+	+	+	+
2.8207	13.00000	+	+	+	+	+

Figure 12. Spectral Response for ZnS

12:00:00

Sub	2.4000		
I	1.5500	1.53220	0.25000
Emu	1.0000		

TOTAL TITON. 1.23220 ml. CHLORO.  
\*\*\*\*\*

2:1:6

$$nR = 9.21020 \text{ and } 1/nR = 0.108690$$

PERCENT CRO-OF-DE REPLICATION AT NORMAL INCUBANCE

```

PC1.      NAME      1      2      3      4      5      10
REFL.     LENGTH  1+++++++1+++++++1+++++++1+++++1+++++1
3.2512     7.500000 +          #
2.4034     7.750000 +          + #
1.0913     8.000000 +          #
1.1221     8.250000 +          #
0.0340     8.500000 +          #
0.3000     8.750000 +          #
0.1549     9.000000 +          #
0.0303     9.250000 +          #
0.0000     9.500000 +          #
0.0331     9.750000 +          #
0.1250    10.000000 +          #
0.2579    10.250000 +          #
0.4515    10.500000 +          #
0.0091    10.750000 +          #
0.9141    11.000000 +          #
1.1308    11.250000 +          #
1.4040    11.500000 +          #
1.7007    11.750000 +          #
2.0000    12.000000 +          #
2.3774    12.250000 +          + #
2.6923    12.500000 +          + #
3.0087    12.750000 +          + #
3.3247    13.000000 +          + #
1 N 1 2 3 4 5 6 7 8 9 10 11 12 13 14 15 16 17 18 19 20 21 22 23 24 25 26 27 28 29 30 31 32 33 34 35 36 37 38 39 40 41 42 43 44 45 46 47 48 49 50 51 52 53 54 55 56 57 58 59 60 61 62 63 64 65 66 67 68 69 70 71 72 73 74 75 76 77 78 79 80 81 82 83 84 85 86 87 88 89 90 91 92 93 94 95 96 97 98 99 100
R = 1.2107      1 = 92.7833      R' = 1.2107
rv1 = 7.500000      rv2 = 13.000000      rv1 = 0.250000
$$$$$$$$$$$$$$$$$$$$

```

Figure 13. Spectral Response for ZnSe

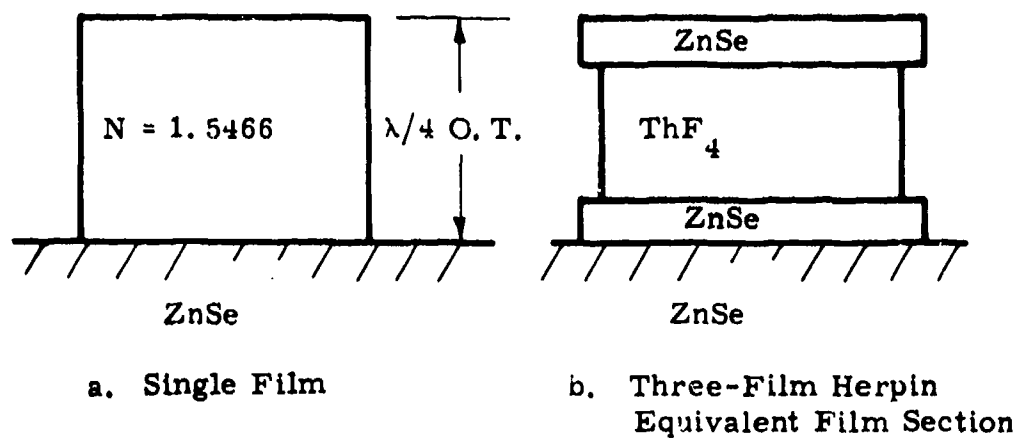


Figure 14. Herpin Equivalent Index Film System

films and one low index film, as shown, or two low index films and one high index film. The selection of the particular arrangement for any two materials would depend on practical considerations such as adhesion to the substrate, abrasion resistance, etc.

Figures 15 and 16 (ZnS and ZnSe, respectively) show the Herpin equivalent film system that replaced the single film previously shown.

#### 4.1.2 Double-Layer Designs

The effective range of antireflection coverage can be extended through the use of double-layer designs using two quarter-wavelength thick films. One solution for such a design occurs when

$$\frac{n_2}{n_1} = \left( \frac{n_s}{n_o} \right)^{\frac{1}{2}}$$

where

$n_1$  is the refractive index of the outer film

$n_2$  is the refractive index of the inner film

By assuming  $n_1$  to be 1.40 ( $\text{ThF}_4$ ) one calculates the theoretical value of  $n_2$  to be 2.07 for ZnS and 2.17 for ZnSe. The spectral response of these coatings is shown in Figure 17 for ZnS and in Figure 18 for ZnSe. By the use of the Herpin equivalent film system,  $n_2$  is replaced by ZnSe and  $\text{ThF}_4$  films. The spectral response of these coatings is shown in Figure 19 for ZnS and in Figure 20 for ZnSe.

#### 4.2 EXPERIMENTAL EFFORT

To increase the durability of these coatings, a thin protective film of  $\text{CeF}_3$  was used as the outer film. The following table lists the coating design and spectral performance curves of 2.0 mm thick ZnS and ZnSe substrates coated on both surfaces.

33105-91500  
A.R.COATINGS

12:14:17

FILM STACK PARAMETERS NR = 9.50000 MICRONS  
NO. MATERIAL THK(MU) OPT.THK.(NR UNITS)

SUB 2.2000  
1 ZNSE 0.13328 0.03367  
2 TiF4 1.16178 0.17416  
3 ZNSE 0.13328 0.03367  
END 1.0000

TOTAL THICK. 1.44035 MICRONS.  
\*\*\*\*\*

33105-91500  
A.R.COATINGS

12:14:40

NR = 9.50000 MICRONS 1/NR = 0.10526

PERCENT END-SIDE REFLECTANCE AT NORMAL INCIDENCE

REFL.	WAVELENGTH	0	2	4	6	8	10
3.5744	7.50000	+	+	+			
2.5354	7.75000	+	+	+			
1.7270	8.00000	+	+	+			
1.1791	8.25000	+	+	+			
0.7136	8.50000	+	+	+			
0.3312	8.75000	+	+	+			
0.1525	9.00000	+	+	+			
0.0407	9.25000	+	+	+			
0.0000	9.50000	+	+	+			
0.0284	9.75000	+	+	+			
0.1125	10.00000	+	+	+			
0.2426	10.25000	+	+	+			
0.4103	10.50000	+	+	+			
0.6075	10.75000	+	+	+			
0.8262	11.00000	+	+	+			
1.0569	11.25000	+	+	+			
1.3191	11.50000	+	+	+			
1.5310	11.75000	+	+	+			
1.6494	12.00000	+	+	+			
2.1217	12.25000	+	+	+			
2.3757	12.50000	+	+	+			
2.6576	12.75000	+	+	+			
2.9423	13.00000	+	+	+			

1 3 1 5 0 8 1 5 0 0 V A L U E S :

R = 1.1525

1 = 95.0470

R' = 1.1525

AVL = 7.500000

AV2 = 13.000000

AV1 = 0.200000

55555555555555555555

Figure 15. Herpin System for ZnS



33105-91500  
A.R.COATINGS

12:04:07

FILM STACK PARAMETERS NR = 9.50000 MICRONS  
NO. MATERIAL THK(MU) OPT.THK.(NR UNITS)

SUB 2.4000  
1 ZNSE 0.18293 0.04621  
2 HF4 0.99795 0.14707  
3 ZNSE 0.18293 0.04621  
ENV 1.0000

TOTAL THICK. 1.36382 MICRONS.  
\*\*\*\*\*

33105-91500  
A.R.COATINGS

12:04:33

NR = 9.50000 MICRONS 1/NR = 0.10526

PERCENT ENR-SIDE REFLECTANCE AT NORMAL INCIDENCE

PC1.	WAVE	0	2	4	6	8	10
REFL.	LENGTH	1+++++	1+++++	1+++++	1+++++	1+++++	1+++++
4.4489	7.50000	+	+	+	+	+	+
3.2121	7.75000	+	+	+	+	+	+
2.2204	8.00000	+	+	+	+	+	+
1.4479	8.25000	+	+	+	+	+	+
0.8555	8.50000	+	+	+	+	+	+
0.4508	8.75000	+	+	+	+	+	+
0.1390	9.00000	+	+	+	+	+	+
0.0432	9.25000	+	+	+	+	+	+
0.0000	9.50000	+	+	+	+	+	+
0.0421	9.75000	+	+	+	+	+	+
0.1543	10.00000	+	+	+	+	+	+
0.3237	10.25000	+	+	+	+	+	+
0.5339	10.50000	+	+	+	+	+	+
0.7904	10.75000	+	+	+	+	+	+
1.0722	11.00000	+	+	+	+	+	+
1.3714	11.25000	+	+	+	+	+	+
1.6385	11.50000	+	+	+	+	+	+
2.0150	11.75000	+	+	+	+	+	+
2.3519	12.00000	+	+	+	+	+	+
2.6210	12.25000	+	+	+	+	+	+
3.0315	12.50000	+	+	+	+	+	+
3.3710	12.75000	+	+	+	+	+	+
3.7079	13.00000	+	+	+	+	+	+

1 N 1 E 3 R A 1 E 0 V A L U E S :

R = 1.4520 1 = 96.5474 R' = 1.4520  
nV1 = 7.500000 nV2 = 13.000000 nV1 = 0.250000

SSSSSSSSSSSSSSSSSSSS

Figure 16. Herpin System for ZnSe

33105-91500  
A.R.COATINGS

12:10:20

FILM STACK PARAMETERS NR = 9.50000 MICRONS  
NO. MATERIAL THK(MU) OPT. THK. (NR UNITS)

SUB	THK	REFL	OPT. THK.
1	2.0700	1.14734	0.25000
2	1.4000	1.09643	0.25000
END	1.0000		

TOTAL THICK. 2.64377 MICRONS.  
\*\*\*\*\*

33105-91500  
A.R.COATINGS

12:10:40

NR = 9.50000 MICRONS 1ZNR = 0.10020

PERCENT TRANSMISSION REFLECTANCE AT NORMAL INCIDENCE

WAVELENGTH	REFL	TRANSM
1.4300	1.14734	0.85266
1.4421	1.13000	0.87000
1.4543	1.11000	0.89000
1.4665	1.09000	0.91000
1.4787	1.07000	0.93000
1.4909	1.05000	0.95000
1.5031	1.03000	0.97000
1.5153	1.01000	0.99000
1.5275	0.99000	1.01000
1.5397	0.97000	1.03000
1.5519	0.95000	1.05000
1.5641	0.93000	1.07000
1.5763	0.91000	1.09000
1.5885	0.89000	1.11000
1.6007	0.87000	1.13000
1.6129	0.85000	1.15000
1.6251	0.83000	1.17000
1.6373	0.81000	1.19000
1.6495	0.79000	1.21000
1.6617	0.77000	1.23000
1.6739	0.75000	1.25000
1.6861	0.73000	1.27000
1.6983	0.71000	1.29000
1.7105	0.69000	1.31000
1.7227	0.67000	1.33000
1.7349	0.65000	1.35000
1.7471	0.63000	1.37000
1.7593	0.61000	1.39000
1.7715	0.59000	1.41000
1.7837	0.57000	1.43000
1.7959	0.55000	1.45000
1.8081	0.53000	1.47000
1.8203	0.51000	1.49000
1.8325	0.49000	1.51000
1.8447	0.47000	1.53000
1.8569	0.45000	1.55000
1.8691	0.43000	1.57000
1.8813	0.41000	1.59000
1.8935	0.39000	1.61000
1.9057	0.37000	1.63000
1.9179	0.35000	1.65000
1.9301	0.33000	1.67000
1.9423	0.31000	1.69000
1.9545	0.29000	1.71000
1.9667	0.27000	1.73000
1.9789	0.25000	1.75000
1.9911	0.23000	1.77000
2.0033	0.21000	1.79000
2.0155	0.19000	1.81000
2.0277	0.17000	1.83000
2.0399	0.15000	1.85000
2.0521	0.13000	1.87000
2.0643	0.11000	1.89000
2.0765	0.09000	1.91000
2.0887	0.07000	1.93000
2.1009	0.05000	1.95000
2.1131	0.03000	1.97000
2.1253	0.01000	1.99000
2.1375	0.00000	2.01000
2.1497	0.00000	2.03000
2.1619	0.00000	2.05000
2.1741	0.00000	2.07000
2.1863	0.00000	2.09000
2.1985	0.00000	2.11000
2.2107	0.00000	2.13000
2.2229	0.00000	2.15000
2.2351	0.00000	2.17000
2.2473	0.00000	2.19000
2.2595	0.00000	2.21000
2.2717	0.00000	2.23000
2.2839	0.00000	2.25000
2.2961	0.00000	2.27000
2.3083	0.00000	2.29000
2.3205	0.00000	2.31000
2.3327	0.00000	2.33000
2.3449	0.00000	2.35000
2.3571	0.00000	2.37000
2.3693	0.00000	2.39000
2.3815	0.00000	2.41000
2.3937	0.00000	2.43000
2.4059	0.00000	2.45000
2.4181	0.00000	2.47000
2.4303	0.00000	2.49000
2.4425	0.00000	2.51000
2.4547	0.00000	2.53000
2.4669	0.00000	2.55000
2.4791	0.00000	2.57000
2.4913	0.00000	2.59000
2.5035	0.00000	2.61000
2.5157	0.00000	2.63000
2.5279	0.00000	2.65000
2.5401	0.00000	2.67000
2.5523	0.00000	2.69000
2.5645	0.00000	2.71000
2.5767	0.00000	2.73000
2.5889	0.00000	2.75000
2.6011	0.00000	2.77000
2.6133	0.00000	2.79000
2.6255	0.00000	2.81000
2.6377	0.00000	2.83000
2.6499	0.00000	2.85000
2.6621	0.00000	2.87000
2.6743	0.00000	2.89000
2.6865	0.00000	2.91000
2.6987	0.00000	2.93000
2.7109	0.00000	2.95000
2.7231	0.00000	2.97000
2.7353	0.00000	2.99000
2.7475	0.00000	3.01000
2.7597	0.00000	3.03000
2.7719	0.00000	3.05000
2.7841	0.00000	3.07000
2.7963	0.00000	3.09000
2.8085	0.00000	3.11000
2.8207	0.00000	3.13000
2.8329	0.00000	3.15000
2.8451	0.00000	3.17000
2.8573	0.00000	3.19000
2.8695	0.00000	3.21000
2.8817	0.00000	3.23000
2.8939	0.00000	3.25000
2.9061	0.00000	3.27000
2.9183	0.00000	3.29000
2.9305	0.00000	3.31000
2.9427	0.00000	3.33000
2.9549	0.00000	3.35000
2.9671	0.00000	3.37000
2.9793	0.00000	3.39000
2.9915	0.00000	3.41000
3.0037	0.00000	3.43000
3.0159	0.00000	3.45000
3.0281	0.00000	3.47000
3.0403	0.00000	3.49000
3.0525	0.00000	3.51000
3.0647	0.00000	3.53000
3.0769	0.00000	3.55000
3.0891	0.00000	3.57000
3.1013	0.00000	3.59000
3.1135	0.00000	3.61000
3.1257	0.00000	3.63000
3.1379	0.00000	3.65000
3.1501	0.00000	3.67000
3.1623	0.00000	3.69000
3.1745	0.00000	3.71000
3.1867	0.00000	3.73000
3.1989	0.00000	3.75000
3.2111	0.00000	3.77000
3.2233	0.00000	3.79000
3.2355	0.00000	3.81000
3.2477	0.00000	3.83000
3.2599	0.00000	3.85000
3.2721	0.00000	3.87000
3.2843	0.00000	3.89000
3.2965	0.00000	3.91000
3.3087	0.00000	3.93000
3.3209	0.00000	3.95000
3.3331	0.00000	3.97000
3.3453	0.00000	3.99000
3.3575	0.00000	4.01000
3.3697	0.00000	4.03000
3.3819	0.00000	4.05000
3.3941	0.00000	4.07000
3.4063	0.00000	4.09000
3.4185	0.00000	4.11000
3.4307	0.00000	4.13000
3.4429	0.00000	4.15000
3.4551	0.00000	4.17000
3.4673	0.00000	4.19000
3.4795	0.00000	4.21000
3.4917	0.00000	4.23000
3.5039	0.00000	4.25000
3.5161	0.00000	4.27000
3.5283	0.00000	4.29000
3.5405	0.00000	4.31000
3.5527	0.00000	4.33000
3.5649	0.00000	4.35000
3.5771	0.00000	4.37000
3.5893	0.00000	4.39000
3.6015	0.00000	4.41000
3.6137	0.00000	4.43000
3.6259	0.00000	4.45000
3.6381	0.00000	4.47000
3.6503	0.00000	4.49000
3.6625	0.00000	4.51000
3.6747	0.00000	4.53000
3.6869	0.00000	4.55000
3.6991	0.00000	4.57000
3.7113	0.00000	4.59000
3.7235	0.00000	4.61000
3.7357	0.00000	4.63000
3.7479	0.00000	4.65000
3.7601	0.00000	4.67000
3.7723	0.00000	4.69000
3.7845	0.00000	4.71000
3.7967	0.00000	4.73000
3.8089	0.00000	4.75000
3.8211	0.00000	4.77000
3.8333	0.00000	4.79000
3.8455	0.00000	4.81000
3.8577	0.00000	4.83000
3.8699	0.00000	4.85000
3.8821	0.00000	4.87000
3.8943	0.00000	4.89000
3.9065	0.00000	4.91000
3.9187	0.00000	4.93000
3.9309	0.00000	4.95000
3.9431	0.00000	4.97000
3.9553	0.00000	4.99000
3.9675	0.00000	5.01000
3.9797	0.00000	5.03000
3.9919	0.00000	5.05000
4.0041	0.00000	5.07000
4.0163	0.00000	5.09000
4.0285	0.00000	5.11000
4.0407	0.00000	5.13000
4.0529	0.00000	5.15000
4.0651	0.00000	5.17000
4.0773	0.00000	5.19000
4.0895	0.00000	5.21000
4.1017	0.00000	5.23000
4.1139	0.00000	5.25000
4.1261	0.00000	5.27000
4.1383	0.00000	5.29000
4.1505	0.00000	5.31000
4.1627	0.00000	5.33000
4.1749	0.00000	5.35000
4.1871	0.00000	5.37000
4.1993	0.00000	5.39000
4.2115	0.00000	5.41000
4.2237	0.00000	5.43000
4.2359	0.00000	5.45000
4.2481	0.00000	5.47000
4.2603	0.00000	5.49000
4.2725	0.00000	5.51000
4.2847	0.00000	5.53000
4.2969	0.00000	5.55000
4.3091	0.00000	5.57000
4.3213	0.00000	5.59000
4.3335	0.00000	5.61000
4.3457	0.00000	5.63000
4.3579	0.00000	5.65000
4.3701	0.00000	5.67000
4.3823	0.00000	5.69000
4.3945	0.00000	5.71000
4.4067	0.00000	5.73000
4.4189	0.00000	5.75000
4.4311	0.00000	5.77000
4.4433	0.00000	5.79000
4.4555	0.00000	5.81000
4.4677	0.00000	5.83000
4.4799	0.00000	5.85000
4.4921	0.00000	5.87000
4.5043	0.00000	5.89000
4.5165	0.00000	5.91000
4.5287	0.00000	5.93000
4.5409	0.00000	5.95000
4.5531	0.00000	5.97000
4.5653	0.00000	5.99000
4.5775	0.00	

33105-91500  
A.R.COATINGS

12:08:04

FILM STACK PARAMETERS NR = 9.50000 MICRONS  
NO. MATERIAL THK(MU) OPT. THK. (NR UNITS)

SUB	2.4000		
1	2.1700	1.09447	0.25000
2	1.4000	1.09043	0.25000
ENN	1.0000		

TOTAL THICK. 2.79090 MICRONS.  
\*\*\*\*\*

33105-91500  
A.R.COATINGS

12:08:25

NR = 9.50000 MICRONS 1/NR = 0.10526

PERCENT ENN-SIDE REFLECTANCE AT NORMAL INCIDENCE

PGT.	WAVE	0	2	4	6	8	10
REFL.	LENGTH	1	1	1	1	1	1
1.3550	7.50000	+	⊗				
0.9146	7.75000	+	⊗				
0.5908	8.00000	+	⊗				
0.3715	8.25000	+	⊗				
0.2154	8.50000	+	⊗				
0.1110	8.75000	+	⊗				
0.0457	9.00000	⊗					
0.0107	9.25000	⊗					
0.0000	9.50000	⊗					
0.0095	9.75000	⊗					
0.0369	10.00000	⊗					
0.0801	10.25000	⊗					
0.1351	10.50000	+	⊗				
0.2101	10.75000	+	⊗				
0.2955	11.00000	+	⊗				
0.3936	11.25000	+	⊗				
0.5040	11.50000	+	⊗				
0.6260	11.75000	+	⊗				
0.7590	12.00000	+	⊗				
0.9023	12.25000	+	⊗				
1.0552	12.50000	+	⊗				
1.2166	12.75000	+	⊗				
1.3865	13.00000	+	⊗				

INTEGRATED VALUES:

R = 0.4483 T = 99.5517 R' = 0.4483  
nV1 = 7.500000 nV2 = 13.000000 nV1 = 0.250000  
\$\$\$\$\$

Figure 18. Spectral Response for ZnSe Double-Layer Design

12:15:20

SUB	2,2000		
1	240E	0.39940	0.10090
2	18F4	0.26090	0.04228
3	240E	0.39940	0.10090
4	18F4	1.09043	0.25000
END	1.0000		

351-91200  
A.M.C. 441100

1 2 3 4 5 6 7 8 9 10 11 12 13 14 15 16 17 18 19 20 21 22 23 24 25 26 27 28 29 30 31 32 33 34 35 36 37 38 39 40 41 42 43 44 45 46 47 48 49 50 51 52 53 54 55 56 57 58 59 60 61 62 63 64 65 66 67 68 69 70 71 72 73 74 75 76 77 78 79 80 81 82 83 84 85 86 87 88 89 90 91 92 93 94 95 96 97 98 99 100 101 102 103 104 105 106 107 108 109 110 111 112 113 114 115 116 117 118 119 120 121 122 123 124 125 126 127 128 129 130 131 132 133 134 135 136 137 138 139 140 141 142 143 144 145 146 147 148 149 150 151 152 153 154 155 156 157 158 159 160 161 162 163 164 165 166 167 168 169 170 171 172 173 174 175 176 177 178 179 180 181 182 183 184 185 186 187 188 189 190 191 192 193 194 195 196 197 198 199 200 201 202 203 204 205 206 207 208 209 210 211 212 213 214 215 216 217 218 219 220 221 222 223 224 225 226 227 228 229 230 231 232 233 234 235 236 237 238 239 240 241 242 243 244 245 246 247 248 249 250 251 252 253 254 255 256 257 258 259 260 261 262 263 264 265 266 267 268 269 270 271 272 273 274 275 276 277 278 279 280 281 282 283 284 285 286 287 288 289 290 291 292 293 294 295 296 297 298 299 300 301 302 303 304 305 306 307 308 309 310 311 312 313 314 315 316 317 318 319 320 321 322 323 324 325 326 327 328 329 330 331 332 333 334 335 336 337 338 339 340 341 342 343 344 345 346 347 348 349 350 351 352 353 354 355 356 357 358 359 360 361 362 363 364 365 366 367 368 369 370 371 372 373 374 375 376 377 378 379 380 381 382 383 384 385 386 387 388 389 390 391 392 393 394 395 396 397 398 399 400 401 402 403 404 405 406 407 408 409 410 411 412 413 414 415 416 417 418 419 420 421 422 423 424 425 426 427 428 429 430 431 432 433 434 435 436 437 438 439 440 441 442 443 444 445 446 447 448 449 450 451 452 453 454 455 456 457 458 459 460 461 462 463 464 465 466 467 468 469 470 471 472 473 474 475 476 477 478 479 480 481 482 483 484 485 486 487 488 489 490 491 492 493 494 495 496 497 498 499 500 501 502 503 504 505 506 507 508 509 510 511 512 513 514 515 516 517 518 519 520 521 522 523 524 525 526 527 528 529 530 531 532 533 534 535 536 537 538 539 540 541 542 543 544 545 546 547 548 549 550 551 552 553 554 555 556 557 558 559 560 561 562 563 564 565 566 567 568 569 570 571 572 573 574 575 576 577 578 579 580 581 582 583 584 585 586 587 588 589 590 591 592 593 594 595 596 597 598 599 600 601 602 603 604 605 606 607 608 609 610 611 612 613 614 615 616 617 618 619 620 621 622 623 624 625 626 627 628 629 630 631 632 633 634 635 636 637 638 639 640 641 642 643 644 645 646 647 648 649 650 651 652 653 654 655 656 657 658 659 660 661 662 663 664 665 666 667 668 669 670 671 672 673 674 675 676 677 678 679 680 681 682 683 684 685 686 687 688 689 690 691 692 693 694 695 696 697 698 699 700 701 702 703 704 705 706 707 708 709 710 711 712 713 714 715 716 717 718 719 720 721 722 723 724 725 726 727 728 729 730 731 732 733 734 735 736 737 738 739 740 741 742 743 744 745 746 747 748 749 750 751 752 753 754 755 756 757 758 759 760 761 762 763 764 765 766 767 768 769 770 771 772 773 774 775 776 777 778 779 780 781 782 783 784 785 786 787 788 789 790 791 792 793 794 795 796 797 798 799 800 801 802 803 804 805 806 807 808 809 810 811 812 813 814 815 816 817 818 819 820 821 822 823 824 825 826 827 828 829 830 831 832 833 834 835 836 837 838 839 840 841 842 843 844 845 846 847 848 849 850 851 852 853 854 855 856 857 858 859 860 861 862 863 864 865 866 867 868 869 870 871 872 873 874 875 876 877 878 879 880 881 882 883 884 885 886 887 888 889 890 891 892 893 894 895 896 897 898 899 900 901 902 903 904 905 906 907 908 909 910 911 912 913 914 915 916 917 918 919 920 921 922 923 924 925 926 927 928 929 930 931 932 933 934 935 936 937 938 939 940 941 942 943 944 945 946 947 948 949 950 951 952 953 954 955 956 957 958 959 960 961 962 963 964 965 966 967 968 969 970 971 972 973 974 975 976 977 978 979 980 981 982 983 984 985 986 987 988 989 990 991 992 993 994 995 996 997 998 999 1000 1001 1002 1003 1004 1005 1006 1007 1008 1009 1010 1011 1012 1013 1014 1015 1016 1017 1018 1019 1020 1021 1022 1023 1024 1025 1026 1027 1028 1029 1030 1031 1032 1033 1034 1035 1036 1037 1038 1039 1040 1

$$m = 9.5(10) \text{ MeV} \quad \text{and} \quad 1/m = 0.10526$$

PERCENT END-SIDE REFLECTION AT NORMAL INCIDENCE

[illegible]

Figure 19. Spectral Response for ZnS Coated With ZnSe and  $\text{ThF}_4$

12810013

SUB	2.4000		
1	LNSE	0.42990	0.10802
2	11F4	0.19317	0.02855
3	LNSE	0.42990	0.10802
4	11F4	1.09043	0.25000
END	1.00000		

\*\*\*\*\*

12810837

PERCENT ENDSIDE REFLECTANCE AT NORMAL INCIDENCE

INTEGRATED VALUES:

$$K = 0.5091 \quad I = 99.4911 \quad K' = 0.5091$$
$$ny1 = 1.500000 \quad ny2 = 13.000000 \quad ny1 = 0.250000$$

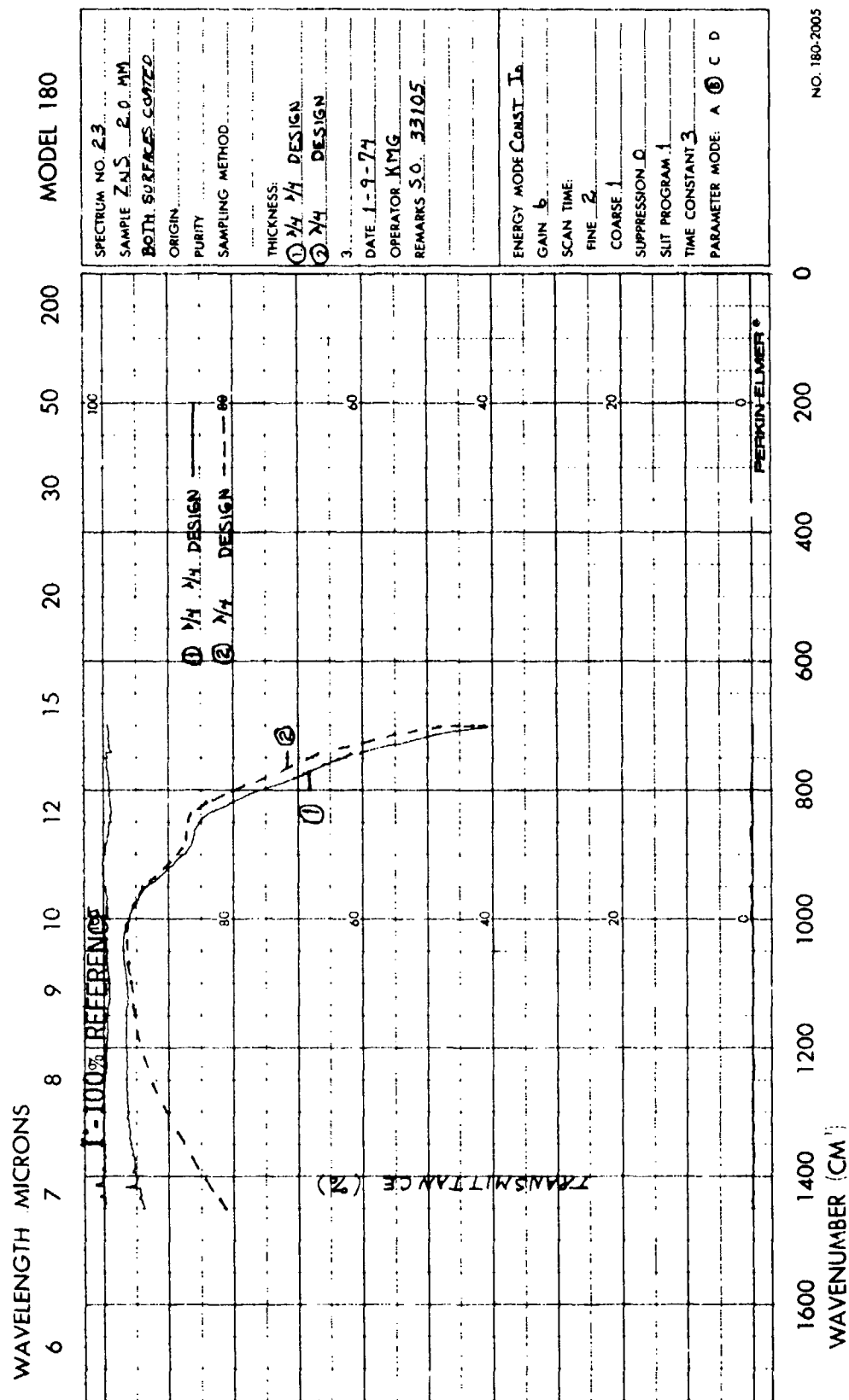
\$ \$

Figure 20. Spectral Response for ZnSe Coated With ZnSe and  $\text{ThF}_4$

Substrate	Theoretical Design	Theoretical Performance	Spectral Curve
ZnS	$\lambda/4$	Figure 15	Figure 21 (2)
ZnS	$\lambda/4 - \lambda/4$	Figure 19	Figure 21 (1)
ZnSe	$\lambda/4$	Figure 16	Figure 22 (2)
ZnSe	$\lambda/4 - \lambda/4$	Figure 20	Figure 22 (1)

The durability of the  $\lambda/4$  and  $\lambda/4 - \lambda/4$  stepdown coatings were evaluated, and the results are shown in the following table.

Test	Specification	Results
Adhesion	MIL-M-13508B	Passed
Abrasion	MIL-C-675A	Passed
Humidity	MIL-C-675A	Passed
Washing	Using Acetone & Alcohol	Passed



NO. 180-2005

Figure 21. Spectral Performance of ZnS With Protective Film Of CeF<sub>3</sub>

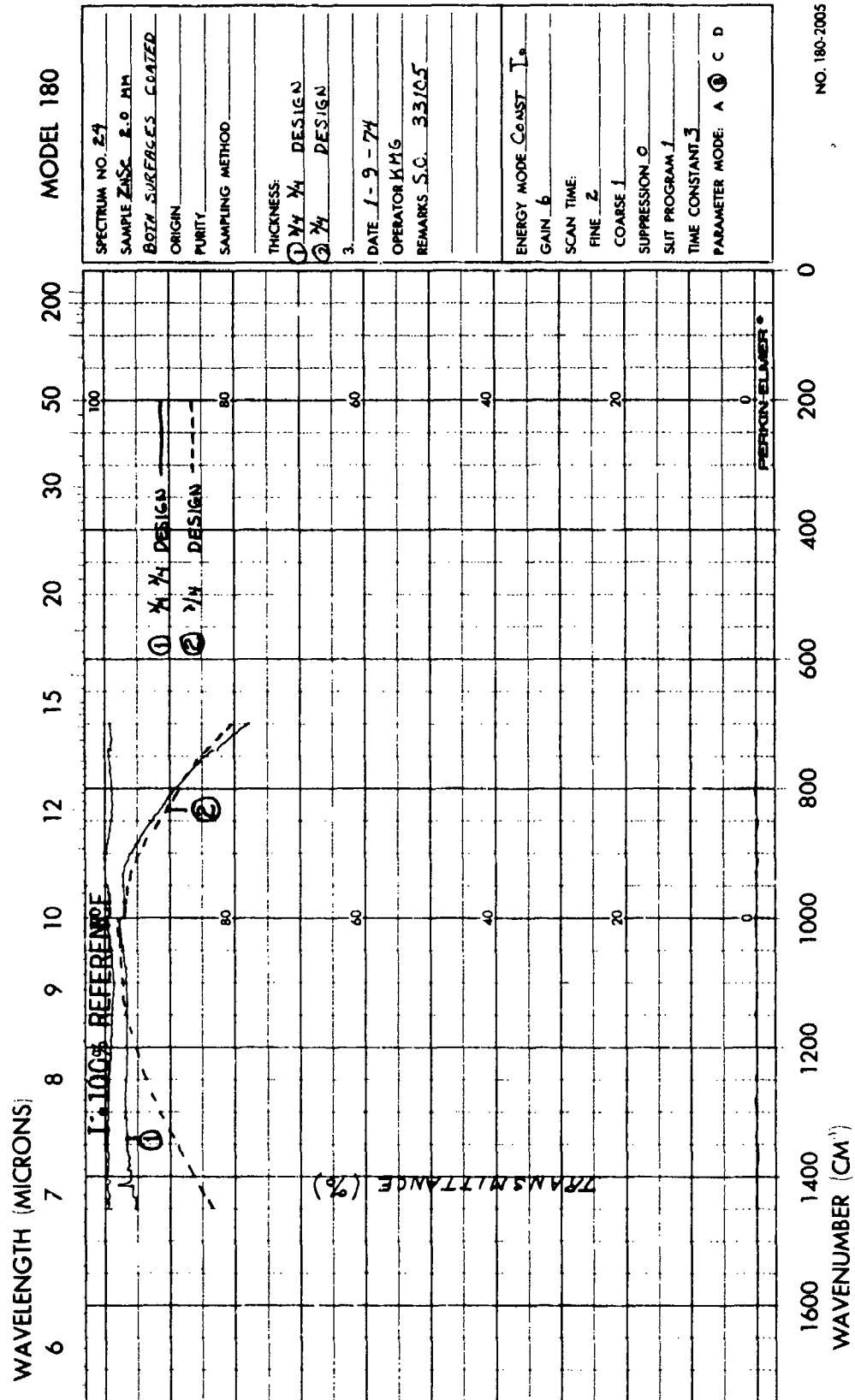


Figure 22. Spectral Performance of ZnSe With Protective Film of CeF<sub>3</sub>



## SECTION 5

### USE OF CONDUCTIVE COATINGS IN NONPARALLEL BUS BAR CONFIGURATIONS

In using thin-film heating systems in relatively high quality transparencies, it is essential to ensure that nonuniformity of power dissipation in the film is avoided. Films made using the Perkin-Elmer conductive oxide process exhibit a high degree of uniformity of bulk resistivity, and any non-uniformity of the sheet resistance/power dissipation would only arise from thickness nonuniformity or effects due to either nonparallelism of the bus bars or end effects at the bus bars.

This phase of the program was intended to demonstrate the use of a non-uniform coating technique applied to a fairly simple irregular configuration such as a trapezoidal or triangular window shape. It was intended to serve two purposes:

- a. A first practical experience with the nonuniform resistance conductive antireflection coating technique applying known technology
- b. A demonstration of significant potential value to the LLLTV portion of the B-1 sensor window program

#### 5.1 NONUNIFORM COATING TECHNIQUES

In many circumstances involving windows of irregular shape (such as those originally planned for the B-1 sensor housing) and spherical (dome) or other nonflat sections, it is not possible to attach electrical connections or bus bars to a window in order to make them parallel. This will create an uneven power dissipation on the element unless it is countered by making the appropriate change in film thickness.

Changing the film thickness or grading of the films could easily be accomplished by using the selective coating technique of the Perkin-Elmer

Glacier<sup>(1)</sup> process. The disadvantage of this method would be that incorporation of the nonuniform films in coating designs would be difficult because of the continually changing thickness. For transparent regions of the conductive film, this problem could be overcome by overcoating the conductive film with a dielectric film of equal refractive index, whose thickness varied in the complementary sense. The two films would then be combined to form a uniform film of known optical thickness that could then be incorporated in anti-reflection coating designs by any of the techniques previously described. Figure 23 schematically illustrates the nonuniform film technique.

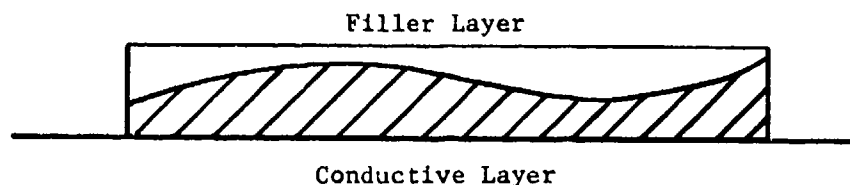


Figure 23. Overcoating of Graded Film

## 5.2 GLACIER PROCESS DESCRIPTION

The basic Glacier process involves a definition phase, a mask preparation phase, and a deposition phase.

### 5.2.1 Definition Phase

The first step in the procedure is to define a point-by-point map description of the desired film thickness required. The values for this approximately rectangular array of locations is required for the mask fabrication process and is inserted into a computer program. The map is used to construct a variable transmission mask that is inserted in the vapor stream of a coating chamber and modifies the flow of coating material to produce a variable thickness coating on the substrate.

### 5.2.2 Mask Preparation

The mask is prepared in several steps. The computer output data is corrected to the final format by point-by-point exposure of photographic film on an automatically controlled precision drafting table. The contrast of the pattern is enhanced by an autopsitive contact printing process. This high-contrast image is then transferred to a layer of photoresist material that has

<sup>(1)</sup> Glacier Program, Perkin-Elmer Report No. 11200.

been laminated on a wire cloth carrier. After development, the remaining photoresist has the pattern that is desired for the final mask. But since the photoresist material is not suitable for use in a vacuum chamber, the pattern is transformed by evaporation, plating, and chemical bathing into an all-metal halftone. The resulting mask is fine enough to permit precise control of evaporant transmission, is sturdy enough to facilitate handling, and is well suited to the vacuum environment.

### 5.2.3 Deposition Phase

The key to the Glacier process is this transmission mask that can effectively regulate the amount of evaporant material deposited on any portion of the optical substrate. The mask consists of a multiplicity of halftone dots or holes in a metallic sheet supported by woven stainless-steel wire cloth. The size of each dot, and therefore its transmission, is controlled individually based upon the input map data. A typical mask may contain over one-half million halftone dots. Because the mask is placed suitably downstream and the evaporant source has an appreciable area, there is no residual halftone structure in the mask shadow on the workpiece. Therefore, smooth surfaces are produced.

The substrate and mask are mounted in the chamber and the alignment of the substrate, mask, and coating source is performed. The deposition of material is initiated by controlling the evaporation sources. Monitoring of deposition rate and thickness is accomplished with two crystal monitors that are mounted on the edge of the substrate. When the crystal monitors indicate the required amount of material has been deposited, the coating process is terminated and the optical element is removed for testing. There is no fundamental limit to the amount of thickness variation that can be achieved.

### 5.3 EXPERIMENTAL EFFORT

Four BK-7 trapezoidal windows were fabricated to achieve a transmission wavefront error less than  $\lambda/15$  at  $6328 \text{ \AA}$ . The two parallel sides of these windows were 3 inches and 6 inches with a height of 4 inches. Two windows (A and B) were coated with a uniform conductive coating, and two windows (C and D) were coated using the Glacier technique to achieve a 2/1 thickness ratio. The latter two windows were then coated with the reverse film thickness variation

using a dielectric film whose index is equal to the conductive film. Figure 24 shows the schematical buildup of this film system. All windows were characterized at each stage of completion and the results are shown in Table 4. Figures 25a and b show the transmission wavefront interferograms before and after coating window B. Figures 25c, d and e show, respectively, the transmission wavefront interferograms before coating, after the 2.3/1 ratio conductive coating, and after correction of window D. Using this process, the observed degradation was less than  $\lambda/20$  at  $6328 \text{ \AA}$ .

Windows B and D were chosen to evaluate the temperature profile of the heatable trapezoidal windows. Figure 26 shows the geometry and electrical connections made to a uniform and nonuniformly coated BK-7 window. The procedure used for this evaluation was to apply ac voltage (slowly) and to record the temperature at positions A through H (as shown in Figure 26) when the window has reached equilibrium ( $\sim 10$  minutes). Table 5 shows recorded temperatures of the nonuniformly coated window and Table 6 shows the uniform coating temperatures.

By comparing the data shown in Tables 5 and 6, one finds that at an average window temperature of approximately  $165^{\circ}\text{F}$ , the nonuniform window had a temperature variation of only  $39.4^{\circ}\text{F}$  as compared with  $65.1^{\circ}\text{F}$  for the uniform coating. This clearly indicates the effectiveness of the nonuniform coating technique to obtain uniform power dissipation. The data also indicates that special techniques for mounting heatable windows may have to be designed to eliminate edge effects. Section 6.9 describes the thermal problems due to lateral heat flow through an IR window to the frame.

#### 5.4 CONCLUSIONS

For the transparent region of conductive films, the nonuniform coating technique described in this section is an ideal solution to the problem of providing a uniform power dissipation in an irregular bus bar configuration if an analytical solution can be determined for the thickness of the conductive film as a function of the geometry. The optical thickness of the coated optic can then be corrected for transmission wavefront uniformity and can be incorporated into a high efficiency multilayer coating.

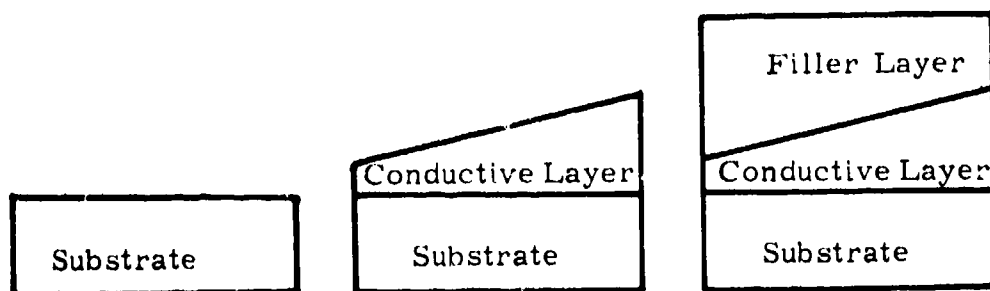


Figure 24. Variable Resistance Coating

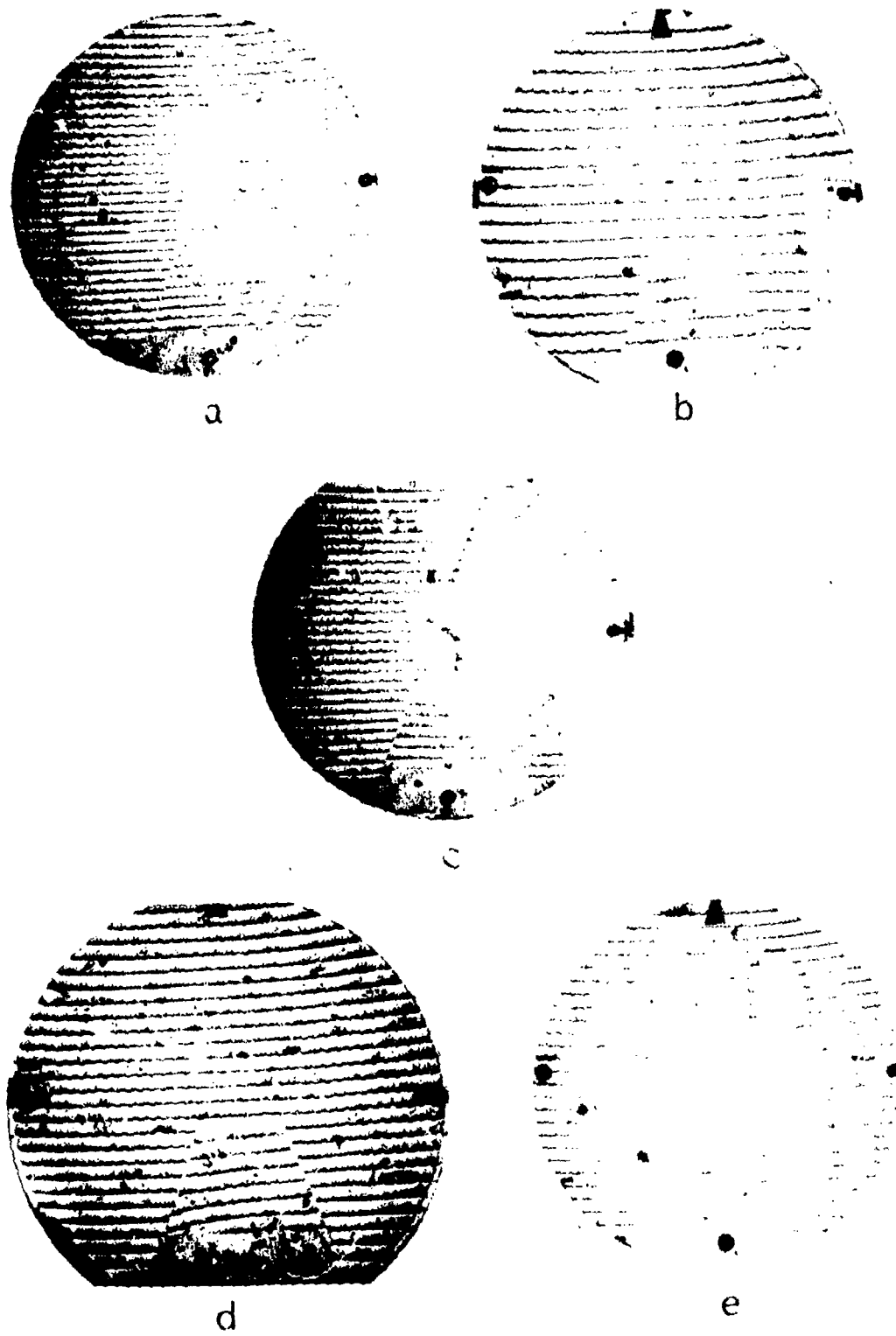


Figure 25. Transmission Wavefront Interferograms

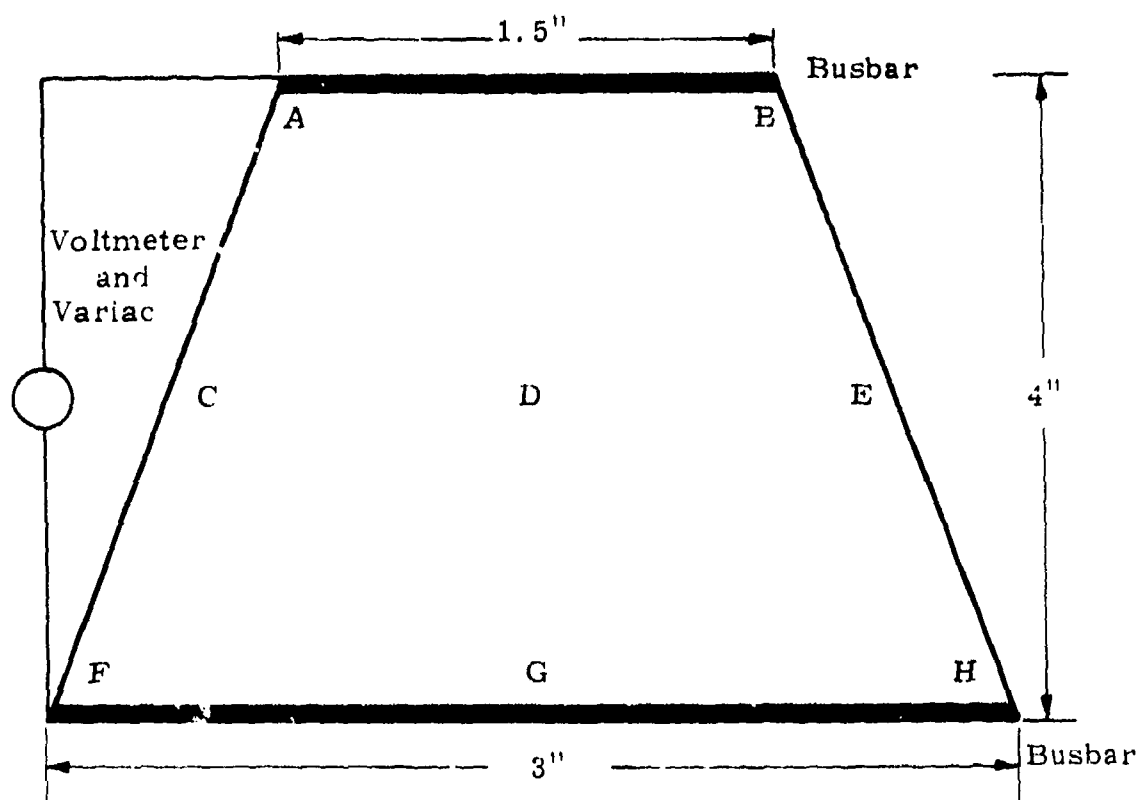


Figure 26. Trapezoidal Window Layout

TABLE 4. WINDOW CHARACTERIZATION

Window	Transmission Wavefront	Optical Thickness of Conductive Film at Center of Optic	Variation of the Transmission Wavefront Over Optic	Thickness Ratio	Optical Thickness of Corrective Film at Center of Optic	Final Variation of the Transmission Wavefront
A	$< \lambda/15$	$\lambda$ at 575 $m\mu$ (finished window)	$< \lambda/15$ at 6328 $\text{\AA}$	1/1	None	$< \lambda/15$ at 6328 $\text{\AA}$
B	$< \lambda/15$	$\lambda$ at 578 $m\mu$ (finished window)	$< \lambda/15$ at 6328 $\text{\AA}$	1/1	None	$< \lambda/15$ at 6328 $\text{\AA}$
C	$< \lambda/15$	$\lambda$ at 620 $m\mu$	$3/4 \lambda$ 's at 6328 $\text{\AA}$	2.3/1	$\lambda$ at 580 $m\mu$	$< \lambda/9$ at 6328 $\text{\AA}$
D	$< \lambda/15$	$\lambda$ at 606 $m\mu$	$3/5 \lambda$ 's at 6328 $\text{\AA}$	1.8/1	$\lambda$ at 610 $m\mu$	$< \lambda/9$ at 6328 $\text{\AA}$



TABLE 5. RECORDED TEMPERATURES OF NONUNIFORMLY COATED WINDOW

WINDOW D

RESISTANCE (BUS TO BUS) = 149.3 OHMS

Voltage (ac) Position (Fig. 26)	Temperature (°F)							
	A	B	C	D	E	F	G	H
15	104.8	104.3	103.8	106.0	104.3	99.1	100.6	97.2
30	146.1	141.0	144.6	147.3	136.1	124.3	130.1	119.1
35	172.6	163.4	169.4	173.3	157.8	140.0	149.7	133.9
60	238.0	237.3	238.8	241.4	220.8	209.3	212.2	185.5

TABLE 6. RECORDED TEMPERATURES OF UNIFORMLY COATED WINDOW

WINDOW B

RESISTANCE (BUS TO BUS) = 236.1 OHMS

Voltage (ac) Position (Fig. 26)	Temperature (°F)							
	A	B	C	D	E	F	G	H
30	96.2	95.9	94.9	95.1	93.5	85.8	89.1	86.8
50	137.4	143.2	130.8	137.4	129.9	106.7	124.3	109.3
60	179.9	176.9	163.2	188.8	171.6	123.7	155.5	131.0

## SECTION 6

### THERMO-OPTICAL ANALYSIS OF CONDUCTIVE FILMS AND PATTERNS

Several infrared window deicing techniques utilizing electrically conductive films or patterns were analyzed to determine the extent of wavefront distortion and the stresses and strains induced by the temperature and pressure gradients imposed by the B-1 flight environment. Window substrate materials were limited to CVD (chemical vapor deposited) zinc sulfide (ZnS), zinc selenide (ZnSe), and zinc sulfo-selenide (ZnSSe) solid solution.

A study of the safety aspects, especially with regard to the possibilities of catastrophic failure due to temperature controller malfunction, was also performed. Several general conclusions were reached:

- a. The maximum window tensile stresses due to temperature and pressure gradients are well within the strength capabilities of the selected window materials with the possible exception of an abnormal situation that results in sudden cooling of a window that has been heated at high power densities.
- b. The wavefront degradation due to axial temperature gradients caused by applying the electrically conductive coating to the interior surface of the window is insignificant at angles of incidence up to  $30^\circ$ .
- c. There is appreciable wavefront distortion for radial (lateral) temperature gradients caused by heat loss to a cold window frame. A method of eliminating these gradients is described.
- d. The thermally-induced optical path differences (window thickness variations) due to striped heater patterns, utilized to increase the average window transmission, will cause negligible wavefront distortion for interior surface coatings on ZnSe at  $4.5 \text{ watts/in}^2$ .

- e. An attractive method for maximizing the overall transmission of the EC-coated window is to add a thin intermediate bus bar centered on the vertical dimension (parallel to the horizontal dimension). This reduces the electrical resistance of the coating by a factor of 4, thus permitting the use of thinner (higher transmission), high resistance EC coatings, uniform or striped.
- f. Thermal stresses are minimized by applying the EC coating to the exterior window surface, although higher power densities are then required to maintain a given interior surface temperature and the exterior coating is more subject to physical damage than an interior coating would be.

#### 6.1 ASSUMED CONDITIONS

For purposes of the analyses, the following conditions were assumed for the IR window:

- Window dimensions, 8.8" x 10" x 0.75", with the 10" dimension horizontal (same as the preliminary dimensions for the B-1 germanium IR window, per Boeing).
- Average power density required, 4.5 to 6.9 watts/in<sup>2</sup> (discussed later).
- Minimum desired average heater-coated window transmission, 0.80.
- Maximum available supply voltage, 230 V rms.
- Aircraft interior temperature, 70°F.
- Interior surface convective film coefficient, 0.5 BTU/hr-ft<sup>2</sup>-°F (calculated value for free convection at 14.7 psia).
- Minimum ambient temperature, -65°F.
- Exterior surface film coefficient, 21.5 BTU/hr-ft<sup>2</sup>-°F (per Joe Stein, NAR).
- Minimum external surface temperature, 35°F (to prevent frosting).
- Window frame is temperature controlled to minimize edge heat losses and concurrently reduce the lateral window temperature gradients.

- The bandpass of the transparent EC coatings is 8 to 12  $\mu\text{m}$ .

The thermal conductivities of ZnS and ZnSe are within 10% of each other; therefore, they are considered interchangeably with regard to the temperature distribution. ZnS<sub>Se</sub> has a thermal conductivity equal to one-half that of ZnS and, therefore, represents the worst case of the three materials in this respect. The properties of these materials were taken from data supplied by Raytheon (Table 7) and References 2 through 6.

## 6.2 BASIC ANALYTICAL PROCEDURE

The transient and steady-state temperature distributions were determined by nodal analysis for selected deicing configurations. From these, the resultant stresses and strains were computed. The latter were then used to calculate the distortion of a plane wavefront assumed to be incident over a selected region of the window.

Of the three potential configurations: (1) EC coating on the exterior surface, (2) EC coating on the interior surface, and (3) EC coating laminated between two window substrates, only the first two were considered because a suitable laminating adhesive having high transmission between 8 and 12  $\mu\text{m}$  was not available at that time.

## 6.3 POWER DENSITY AND TEMPERATURE CONTROL REQUIREMENTS

The initial axial temperature gradient analysis was based on the heat flux specified for the B-1 LLLTV window, 6.9 watts/in<sup>2</sup> (Ref. 7). Subsequent

- 
- (2) Caren, R.P., Funai, A.I., Frye, W.E. and Sklensky, A.F., "Properties of Infrared Sensor Materials", Materials Research and Standards, MTRSA, Volume 11, No. 6, June, 1971, p. 10.
  - (3) Technical Report AFAL-TR-73-252, "Chemical Vapor Deposition of Multi-spectral Windows", Air Force Avionics Laboratory, Wright Patterson Air Force Base, July, 1973, pp. 29, 30.
  - (4) "Raytran ZnSe", Raytheon Data Sheet, Raytheon Research Division, 28 Seyon Street, Waltham, Massachusetts 02154
  - (5) Telecon, James Pappis, Raytheon with E.A. Strouse, Perkin-Elmer, December 1974, re: Recent CVD ZnSe Data.
  - (6) Letter, James Pappis, Raytheon to E.A. Strouse, Perkin-Elmer, June 28, 1973, re: Properties of CVD ZnS, ZnSe and ZnS<sub>Se</sub>.
  - (7) Specification No. L330C2001-1, Rockwell International, B-1 Division, p. 3.

TABLE 7. CVD MATERIAL PROPERTIES (REF. 3,  
EXCEPT ASTERISKED DATA AS NOTED)

Property	Standard ZnSe	ZnSSe	ZnS
Density (gm/cc)	5.27	5.15	4.08
Refractive Index (10.6 $\mu\text{m}$ )	2.405* (10.6 $\mu\text{m}$ )	2.38 (est)	2.20
Absorption Coefficient (10.6 $\mu\text{m}$ , 1/cm)	0.002 - 0.005**	0.007**	$\sim 0.15^{**}$
Transmission Limits	0.5 - 22 $\mu\text{m}$	0.5 - 16 $\mu\text{m}$	0.5 - 14 $\mu\text{m}$
Hardness (Knoop 50 gm)	100	190	250*
Grain Size (Microns)	70*	100	(20 - 100)
Flexural Strength (psi, 4-point loading)	8000*	7700	16000*
Young's Modulus (psi)	$9.75 \times 10^6$	$9.16 \times 10^6$	$10.8 \times 10^6$
Thermal Expansion Coefficient (1/°C) RT-500°C	$8.53 \times 10^{-6}$	$8.30 \times 10^{-6}$	$7.85 \times 10^{-6}$
RT - 170°C	$7.57 \times 10^{-6*}$		
Thermal Conductivity (25°C, cal/sec-cm-°C)	0.043	0.02	0.040
Specific Heat (cal/gm-°C)	0.085	0.088 (est)	0.112
Electrical Resistivity (ohm-cm)	$\sim 10^{12}$	$\sim 10^{12}$	$\sim 10^{12}$
dn/dt (10.6 $\mu\text{m}$ , 1/°C)	$5.9 \times 10^{-5*}$		
Turbidity Coefficient (1/cm)			
0.6328 $\mu\text{m}$	0.16 - 0.43*		
10.6 $\mu\text{m}$	$1.5 - 3 \times 10^{-4*}$		
Inhomogeneity 10.6 $\mu\text{m}$	$1.3 \times 10^{-6}$		

\* Ref. 5

\*\* Ref. 6

discussions with the Thermodynamics Section personnel at Rockwell during September 1973 revealed that the nominal heat flux requirement for the B-1 IR window could be as low as 4 watts/in<sup>2</sup> (approximately 2000 BTU/hr-ft<sup>2</sup>) to maintain the exterior surface above 35°F. Perkin-Elmer analysis has indicated that a minimum of 4.5 watts/in<sup>2</sup> (approximately 2200 BTU/hr-ft<sup>2</sup>) is required to achieve this condition with the -65°F exterior ambient temperature specified for the B-1 LLLTV window. Consequently, 4.5 watts/in<sup>2</sup> was ultimately selected for the minimum required value. (Note that MIL-T-5842A, Ref. 8, requires a maximum of 4.3 watts/in<sup>2</sup> for windshield anti-icing heating at air speeds greater than 300 knots.) However, as will be shown later, higher power densities may be needed to prevent fogging on the interior surface with low exterior ambient temperatures.

This situation is primarily due to the relatively high thermal conductivity of the selected window substrates (near that of the austenitic stainless steels), which results in much lower axial temperature gradients than are usually encountered with the more common window glasses. The latter have thermal conductivities that are lower by factors of up to 10 or more. Therefore, the temperature control circuit should be designed to automatically deliver sufficient power to ensure that the minimum interior surface temperature is always maintained above the interior dewpoint temperature in addition to satisfying the 35°F minimum exterior surface temperature requirements. It is possible to provide a control system that will make the minimum interior surface temperature track the interior atmosphere dewpoint with a positive temperature differential of a few degrees. This method would minimize the heater power requirements. A simpler, alternate approach (which will obviously waste power at relative humidities of less than 100%) is to track the interior ambient atmosphere temperature with a small positive differential.

There is the possibility that a combination of circumstances can result in fogging of the exterior surface, e.g., this surface, operating near 35°F, is suddenly exposed to a warmer, high humidity environment during a flight maneuver. An external dewpoint or ambient temperature sensor track circuit,

---

(8) Military Specification MIL-T-5842A, "Transparent Areas, Anti-Icing, Defrosting and Defogging Systems, General Specification for", September, 1950.

similar to that just described for the interior surface, would also be required if there is a chance that these circumstances would occur when the IR window is in use.

A schematic of the complete control system described above is shown in Figure 27. The edge guard (subframe) heater is required to minimize the optical degradation resulting from radial (lateral) temperature gradients (to be discussed later). The bimetallic, Klaxon-type thermostat will shut down both controllers in the event of a circuit malfunction that causes the heater to inadvertently stay on, e.g., open circuit in any of the positive temperature coefficient ambient temperature sensors, shorted control transistor or thyristor, shorted positive temperature coefficient surface temperature sensor, etc. Control redundancy can thereby be provided by using a narrow differential thermostat having an actuating temperature above the highest anticipated interior dewpoint, which would automatically maintain the window fog- or frost-free but at the expense of higher power consumption and/or EMI caused by the ON-OFF switching transients.

#### 6.4 STEADY STATE THERMAL STRESSES

The results of the steady state nodal analyses are summarized in Table 8 for the range of power densities considered here. The intermediate values listed therein are those necessary to maintain the interior window surface at the assumed interior ambient temperature (70°F) for either EC coating location. This condition guarantees that there will be no fogging on the interior surface at very high humidities.

The thermally induced stresses were calculated for 4.5 and 6.9 watts/in<sup>2</sup> using the equation for the bending stress in a flat plate of uniform thickness with a linear temperature gradient and fixed edges<sup>(9)</sup>:

$$\text{Stress} = 0.5 \cdot \Delta T \cdot \alpha \cdot E / (1 - \nu)$$

where

$\Delta T$  = temperature gradient, °F

$\alpha$  = expansion coefficient, 1/°F

$E$  = modulus of elasticity, psi

$\nu$  = Poisson's ratio (dimensionless) = 0.3 (Ref. 2)

<sup>(9)</sup>Timoshenko, S. and Woinowsky-Krieger, S., "Theory of Plates and Shells", McGraw-Hill, 1959.

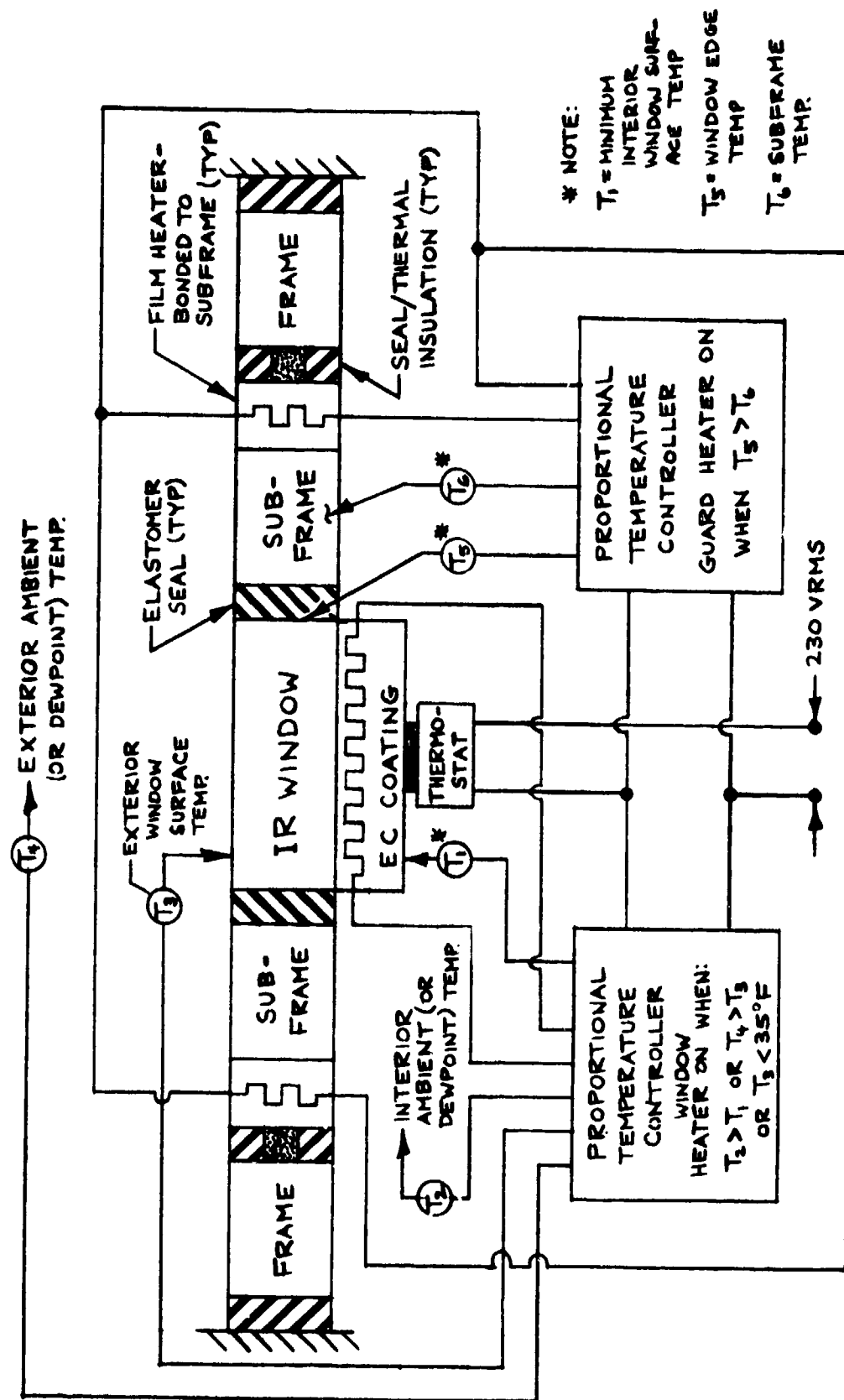


Figure 27. Temperature Control Schematic, IR Window Defogger/Deicer With Guard Heater



TABLE 8. SUMMARY OF EC-COATED ZnSe AND ZnSse WINDOW  
(STEADY-STATE TEMPERATURES BETWEEN  
4.5 AND 6.9 WATTS)/IN<sup>2</sup>)

Window Material	Power Density ( $\frac{\text{Watts}}{\text{in}^2}$ )	EC Coating On Interior Surface			EC Coating On Exterior Surface		
		Interior Surface Temp(°F)	Exterior Surface Temp(°F)	Temp Gradient (°F)	Interior Surface Temp(°F)	Exterior Surface Temp(°F)	Temp Gradient (°F)
ZnSe	4.50	51.62	38.28	13.34	38.68	38.58	0.10
	5.23	70.00	54.55	15.45	54.96	54.91	0.05
	5.91	86.99	69.60	17.39	70.00	70.00	0.00
	6.90	111.98	91.73	20.25	92.13	92.20	-0.07*
ZnSse	4.50	66.51	37.93	28.58	38.78	38.58	0.20
	4.62	70.00	40.66	29.34	41.51	41.33	0.18
	5.91	106.40	69.15	37.25	70.00	70.00	0.00
	6.90	134.58	91.21	43.37	92.06	92.20	-0.14*

\* Negative temperature gradient indicates that heat flows from exterior to interior surface.

Conditions:

1. Window dimensions, 8.8" x 10" x 0.75" thick
2. No lateral heat flow
3. Interior ambient temp, 70°F
4. Exterior ambient temp, -65°F
5. Interior surface film coefficient, 0.5 BTU/hr-ft<sup>2</sup>-°F
6. Exterior surface film coefficient, 21.5 BTU/hr-ft<sup>2</sup>-°F

The results are given in Table 9 for interior and exterior EC coatings on ZnSe and ZnSSe. The corresponding stresses for ZnS are within 10% of those listed for ZnSe.

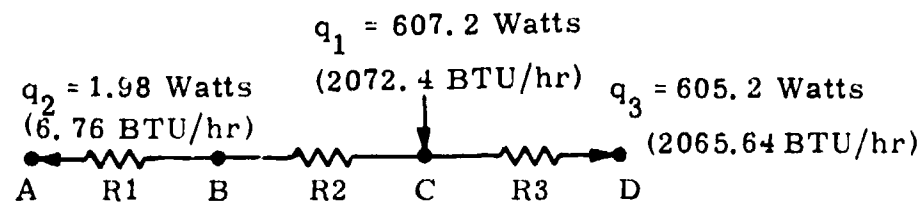
Obviously, each of the three substrate materials, ZnS, ZnSe and ZnSSe, is suitable from a stress standpoint when the EC coating is deposited on the exterior surface of the window. The exterior surface thermal resistance (R3, Figure 28), due to forced convection in flight, is much smaller than the interior surface resistance (R1). Consequently, most of the electrical heat flux must flow through R3. This, combined with the relatively high conductance of the window substrate material, results in an extremely small axial (thickness) temperature gradient, e.g.,  $0.10^{\circ}\text{F}$  for ZnS or ZnSe and  $0.20^{\circ}\text{F}$  for ZnSSe at  $4.5 \text{ watts/in}^2$ , with a correspondingly negligible stress. With the heater coating deposited on the interior surface (Figure 29), all three materials still have acceptable stresses despite the considerable increase in thermal gradient compared to the previous configuration (from  $0.07^{\circ}\text{F}$  to  $20.25^{\circ}\text{F}$  for ZnSe) because most of the applied electrical power must now flow through the substrate to the exterior ambient. Note that even at  $6.9 \text{ watts/in}^2$ , very little of the total electrical input (3.8 watts or 0.63%) is dissipated to the interior ambient because of the aforementioned large free convection resistance at the interior surface.

#### 6.5 COMBINED STEADY-STATE STRESSES (AT EXTERIOR SURFACE)

The maximum stresses due to the temperature and pressure gradients were calculated<sup>(9)</sup> for three basic window support conditions at  $\Delta p$ 's of 2.5 and 10.5 psi (maximum expected  $\Delta p$  per Ref. 10). The worst case results, for ZnSSe at  $6.9 \text{ watts/in}^2$ , are summarized in Table 10. Raytheon<sup>3</sup> has determined that the room temperature flexural strength of this hybrid material, (with 10 percent sulfur substituted for selenium) is 7700 psi  $\pm 10\%$ ; therefore, the material would be conservatively loaded, especially since the soft elastomers, normally used for the window support to eliminate stress concentrations in the brittle substrates, provide conditions that approach the free edge case.

---

(10) Telecon, Phil Mueller and Ron Brigstorke of Boeing to E.A. Strouse, Perkin-Elmer, July 1973, re: B-1 Flight Parameters.



Nodes:

A = Interior Ambient,  $t_A = 70^\circ\text{F}$

B = Interior Window Surface,  $t_B = 92.13^\circ\text{F}$

C = Exterior Window Surface,  $t_C = 92.20^\circ\text{F}$

D = Exterior Ambient,  $t_D = -65^\circ\text{F}$

Temp gradient through window =  $t_B - t_C = -0.07^\circ\text{F}$

Resistances (Based on assumptions stated earlier):

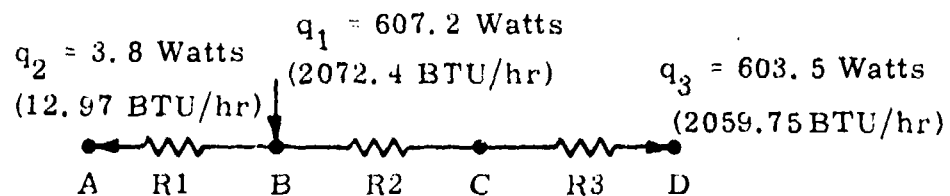
$R_1 = 3.2727^\circ\text{F} \cdot \text{hr}/\text{BTU}$

$R_2 = 0.0098^\circ\text{F} \cdot \text{hr}/\text{BTU}$

$R_3 = 0.0761^\circ\text{F} \cdot \text{hr}/\text{BTU}$

Note: It is assumed that heat flow is unidirectional-perpendicular to window plane (an edge guard heater eliminates heat transfer to the window frame)

Figure 28. Thermal Schematic of Heated 8.8" x 10" x 0.75" ZnSe Window with EC Coating on Exterior Surface ( $6.9 \text{ watts/in}^2$ )



Nodes:

A = Interior Ambient,  $t_A = 70^\circ\text{F}$

B = Interior Window Surface,  $t_B = 111.98^\circ\text{F}$

C = Exterior Window Surface,  $t_C = 91.73^\circ\text{F}$

D = Exterior Ambient,  $t_D = -65^\circ\text{F}$

Temp gradient through window,  $t_B - t_C = 20.25^\circ\text{F}$

Resistances (Based on assumptions stated earlier):

$R1 = 3.2727^\circ\text{F} \cdot \text{hr}/\text{BTU}$

$R2 = 0.0098^\circ\text{F} \cdot \text{hr}/\text{BTU}$

$R3 = 0.0761^\circ\text{F} \cdot \text{hr}/\text{BTU}$

Figure 29. Thermal Schematic of Heated 8.8" x 10" x 0.75" ZnSe Window with EC Coating on Interior Surface (6.9 watts/in<sup>2</sup>)

TABLE 9. STEADY-STATE THERMAL STRESSES FOR UNIFORMLY HEATED  
8.8" X 10" X 0.75" ZnSe AND ZnSSe WINDOWS AT 4.5  
AND 6.9 WATTS/IN<sup>2</sup> POWER DENSITY

Window Substrate	Maximum Tensile Stress* at 4.5 watts/in <sup>2</sup> (psi)		Maximum Tensile Stress* at 6.9 watts/in <sup>2</sup> (psi)	
	Exterior Coating	Interior Coating	Exterior Coating	Interior Coating
ZnSe	2.6	372	1.9	589
ZnSSe	5.2	732	4.1	1163

\* Occurs at colder surface (Table 8) and assumes rigidly held (fixed) edges; actual stress levels are usually reduced by deflection of the flexible elastomer sealant or gasket retaining the window.

TABLE 10. EFFECT OF WINDOW SUPPORT CONDITIONS ON STEADY-STATE WINDOW STRESSES AT EXTERIOR SURFACE

Edge Condition	Maximum Thermal Stress (psi)	Maximum Pressure Stress* (psi)		Worst Combined Stress (psi)
		$\Delta p = 2.5$ psi	$\Delta p = 10.5$ psi	
Fixed	+1163 (at edge)	-124 (at edge)	-522 (at edge)	+1039 (at edge)
Simply Supported	+ 814 (at center)	+120 (at center)	+503 (at center)	+1317 (at center)
Free**	0 (all over)	+160 (at center)	+673 (at center)	+673 (at center)

\*Positive sign indicates tensile stress; negative sign, compressive stress.

\*\*Window is allowed to assume a spherical curvature with radius  $t/\Delta T \alpha$ , where  $t$  = thickness (corners not secured).

Conditions:

1. 8.8" x 10" x 0.75" ZnS<sub>Se</sub> window
2. Uniform EC Coating on interior surface
3. 6.9 watts/in<sup>2</sup> power density,  $\Delta T = 43.4^\circ\text{F}$

## 6.6 TRANSIENT THERMAL STRESSES

During transient heating of the window with the EC coating on the interior surface, the thermal tensile stress does not exceed the steady-state values given in Table 7. If the heater power is interrupted after the steady-state temperature gradient is established, the tensile stress will increase due to the cooling of the exterior surface to approximately 650 psi for the ZnS material and to approximately 1240 psi for the ZnSSe material. These values are all acceptable; however, if the steady-state power input is increased to above 4.5 watts/in<sup>2</sup>, the ZnSSe material may become marginal. For the case where the EC coating (and the power input) is applied to the exterior surface of the window, there is no transient thermal stress problem.

The time to heat the outer surface of the ZnS window to 35°F, at -65°F ambient, is approximately 22 minutes when the EC coating is on the interior surface and 20 minutes when the coating is on the exterior surface. An increase in the maximum power input to above 4.5 watts/in<sup>2</sup> will decrease this time. The ZnSSe material will require approximately 10% longer to come up to temperature.

The transient thermal response, thermal stress, and thermal runaway equilibrium temperature have not been computed separately for the ZnSe material. This was considered unnecessary since the response of the ZnSe material would be almost identical to the ZnS material. The thermal conductivity, thermal capacity, thermal stress, and thermal diffusivity for both materials are very similar (within a few percent).

## 6.7 TEMPERATURE CONTROL CIRCUIT MALFUNCTION

Although the proposed circuit for the window heater controller includes a thermostatic switch bonded to the window to cut off power in case of excessive temperature, calculations indicate that 4.5 watts/in<sup>2</sup> could be continuously applied to the EC coating with the local ambient at 70°F on both sides of the window. The ZnS window would stabilize below 200°F if the air stream velocity exceeds 500 ft/sec (340 mph). The temperature gradient (and hence, the thermal stress) would not be significantly different than for steady-state conditions. Only in the case of prolonged overheating followed by a power failure and simultaneous greatly reduced ambient would the thermal

stress indicate a probable window failure. With the EC coating on the outside, a structural failure due to overheating is unlikely.

#### 6.8 WAVEFRONT DEGRADATION (UNIFORM EC COATING ON INTERIOR SURFACE)

A raytrace and wavefront analysis was performed for each of the three materials (ZnSe, ZnS, and ZnSSe) for a temperature gradient due to 6.9 watts/in<sup>2</sup> accompanied by a flight pressure differential of 2.5, 5.0 and 10.0 psi at angles of incidence of 0°, 15° and 30°. The deflection due to the pressure differential tends to compensate for the thermal distortion; therefore, the worst case is for the largest  $\Delta T$  (for ZnSSe material with its lower thermal conductivity), the smallest pressure gradient, and the highest angle of incidence. The results for this combination are shown in Figure 30; wavefront degradation is insignificant and will obviously be less for lower power densities.

#### 6.9 LATERAL TEMPERATURE GRADIENTS

A serious problem does exist with regard to lateral heat flow through the window to the frame. For the mount configuration shown in Figure 31, the conduction between the window and frame, through the 0.13-inch thick silicone elastomer, is on the order of 1.9 watts per degree F of their temperature difference (with the thermal conductivity of the silicone rubber = 0.18 BTU-ft/hr-ft<sup>2</sup>-°F). Therefore, the heat loss could be as high as 331 watts for the extreme case of a ZnSSe window at 6.9 watts/in<sup>2</sup> (average edge temperature = 112.9°F) and a frame temperature of -65°F.

A nodal analysis was made to determine the in-plane temperature gradients due to conduction to the window frame. It was assumed that the frame was attached to the exterior of the turret in the usual fashion. The following typical flight conditions, obtained from Rockwell B-1 Section personnel, were used for these computations:

- Aircraft velocity, 500-600 ft/sec
- Altitude 8000 - 10000 ft
- Ambient air temperature, 483°R (23°F)
- Exterior surface film coefficient, 21.5 BTU/hr-ft<sup>2</sup>-°F
- Average turret diameter, 12" (looking forward)



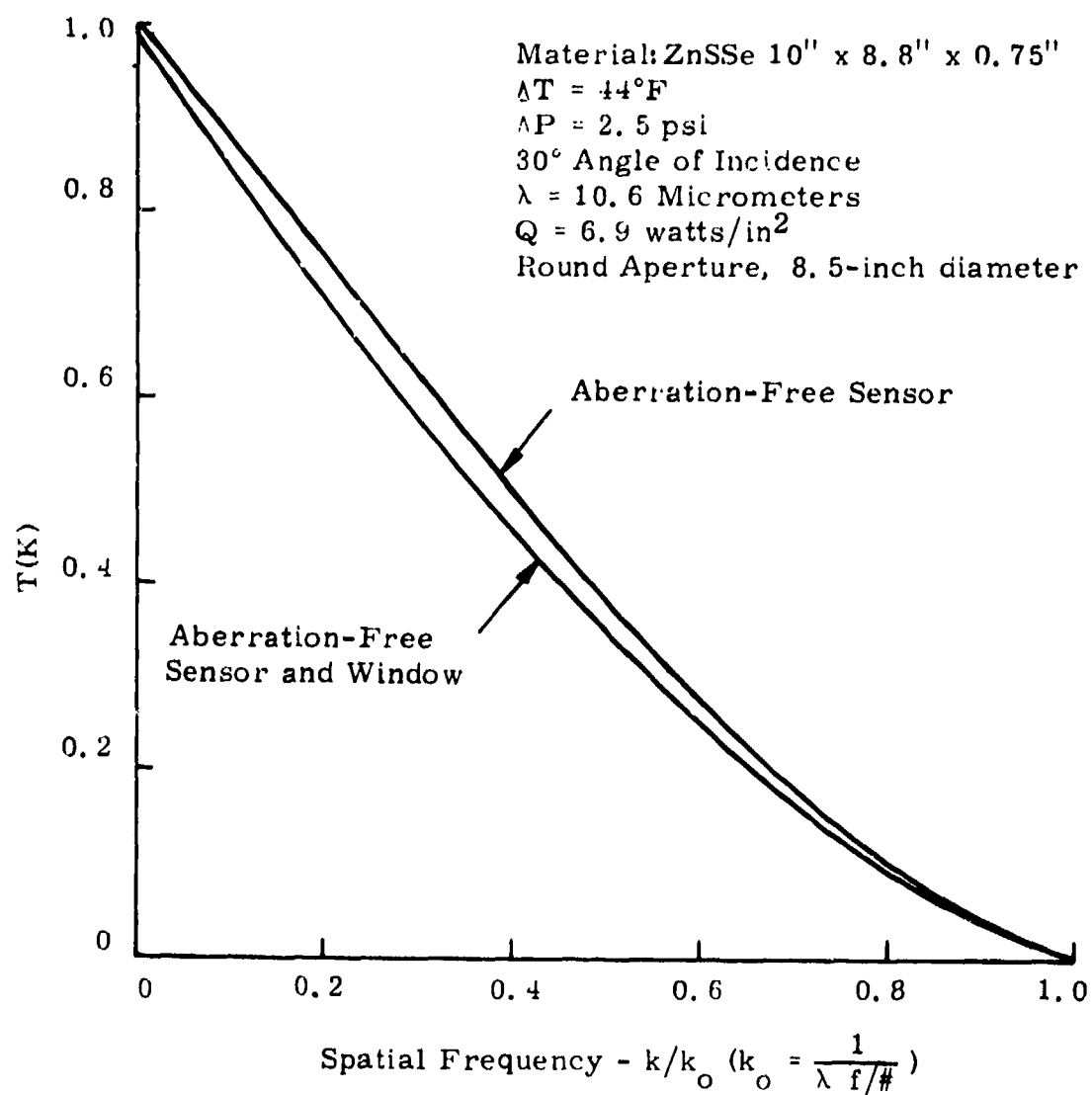


Figure 30. Loss of Performance Due to Window with Axial Temperature Gradient and Pressure Differential

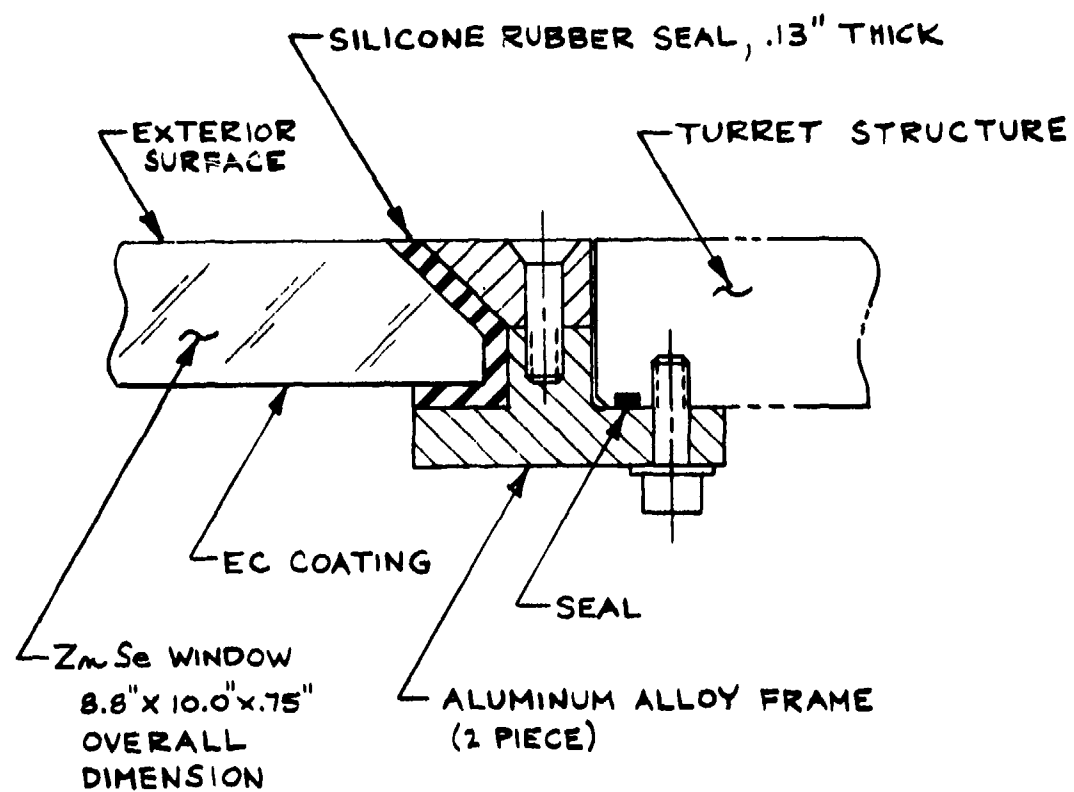


Figure 31. Window Mount Concept

The stagnation temperature for the first three conditions is 500.7°R or 41°F at a Mach number of 0.464 (500 ft/sec). This value was used here for the frame temperature.

Figure 32 shows the thermal contours for one quarter of the window. Figures 33, 34, and 35 show that significant wavefront degradation is caused by this temperature profile with ZnSe. The analysis is based on the value of  $dn/dT$  for the ZnSe material obtained at 6328 Å. Values of  $dn/dT$  for ZnSSe are presently unknown.

If, in order to eliminate lateral gradients, an additional 0.13-inch thickness of silicone rubber and closed-cell polyurethane foam were used to enhance the thermal insulation between the window and frame (Figure 36), approximately 247 watts would be required to maintain the added subframe at the maximum average edge temperature of 112.9°F for the ZnSSe window (frame at -65°F; thermal conductivity, BTU-ft/hr-ft<sup>2</sup>-°F, for silicone rubber = 0.18 and for polyurethane foam = 0.022). This is a relatively large amount compared to that required for the window heater, but it appears to be essential for maintaining high optical performance. Note that extra power would be required anyway to compensate for the edge losses that are present with the simple window mount shown in Figure 31, as mentioned above. The extra power, if delivered to the subframe heater instead, is used more effectively to eliminate lateral gradients. Power is conserved by maximizing the ratio of polyurethane insulating foam to silicone rubber used between the subframe and frame, consistent with seal and support requirements.

#### 6.10 INCREASING COATED WINDOW TRANSMISSION WITH CONDUCTIVE PATTERNS

A basic disadvantage of the electrically-conductive coatings considered here is their inherent decrease in optical transmission with decreasing resistivity (increasing thickness). Three possible approaches to solving this problem were selected for thermo-optical analysis. They are, not necessarily in order of preference:

- a. Application of opaque, electrically-conductive nichrome films to the antireflection coated window in a regular pattern of narrow, parallel linear stripes.

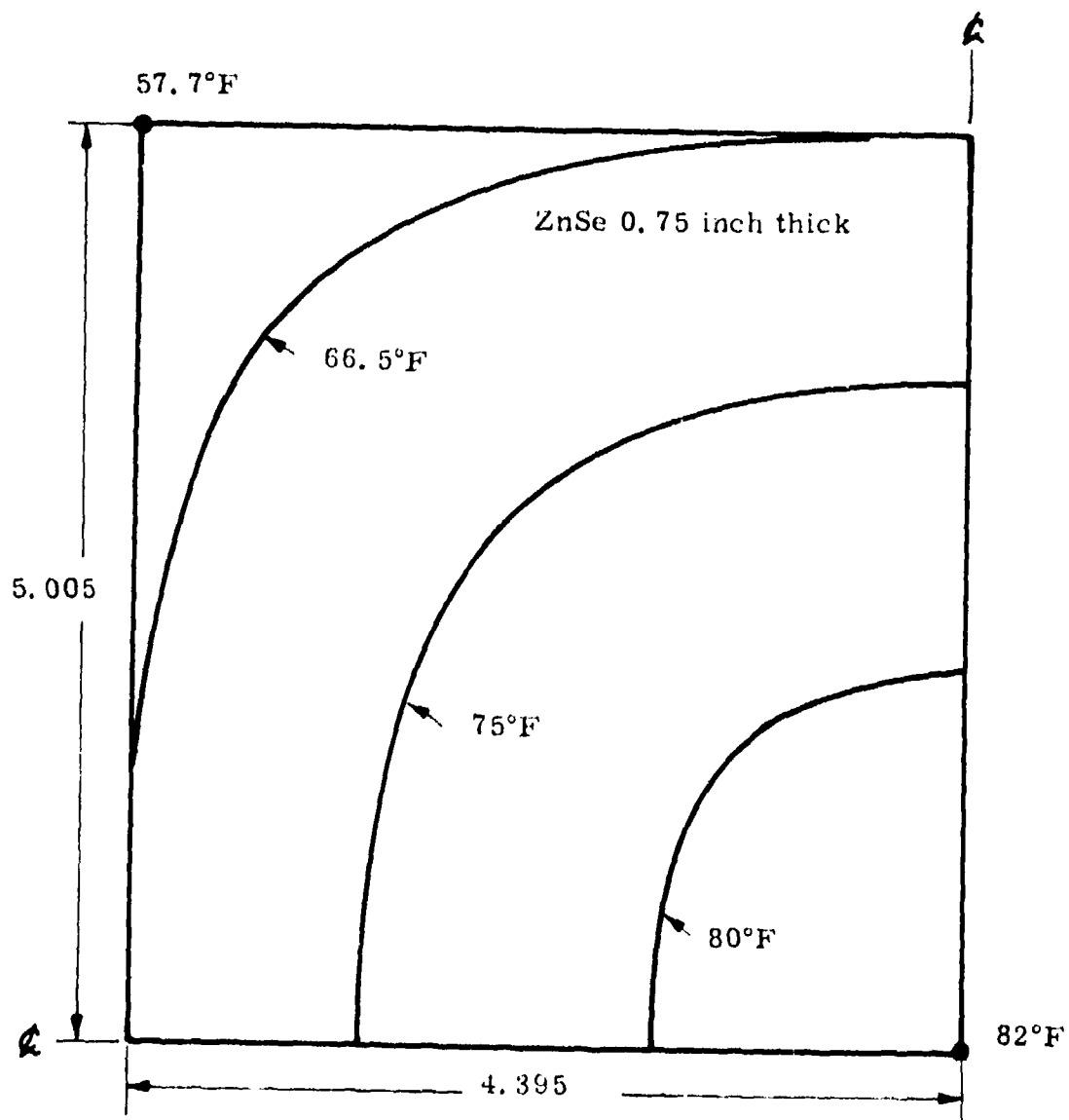


Figure 32. Temperature Gradients in Quarter Window

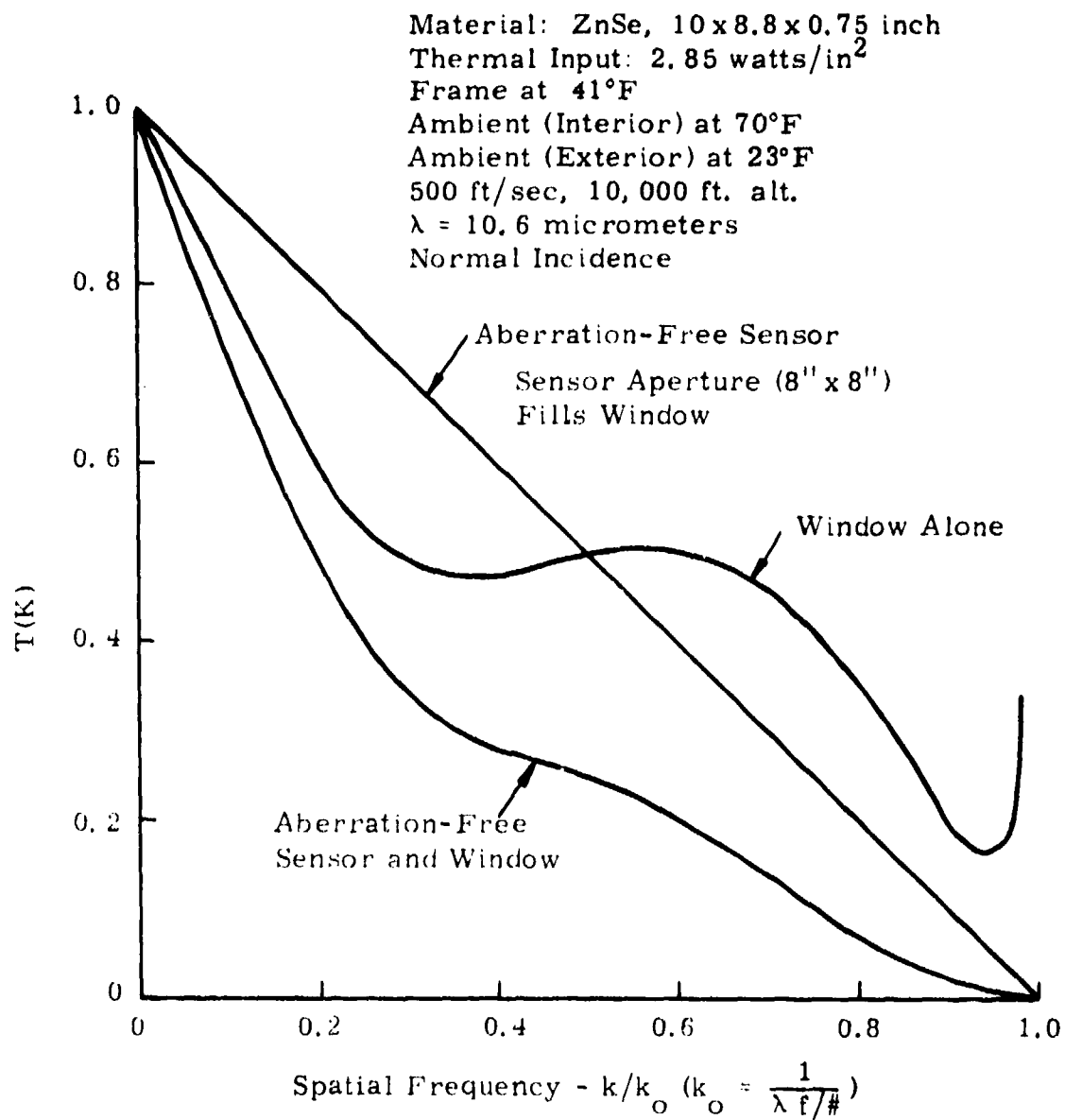


Figure 33 Loss of Performance Due to Window with Radial Temperature Gradient Resulting from Conduction of Deicing/Defogging Heat to Frame

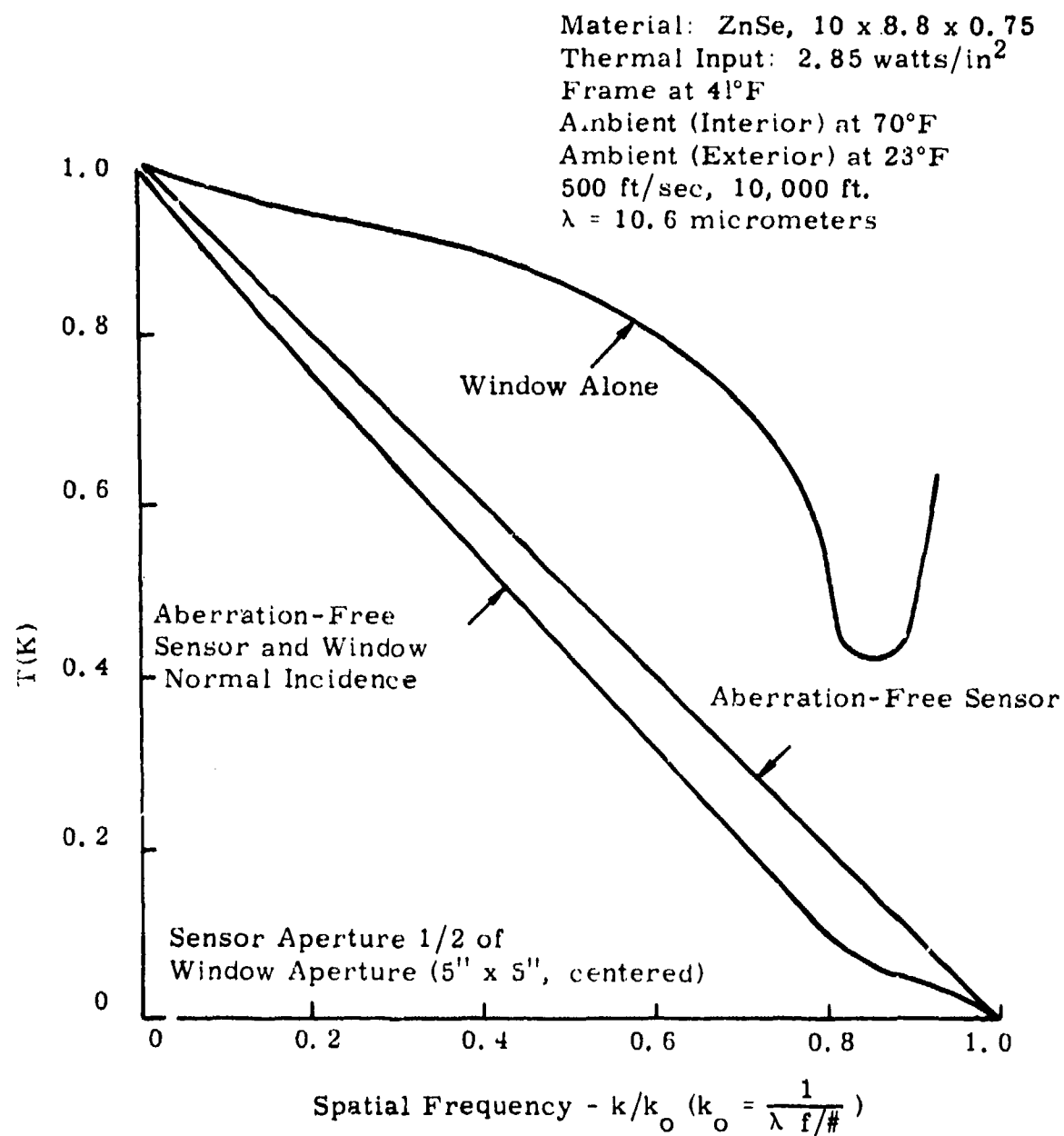


Figure 34. Loss of Performance Due to Window with Radial Temperature Gradient Resulting from Conduction of Deicing Heat to Frame

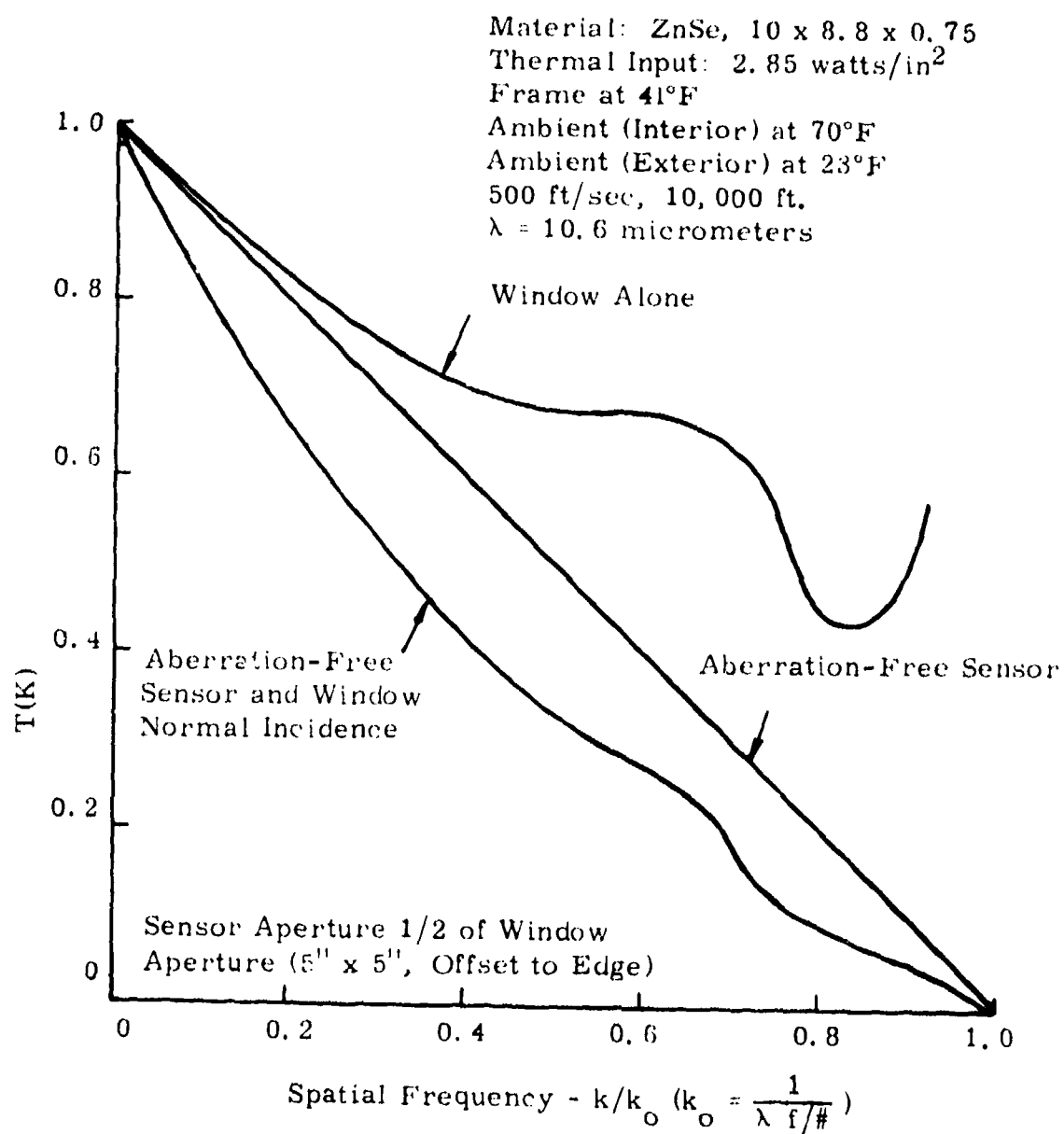


Figure 35. Loss of Performance Due to Window with Radial Temperature Gradient Resulting from Conduction of Deicing Heat to Frame

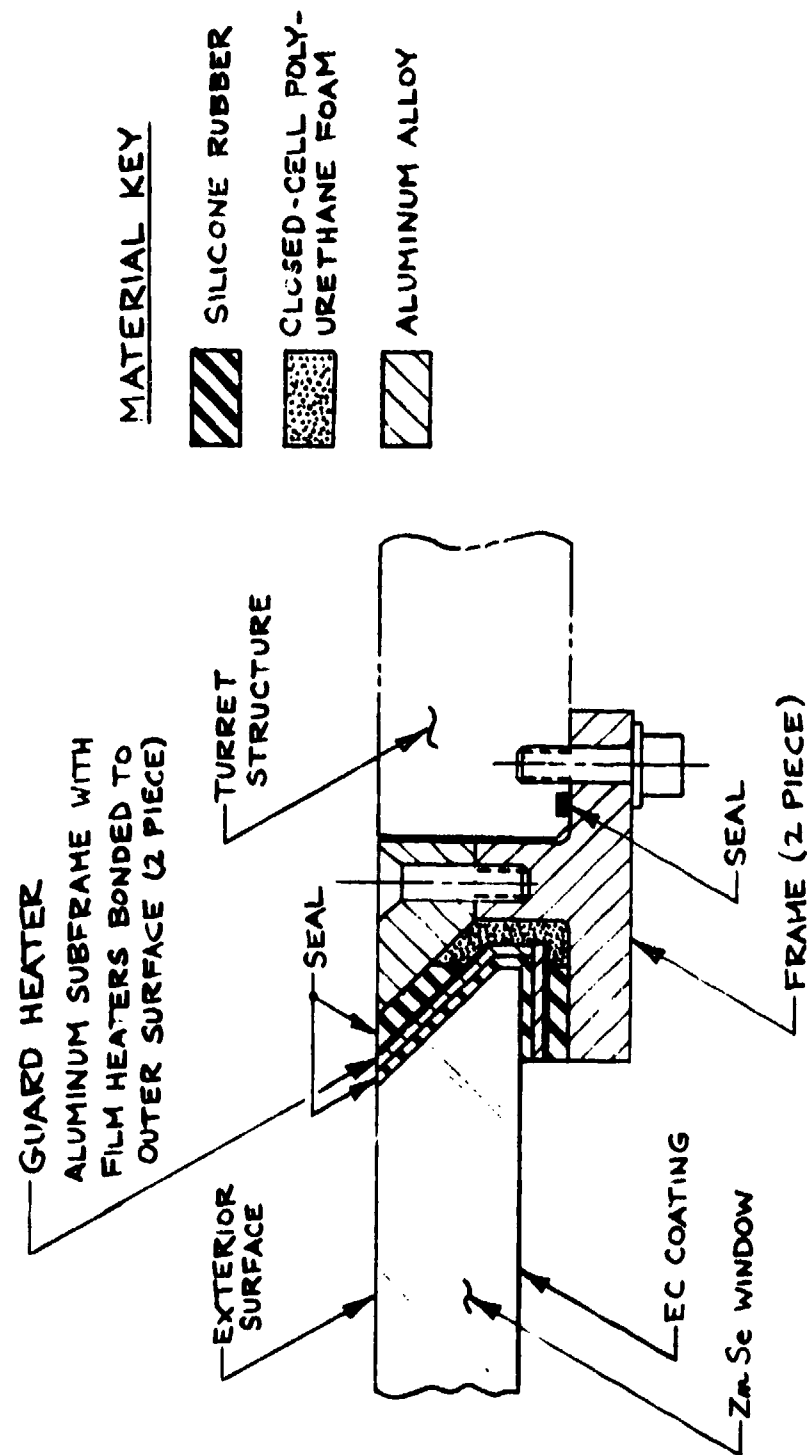


Figure 36. Insulating Window Mount Concept



- b. The use of additional narrow intermediate bus bars located within the window clear aperture to permit the use of full sheet, uniform multilayer EC coatings having higher electrical resistance than those being considered and, possibly, higher optical transmission. The additional bus bars would minimize the supply voltage requirements by reducing the path lengths for current flow.
- c. Application of low sheet resistance, semi-transparent EC coatings to the antireflection coated window in a regular pattern of parallel linear stripes.

For the first approach considered (the opaque nichrome stripes), a pattern was chosen to give the minimum clear aperture obscuration for an average power density of 4.5 watts/in<sup>2</sup>, consistent with the maximum recommended stripe power density for thin-film resistors of 50 watts/in<sup>2</sup> (Ref. 11). This pattern, which provides an overall transmission of 0.88, consists of nine 0.12-inch (3 mm) wide nichrome stripes spaced 1 inch (25.4 mm) apart and oriented parallel to the 10" window dimension, symmetrical with the window centerline. Because of the high local power density, this configuration will produce the highest temperature gradients in a given material and thus the worst case optical path differences.

The major optical effect of this arrangement is the spurious diffraction image it produces, a regularly spaced set of images displaced along a line perpendicular to the opaque conducting stripes at angles ( $\theta$ ) from the real image, where

$$\theta = \frac{m\lambda}{d}$$

with intensity ratio (with respect to the axial intensity)

$$I(\theta) = \left( \frac{s}{d-s} \right)^2 \left[ \frac{\sin\left(\frac{m\pi s}{d}\right)^2}{\left(\frac{m\pi s}{d}\right)} \right]$$

(11) Rea, S.N. and Wriston, R.S., Development of Deicing Methods for Chalcogenide Windows for Reconnaissance and Weapon Delivery", Technical Report AFAL-TR-73-340, Air Force Avionics Laboratory, Air Force Systems Command, Wright-Patterson AFB, Ohio, October, 1973, p. 9.

where

$d$  = center-to-center separation of the stripes

$s$  = width of stripes

$m$  = integer 1, 2, 3, ...

$\lambda$  = wavelength

$I(\theta)$  versus  $m$  is given in Table 11. The main effects of these diffraction images are crosstalk among the detectors in an array and extraneous signals from an out-of-field bright object.

TABLE 11. DIFFRACTED IMAGE INTENSITY

$m$	$\theta(\lambda = 10 \mu\text{m})$	$I(\theta)$
1	$4.0 \times 10^{-4}$	0.017
2	$8.0 \times 10^{-4}$	0.015
3	$1.2 \times 10^{-3}$	0.014
4	$1.6 \times 10^{-3}$	0.008
5	$2.0 \times 10^{-3}$	0.005
6	$2.4 \times 10^{-3}$	0.002

In addition to the diffracted images produced by a regular array of opaque conductors, the total diffracted energy outside of a given angle from the image of a point source is obtained from a simple formula. If  $L$  is the total length of edges in the aperture of the optical system at which diffraction can occur,  $L\lambda H$  is the total energy scattered outside a  $3^\circ$  cone, where  $H$  is the irradiance at the diffracting edges and  $\lambda$  is the wavelength of the incident radiation. The scattered energy is essentially independent of the curvature of the edges as long as it is not too great. This formula points out the necessity of utilizing a small value of  $L$  (i.e., as few conductors as possible), which suggests the second approach in its simplest form (one narrow conductor) centered on the 8.8-inch dimension and parallel to the 10-inch dimension. Obviously, diffraction effects are substantially reduced when compared with the nichrome striped pattern, which has 9 times the total edge length. The single intermediate bus bar will lower the terminal resistance by a factor of 4, allowing the use of EC coatings having sheet resistivities of  $600\Omega/\text{sq.}$  to produce a power density of  $4.5 \text{ watts/in.}^2$  with a 230 volt

supply. Furthermore, the central conductor can be grounded and the high voltage bus bars can be located, as usual, near the window frame, well shielded from accidental contact.

Another benefit of running the conductor along the horizontal dimension of the window is that it is probably the direction of scan of a potential IR sensor. If the scan is along the centerline of the window, the length of conductor seen at the focal plane will be constant over the scan. Had the conductor been placed along the other dimension of the window, the length in the field of view would vary with the frequency of the scan. In this case, any radiation emanating from the conductor because of its finite emissivity would be modulated and added to the signal instead of being averaged out as noise.

The key to the feasibility of this approach is how much of a transmission advantage the higher sheet resistance coatings (300 to 600  $\Omega$ /sq.) would have over the existing 75 to 100  $\Omega$ /sq. coatings.

Note that there is another parameter that can be varied to possibly eliminate the necessity for intermediate bus bars--the level of the supply voltage. For a given power density, doubling the sheet resistance requires  $\sqrt{2}$  times the voltage. The maximum voltage permissible, no doubt, is limited by safety considerations in addition to EMI requirements and problems with arc-over or corona, which might occur in an unpressurized or depressurized area.

A steady-state computer nodal analysis was run for the case of the opaque, striped nichrome pattern on ZnS and ZnSSe substrates to obtain a comparison with the uniform sheet coating. A summary of the results is given in Table 12 and Figure 37.

As mentioned previously, the interior surface temperatures are below the aircraft interior temperature in all cases except on or adjacent to the nichrome stripe on the ZnSSe window, even though the exterior surface temperature is high enough to prevent frosting. This condition and the excellent temperature uniformity on the exterior surface are due to the relatively high substrate conductivity.

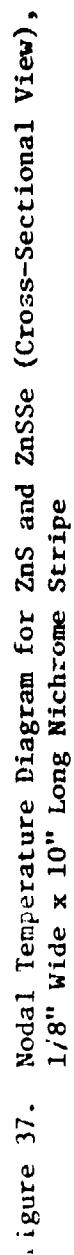


TABLE 12. TEMPERATURE DISTRIBUTION COMPARISON (0.12" WIDE NICHROME STRIPES VERSUS UNIFORM EC COATING)

Material	Interior Surface			Exterior Surface		
	Maximum Temp. (°F)	Minimum Temp. (°F)	Maximum Lateral ΔT (°F)	Maximum Temp. (°F)	Minimum Temp. (°F)	Maximum Lateral ΔT (°F)
<u>ZnS</u>						
0.12" Nichrome Stripes	59.7*	46.3**	13.4	36.2*	35.8**	0.4
Uniform Sheet	52.6	52.6	0	38.2	38.2	0
<u>ZnS<sub>Se</sub></u>						
0.12" Nichrome Stripes	83.0*	56.1**	26.9	36.1*	35.3**	0.8
Uniform Sheet	66.6	66.6	0	37.9	37.9	0

\*At center of stripe

\*\*At midpoint between stripes

Conditions: Average Power Input      4.5 watts/in<sup>2</sup>

Nichrome Stripe Power Density      50 watts/in<sup>2</sup>

Exterior Ambient Temperature      -65°F

Interior Ambient Temperature      70°F

The third approach considered, a pattern of semi-transparent stripes, would also produce diffraction effects similar to those obtained with the opaque stripes, but with somewhat lower intensities. The main problem with semi-transparent stripes is that they introduce a phase shift over the part of the aperture they cover with respect to the rest of the window. For a wavelength in the range of interest, this differential phase shift is  $\sim \pi$ , corresponding to a half-wave, resulting in a reduction of axial intensity from 1.00 to 0.89 for an EC coating having a transmission of 0.60, using the same dimensions as given for the opaque conductors. This loss of energy on-axis is redistributed among the rings of the diffraction image, corresponding to a larger blur circle. Obviously, this problem can be eliminated if the nonconducting portions of the window surface are covered with a coating having the same phase shift characteristics as the conductive coating.

Another disadvantage of semi-transparent stripes is the relatively high electrical resistance per stripe, requiring that the supply voltage be increased above 230 volts to obtain an average power density of 4.5 watts/in<sup>2</sup>. For example, if it is assumed that the minimum sheet resistance available is 75 $\Omega$ /sq., a pattern consisting of 1/2" wide stripes spaced 1" apart would give an overall transmission of 0.80 (with a coating transmission of 0.60) but would require 257.1 volts for 4.5 watts/in<sup>2</sup>, unless perpendicular intermediate bus bars were introduced.

#### 6.11 WAVEFRONT DISTORTION OF HEATER PATTERNS

Steady-state computer nodal temperature analyses were run for four different semi-transparent (Perkin-Elmer multilayer EC coating) striped window heater patterns, each producing an average power density of 4.5 watts/in<sup>2</sup> (for a total power input of 396 watts) with a pitch (spacing) of 1 inch. The window dimensions are 8.8" x 10" x 0.75" thick; material is either ZnS or ZnSe since they have similar thermal conductivities. The four configurations are as follows:

- Nine 1/2-inch wide x 10-inch long stripes, 4.4 watts/linear inch
- Ten 1/2-inch wide x 8.8-inch long stripes, 4.5 watts/linear inch

- Ten 1/4-inch wide x 8.8-inch long stripes, 4.5 watts/linear inch and also with 6 watts/linear inch (6.0 watts/in<sup>2</sup> or 528 watts total) to demonstrate the effects of higher power densities
- Ten 1/8-inch wide x 8.8-inch long stripes, 4.5 watts/linear inch

In addition, the nodal analysis for the 1/8-inch wide x 10-inch long nichrome stripe pattern was rerun for a direct comparison.

A summary of the results of these analyses is given in Table 13 and Figures 38, 39, and 40. A finer nodal network was used for these runs, thus giving slightly different (more accurate) temperatures than previously reported for the case of the 1/8" wide nichrome stripes. Note that the temperatures obtained for the 1/8" x 10" stripes are lower than those for the 1/8" x 8.8" stripes, which is due solely to the fact that the total length is somewhat greater for nine 10-inch long stripes than ten 8.8-inch long stripes, thus giving a slightly lower linear power density for the former pattern (4.4 watts/linear inch compared to 4.5 watts/linear inch).

From an inspection of Table 13 and Figures 38, 39, and 40, it is clear that, as expected, the wider stripes produce a more uniform temperature distribution. The maximum lateral temperature gradient at the upper (heated) surface ranges from a high of 16.1°F for the 1/8" x 10" stripes to a low of 6.5°F for the 1/2" x 10" stripes.

For comparison, the average transmission of each configuration, given in Table 14, was calculated based on a simple area ratio, assuming the following transmissions in the 8-12  $\mu$ m region: 0.60 for the semi-transparent EC coating, 0.95 for the antireflection coated intermediate regions (it has been assumed that this coating has the same phase shift characteristics as the EC coating), and 0.0 for the opaque nichrome stripes. The effects of diffraction caused by the regularly varying transmission perpendicular to the stripes have not been considered here. Note that the orientation of the stripes makes very little difference in the overall transmission as evidenced by the calculated values for the 1/2" wide stripes.

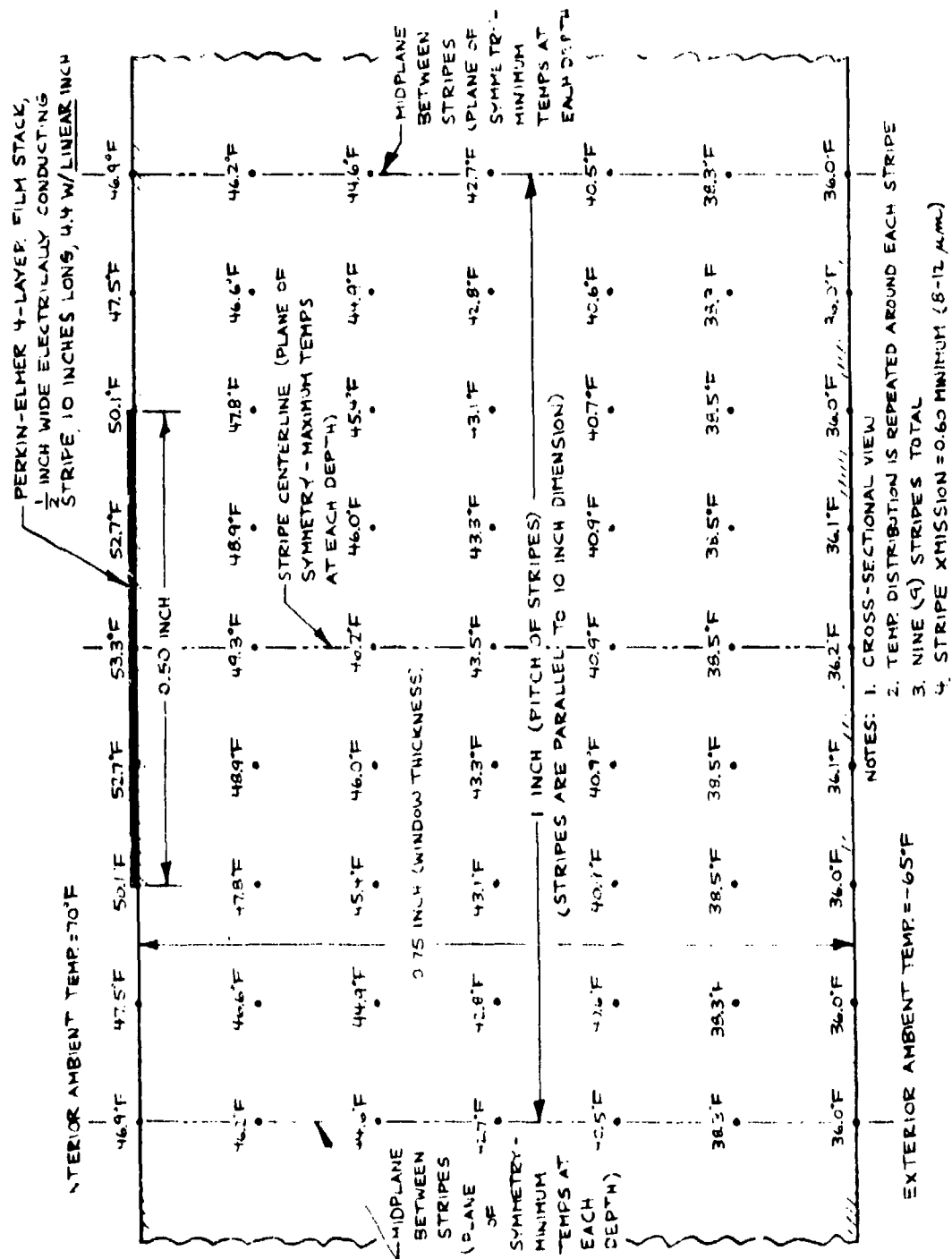


Figure 38. Nodal Temperature Diagram, ZnS or ZnSe, 8.8" x 10" x 0.75", 4.5 w/in<sup>2</sup>, 396w Total Power, 1/2-inch Wide Electrically Conducting Stripe



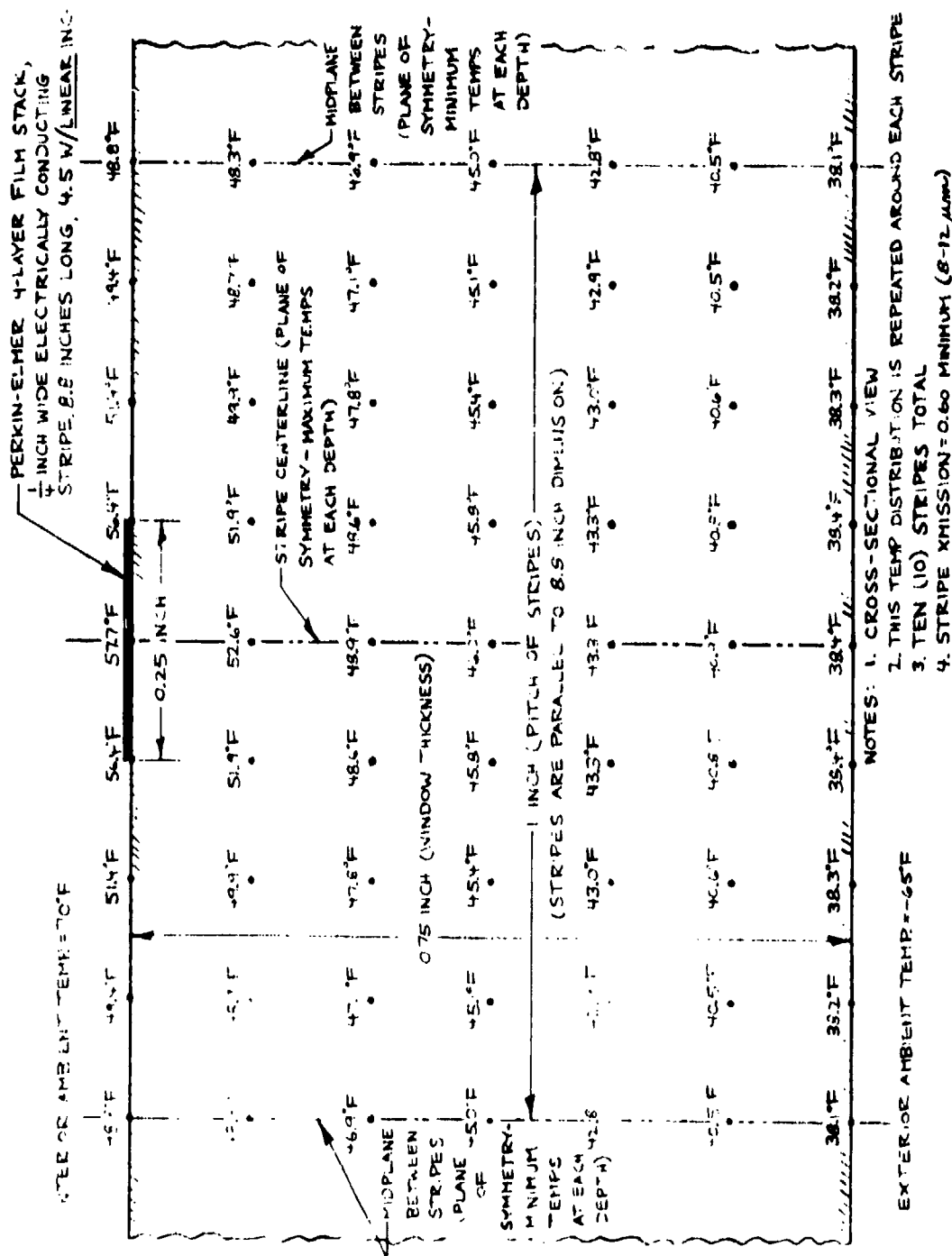




TABLE 13. TEMPERATURE DISTRIBUTION COMPARISON (SEMI-TRANSPARENT EC STRIPES OF VARIOUS WIDTHS VERSUS OPAQUE NICHROME STRIPES AND UNIFORM EC COATING)

Pattern Configuration	Zinc Sulfide or Zinc Selenide, $4.5 \frac{\text{watts}}{\text{in}^2}$ Average Power Input					
	Interior Surface			Exterior Surface		
	Maximum Temp. (°F)	Minimum Temp. (°F)	Maximum Lat. ΔT (°F)	Maximum Temp. (°F)	Minimum Temp. (°F)	Minimum Lat. ΔT (°F)
9 - 1/2" x 10" EC Stripes	53.3*	46.9**	6.5	36.2*	36.0**	0.2
9 - 1/8" x 10" Nichrome (or EC) Stripes	61.0*	45.9**	16.1	36.1*	35.8**	0.3
10 - 1/2" x 8.8" EC Stripes	55.9*	49.3**	6.6	38.4*	38.2**	0.2
10 - 1/4" x 8.8" EC Stripes	57.7*	48.8**	8.9	38.4*	38.1**	0.3
10 - 1/4" x 8.8" EC Stripes at 6.0 watts/in <sup>2</sup>	97.4*	85.6**	11.8	71.9*	71.5**	0.4
10 - 1/8" x 8.8" EC (or Nichrome) Stripes	63.9*	48.5**	15.4	38.5*	38.1**	0.4
Uniform EC Coating (For Reference)	52.6	52.6	0	38.2	38.2	0

\*At center of stripes

\*\*At midpoint between stripes

Conditions:

Exterior Ambient Temperature -65°F

Interior Ambient Temperature 70°F

TABLE 14. AVERAGE TRANSMISSION OF STRIPED WINDOW HEATER PATTERNS

Pattern Configuration	Average Transmission
9 - 1/2" x 10" EC Stripes	0.77
9 - 1/8" x 10" Nichrome Stripes	0.83
10 - 1/2" x 8.8" EC Stripes	0.78
10 - 1/4" x 3.8" EC Stripes	0.86
10 - 1/8" x 8.8" EC Stripes	0.91
Uniform EC Coating	0.60

The 1/4" x 8.8" pattern on ZnSe operating at an average power density of 4.5 watts/in<sup>2</sup> was selected for detailed optical analysis. The optical path differences (OPD's) were calculated for this configuration in 1/8" wide lateral and 1/8" thickness increments corresponding to the node spacings shown in Figure 39 using the following equation:

$$OPD = \sum_{i=0}^{i=6} t \Delta T_i \left[ \frac{dn}{dT} + (n-1)(\alpha) \right]$$

where

$t$  = thickness increment = 0.125 inch = 3.175 mm

$\Delta T_i$  = temperature differential between lateral increments

$\frac{dn}{dT}$  = temperature coefficient of the index of refraction  
for ZnSe =  $4.8 \times 10^{-5}$  1/°C (Ref. 4)

$n$  = index of refraction for ZnSe = 2.40

$\alpha$  = thermal expansion coefficient for ZnSe =  $7.2 \times 10^{-6}$   
1/°C between 270 and 290°K (26 and 62°F) (Ref. 12)

The calculated OPD values, which repeat around each stripe, are listed in Table 15. The maximum OPD of  $0.132\lambda$  satisfies the Rayleigh criterion,

(12) "Kodak Intran Infrared Optical Materials", Publication U-72, Eastman Kodak Company, Rochester, New York, 14650, September, 1971, p. 20.

TABLE 15. OPTICAL PATH DIFFERENCE DISTRIBUTION AROUND EACH STRIPE

Distance from Edge of Window (Inches)	Optical Path Difference (OPD) (Waves at 10 $\mu$ m)
0	-0.132 $\lambda$
1/8	-0.121 $\lambda$
1/4	-0.085 $\lambda$
3/8 (edge of stripe)	-0.021 $\lambda$
1/2 (center line of stripe)	0 (reference thickness)
5/8 (edge of stripe)	-0.021 $\lambda$
3/4	-0.085 $\lambda$
7/8	-0.121 $\lambda$
1 (midpoint between stripes)	-0.132 $\lambda$

which states that an OPD of less than  $0.25\lambda$  will not sensibly affect the image quality. (A similar calculation for ZnS gives a slightly higher maximum OPD of  $0.187\lambda$  still satisfying this criterion.)

The shape of the distribution curve, plotted in Figure 41, is closely approximated by the cosine function:

$$\text{OPD} = -0.066 \cos(2\pi x - 2\pi) - 0.066$$

(where  $x$  = distance divided by stripe pitch, dimensionless)

also plotted for comparison. Therefore, for purposes of this analysis, the OPD distribution was assumed to have a regular cosine variation with a peak-to-peak value of 0.13 wave (at 10  $\mu$ m) in a direction perpendicular to the stripes. This function was used to calculate the optical modulation transfer function (MTF) and point spread function (PSF) for an 8.8-inch diameter circular aperture within a window having this striped heater pattern. The Perkin-Elmer computer program OTFGEN was used to determine these two functions. The results of these runs are plotted in Figures 42 and 43.

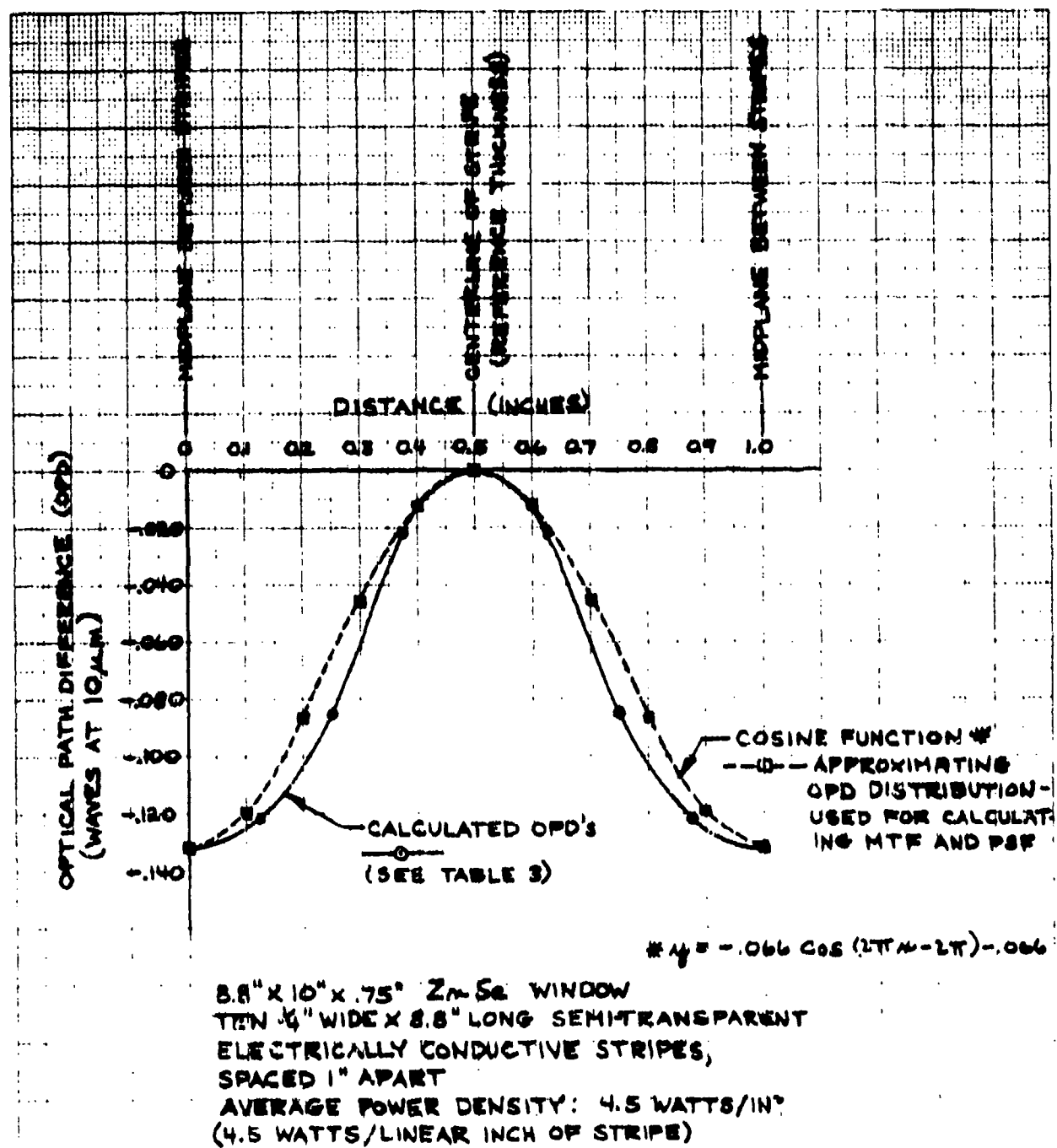


Figure 41. Distribution of Optical Path Difference Around Each Heater Stripe

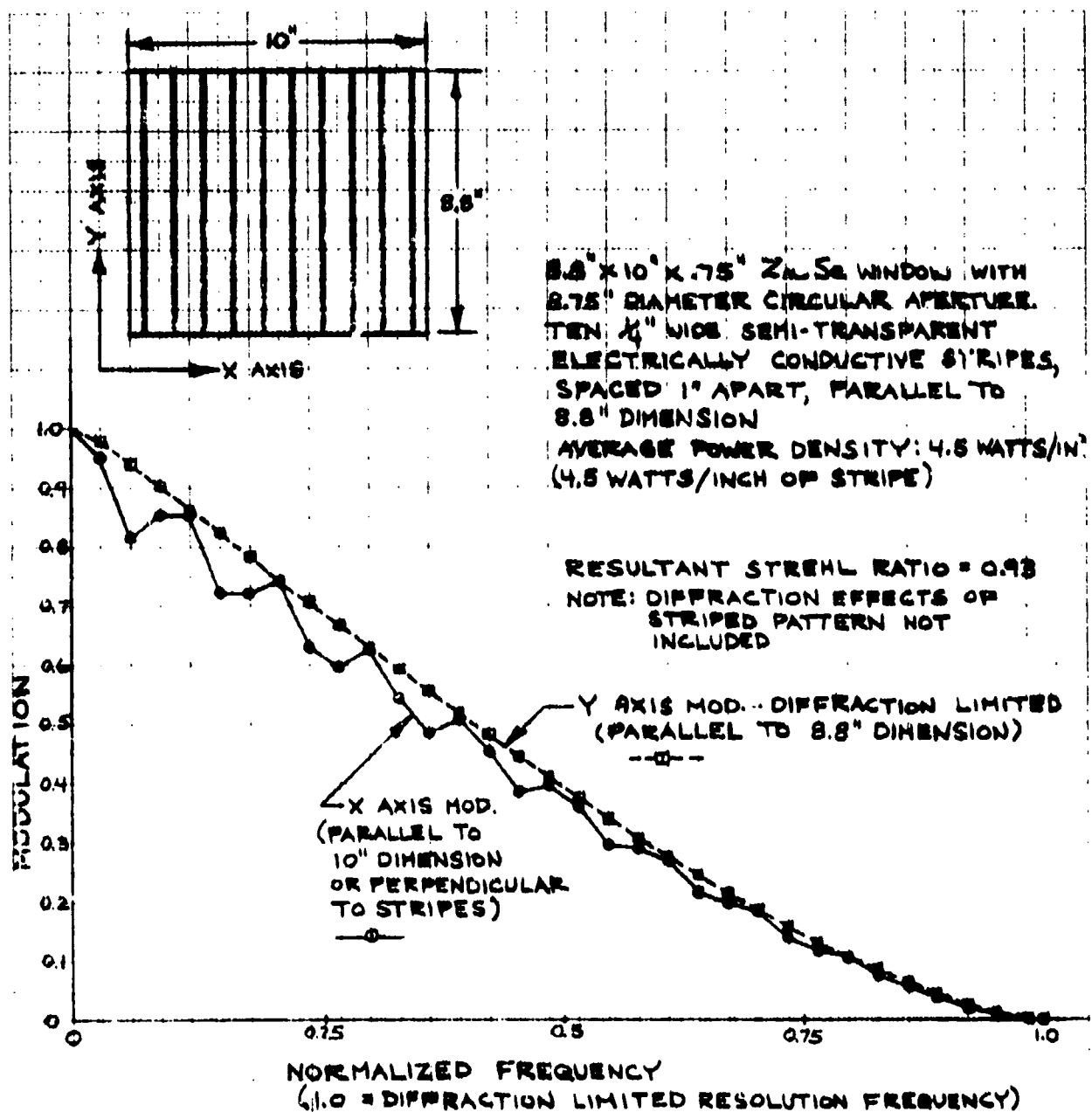


Figure 42. Affect of Thermally-Induced Optical Path Differences on Modulation Transfer Function

8.8" x 10" x .75" ZnSe WINDOW, 8.75" DIA. APERTURE  
 TEN  $\frac{1}{4}$ " WIDE x 8.8" LONG SEMI-TRANSPARENT  
 ELECTRICALLY CONDUCTIVE STRIPES,  
 SPACED 1" APART  
 AVERAGE POWER DENSITY: 4.5 WATTS/IN<sup>2</sup>  
 (4.5 WATTS/LINEAR INCH OF STRIPE)

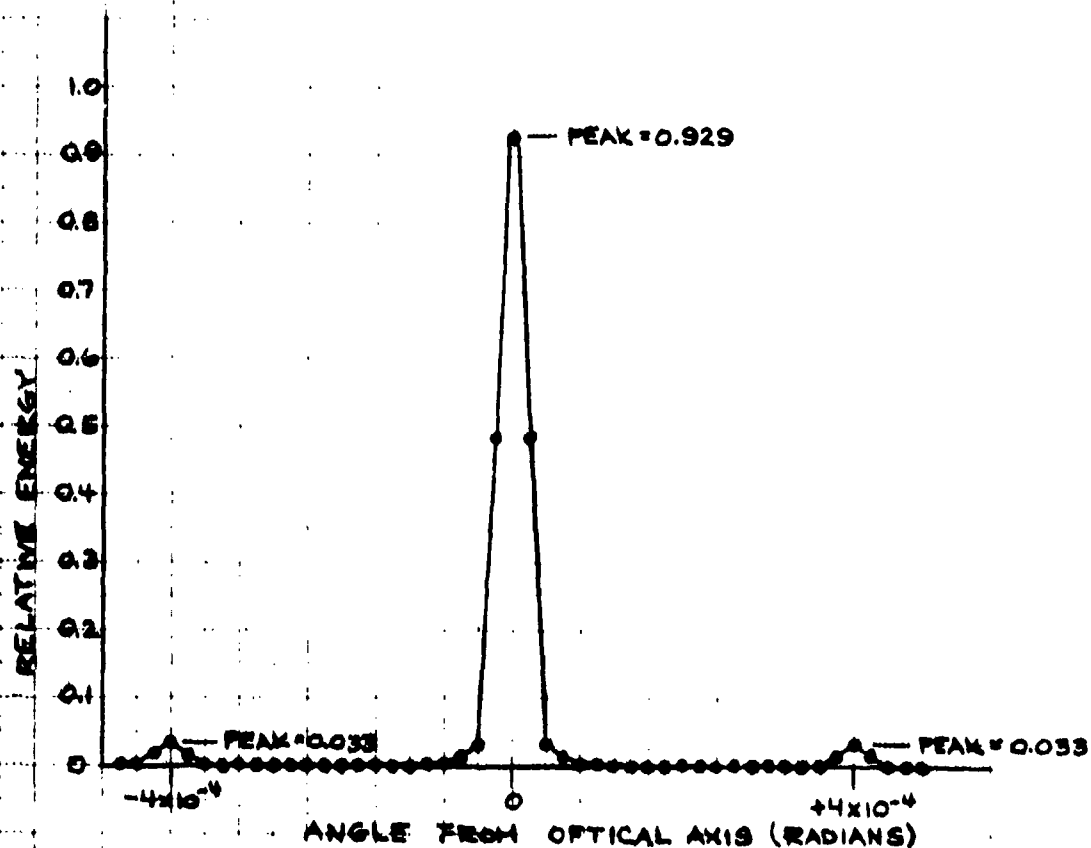


Figure 43. Thermally-Induced Point Spread Function  
 Perpendicular to Stripes (X Axis)



The shape of the resultant MTF curve in the worst case direction (perpendicular to that of the stripes) and the relatively high Strehl ratio\* of 0.93 indicate that the optical path variation across the window will not significantly degrade image quality, thereby substantiating the  $0.25\lambda$  Rayleigh criterion mentioned previously. The MTF curve for the direction parallel to the stripes, also plotted in Figure 42, is equivalent to the ideal curve for a diffraction-limited system since there is no OPD variation due to the heated stripes in that direction.

The point spread function for the thermally-induced OPD variation perpendicular to the stripes is plotted in Figure 43. Note that most of the energy is concentrated around the axis with small amounts of energy distributed in spurious diffraction images displaced  $4 \times 10^{-4}$  radian from the real image, again substantiating the small amount of degradation attributable to the heated stripes. In the direction parallel to the stripes, the energy distribution is similar with the same peak value but slightly more concentrated; however, there are no spurious diffraction images produced due to the absence of optical path variations.

With the  $1/4'' \times 8.8''$  long stripes having a minimum resistance of  $75\Omega/\text{sq.}$ , the maximum power available for a supply voltage of 230V would be only 200 watts. However, by adding a third bus bar at the center of the window perpendicular to the stripes (Figure 44), the maximum power available with the same supply voltage is increased to 802 watts--more than sufficient to produce  $4.5 \text{ watts/in}^2$ --since the effective resistance of the pattern is reduced by a factor of 4 (coating resistivity remaining at  $75\Omega/\text{sq.}$ ). Alternately, with this central bus bar, the resistivity can increase to  $152\Omega/\text{sq.}$  and still produce the desired average power density of  $4.5 \text{ watts/in}^2$ .

Thus, it can be concluded that the EC neater pattern consisting of ten equally spaced  $1/4'' \times 8.8''$  stripes with three bus bars (one centrally located) is an attractive compromise approach for significantly increasing the average transmission of heated infrared windows over that obtainable with a uniform EC coating (0.86 versus 0.60) without introducing appreciable thermal-optical degradation within the wavelength range of interest.

---

\*Ratio of the energy intensity at the peak of the diffraction pattern of an aberrated image to that at the peak of an aberration-free image (diffraction limited).

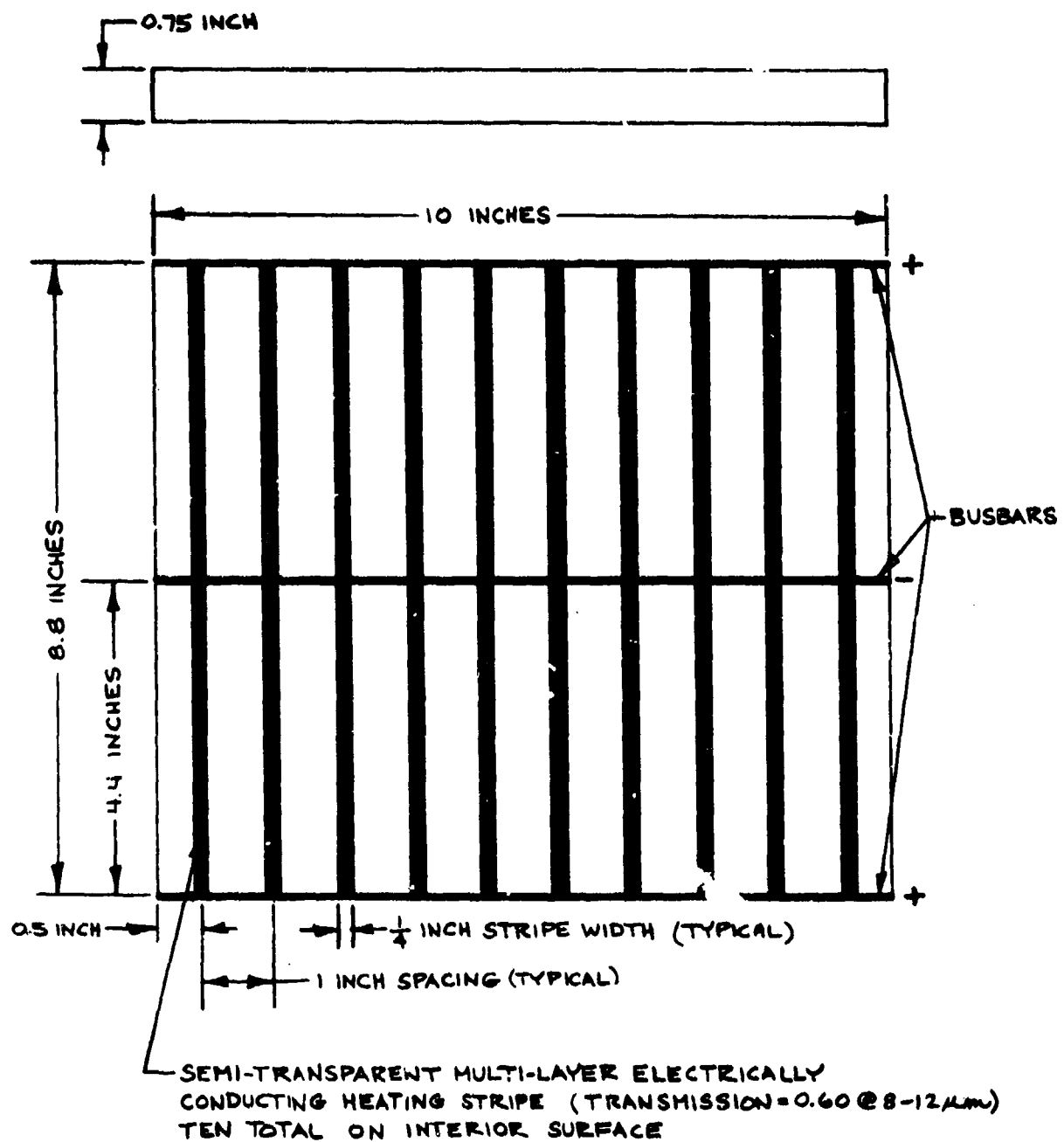


Figure 44. Striped Pattern Window Heater With Central Bus Bar

## SECTION 7

### FABRICATION AND EVALUATION OF COATED ZINC SULFIDE WINDOWS

Three ZnS windows were fabricated and coated using the designs developed during the experimental work on this program. The windows were evaluated for the following:

- MTF measurements were made before and after coating
- Transmission and reflection curves were made of one-inch diameter witness pieces at various operational temperatures
- Coating durability was evaluated on the one-inch diameter witness pieces
- Measurements were made of the thermal profile across a heated window

#### 7.1 FABRICATION OF TEST FIXTURES

A test fixture was designed and fabricated to measure the transmission of the one-inch diameter witness pieces at 0°F, ambient temperature, and 120°F. Figure 45 shows the detailed drawing of this fixture.

A second fixture was designed and fabricated to hold a window in the "cold box" to perform a thermal profile of a heated window under operational condition. Figure 46 shows the detailed drawing of the housing.

#### 7.2 FABRICATION OF WINDOWS

Six ZnS windows 4.0" x 3.5" x 0.3" were fabricated and the best three were chosen to be fully coated and were used to evaluate the design concept. The coating design used for conductive antireflective coating is shown in Table 3 and the coating design for the antireflection coating is shown in Figure 19.

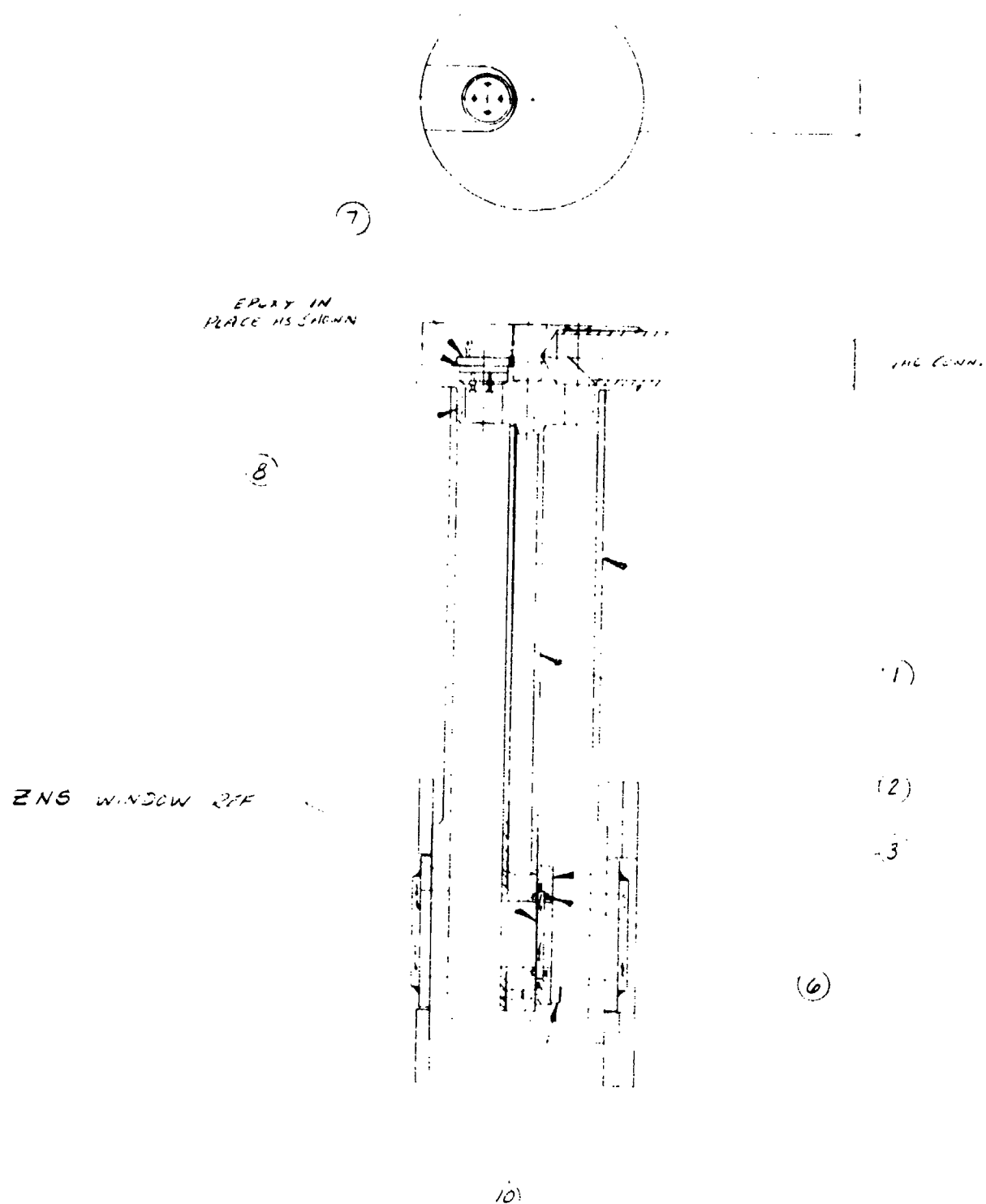


Figure 45. Thermal Vacuum Chamber



## 7.3 EVALUATION OF ZnS WINDOWS

### 7.3.1 MTF Measurements

MTF measurements were made by Texas Instruments on two windows (P/N 610-5457-2 and P/N 610-5457-6) before and after coating. The data received from Texas Instruments are given in Appendix A for before coating and in Appendix B for after coating.

Table 16 compares the before and after coating MTF values at 10 lp/mm and 20 lp/mm. Also given is the effective MTF of the coating only. Since there is a limited range of lp/mm, the image spread function cannot be calculated. The image spoiling effects due to the coating must be inferred by the MTF coating-only data at single frequencies (lp/mm).

TABLE 16. MTF MEASUREMENTS

S/N	Orientation	10 lp/mm MTF			20 lp/mm MTF		
		Before Coating	After Coating	Coating Only	Before Coating	After Coating	Coating Only
610-5457-6	0°	0.979	0.973	0.994	0.947	0.900	0.950
610-5457-6	90°	0.955	0.975	1.021	0.893	0.972	1.089
610-5457-2	0°	0.972	0.973	1.001	0.949	0.955	1.006
610-5457-2	0°	0.972	0.992	0.999	0.922	1.043	1.123

Bob Crossland (Texas Instruments) stated that all existing FLIR systems are limited to frequencies of less than 20 lp/mm because of their short focal lengths (3 to 20 inches) and detector size. Since the MTF measurements are reproducible to  $\pm 0.02$ , the change in the MTF due to the coatings was not measurable. The apparent increase of the coating-only MTF is due to the use of a narrower bandpass filter to define the in-band transmission region. Therefore, any image spoiling effects will be caused by temperature gradients across the window and must be controlled by using appropriate mounting techniques and edge heaters.

### 7.3.2 Optical Performance of Coated Witness Pieces

One-inch diameter witness pieces, coated with the window, were evaluated for spectral performance. Table 17 lists the types of spectral measurement,

conditions under which the measurement was made, and the corresponding figure numbers. The following summarizes the results of these measurements:

- The transmission of the coatings remains unchanged from 0°F to 120°F
- The average transmission for the three windows is 68% in the 8 to 11 micron region
- The average reflectance for the three windows is 6% in the 8 to 11 micron region
- The peak transmission is 72% at approximately 9.5 microns

### 7.3.3 Coating Durability

One witness piece from each coating run was evaluated for coating durability. Table 18 summarizes the test method and results.

### 7.3.4 Measurement of the Thermal Profile Across a Heated Window

Bus bars were soldered to the window along the two four-inch sides of the window and were mounted in the test fixture shown in Figure 46 using RTV. Eight thermocouples were attached onto conductive coatings (inside the box). The position of the thermocouples and recorded temperatures at steady-state are shown in Figure 56. Three thermocouples were attached to the external surface (antireflection coating). The positions and recorded temperatures at steady state are shown in Figure 57. A small piece of plastic foam was placed over these thermocouples to insure that the temperature readings were of the window surface and not the cold air stream.

The fully instrumented package was placed in a cold box at an angle of 45° to the air stream. At the steady-state condition, the following parameters were recorded:

- Cold air temperature = 0°F
- Air velocity, 5850 feet per minute
- Window was drawing 107 watts (107 volts and 1 amp)
- Power dissipation approximately 8.9 watts/in<sup>2</sup>
- Starting from ambient conditions, the steady-state condition is reached in thirty minutes

TABLE 17. OPTICAL PERFORMANCE

P/N	Measurement	Conditions	Figure No.
610-5457-1	Transmission	70.8°F	47
610-5457-1	Reflectance	Ambient	48
610-5457-1	Transmission	0°F & 120°F	49
610-5457-6	Transmission	70.0°F	50
610-5457-6	Reflection	Ambient	51
610-5457-6	Transmission	0°F & 120°F	52
610-5457-2	Transmission	69.0°F	53
610-5457-2	Reflection	Ambient	54
610-5457-2	Transmission	0°F & 120°F	55

TABLE 18. COATING DURABILITY

Test	Antireflection Coating	Conductive Coating
Washing	Passed	Passed
Scotch-Tape Test per MIL-M-13508B	Passed	Passed
Abrasion Test per MIL-M-13508B	Passed	Passed
Abrasion Test per MIL-C-675A	Passed	Failed
Humidity Test per MIL-C-675A	Passed	Passed





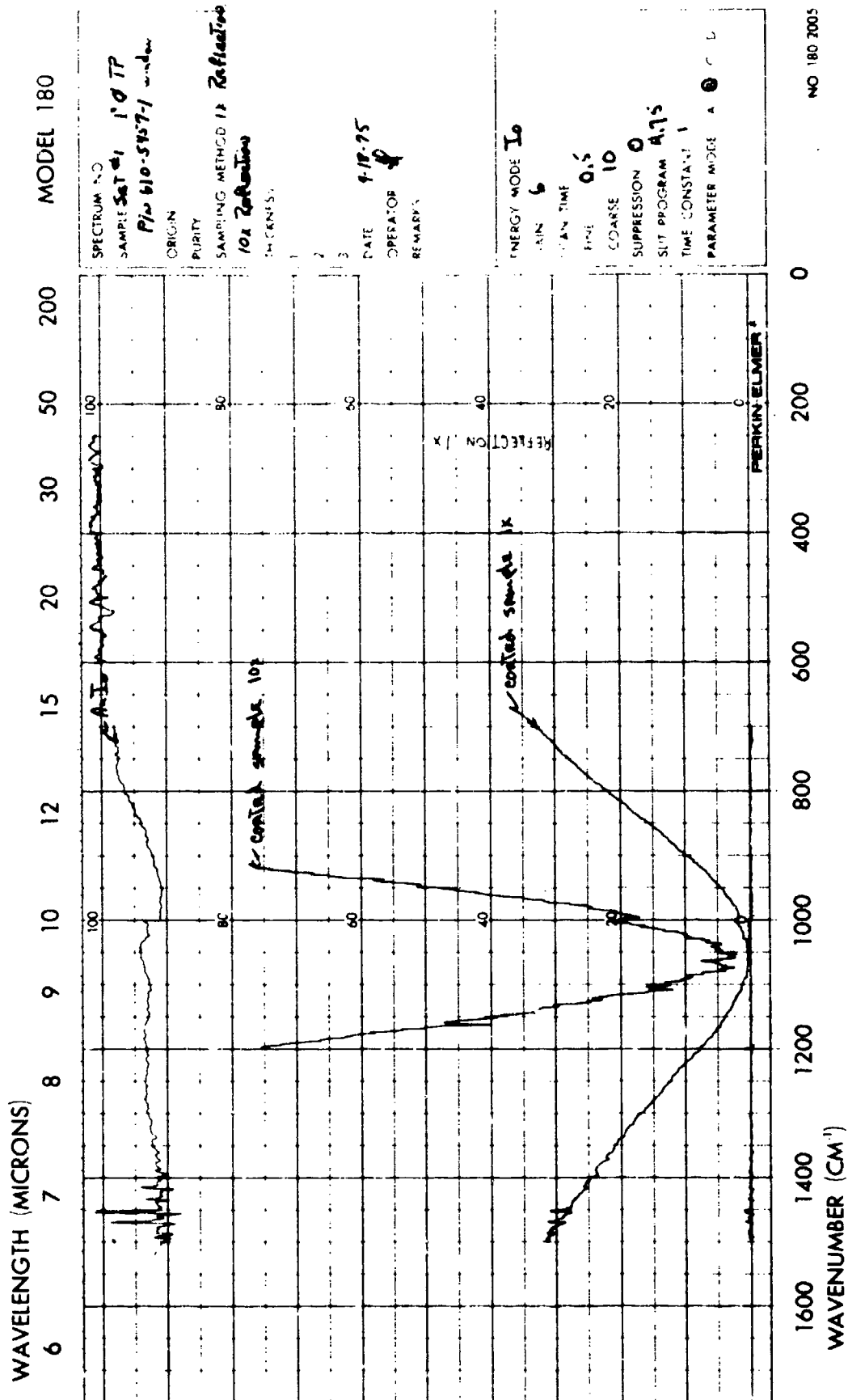


Figure 48. Spectral Performance at Ambient





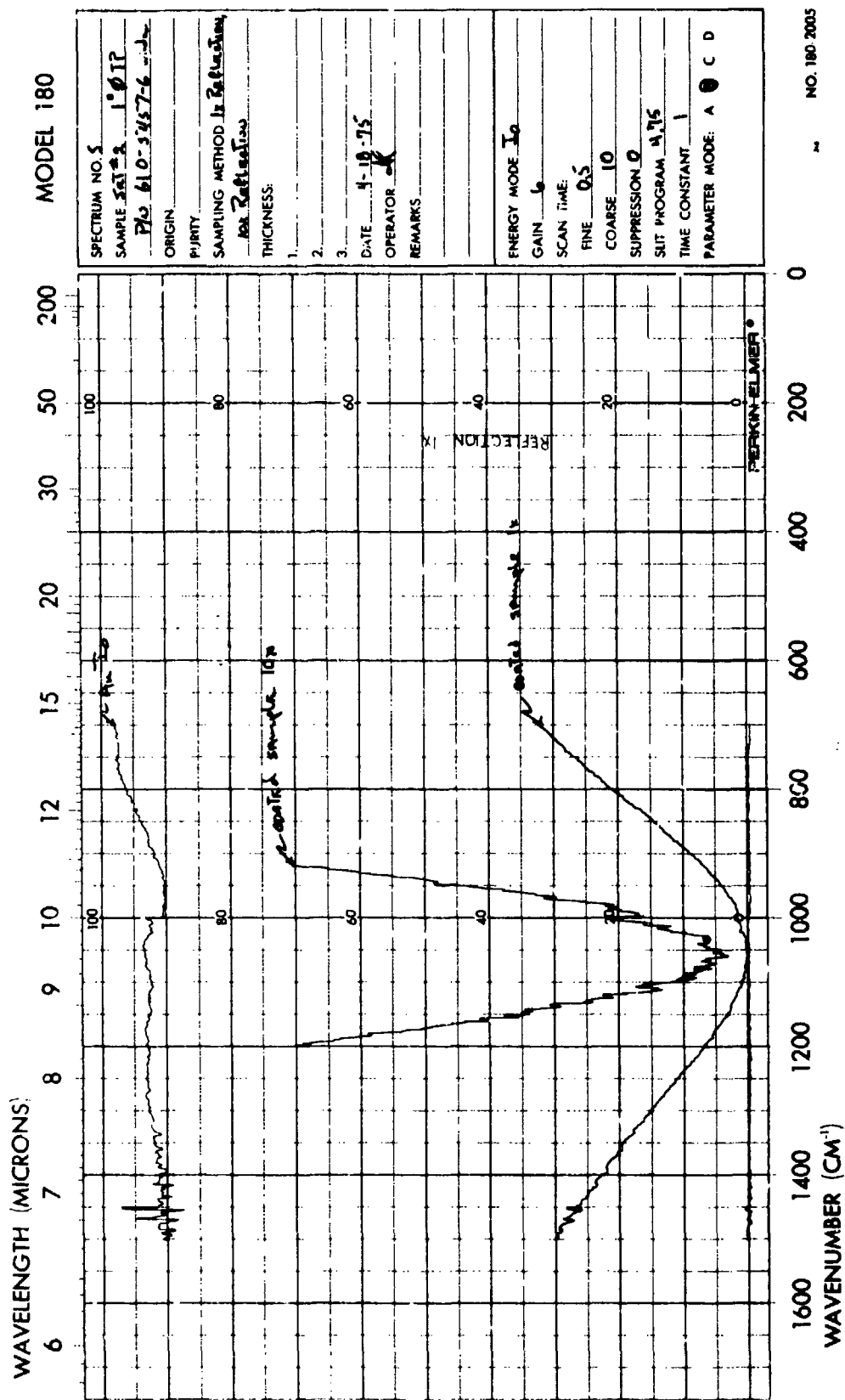


Figure 51. Spectral Performance at Ambient

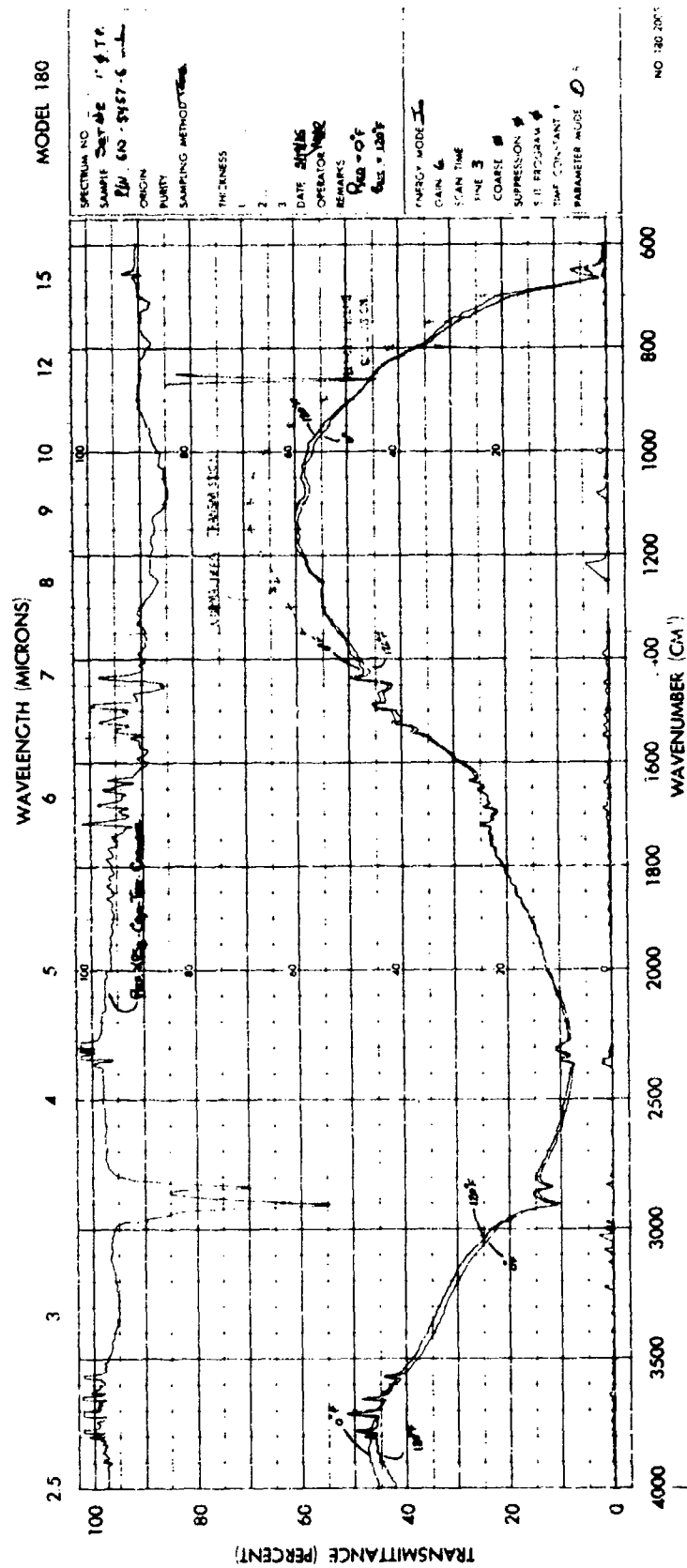


Figure 52. Spectral Performance at 0°F and 120°F









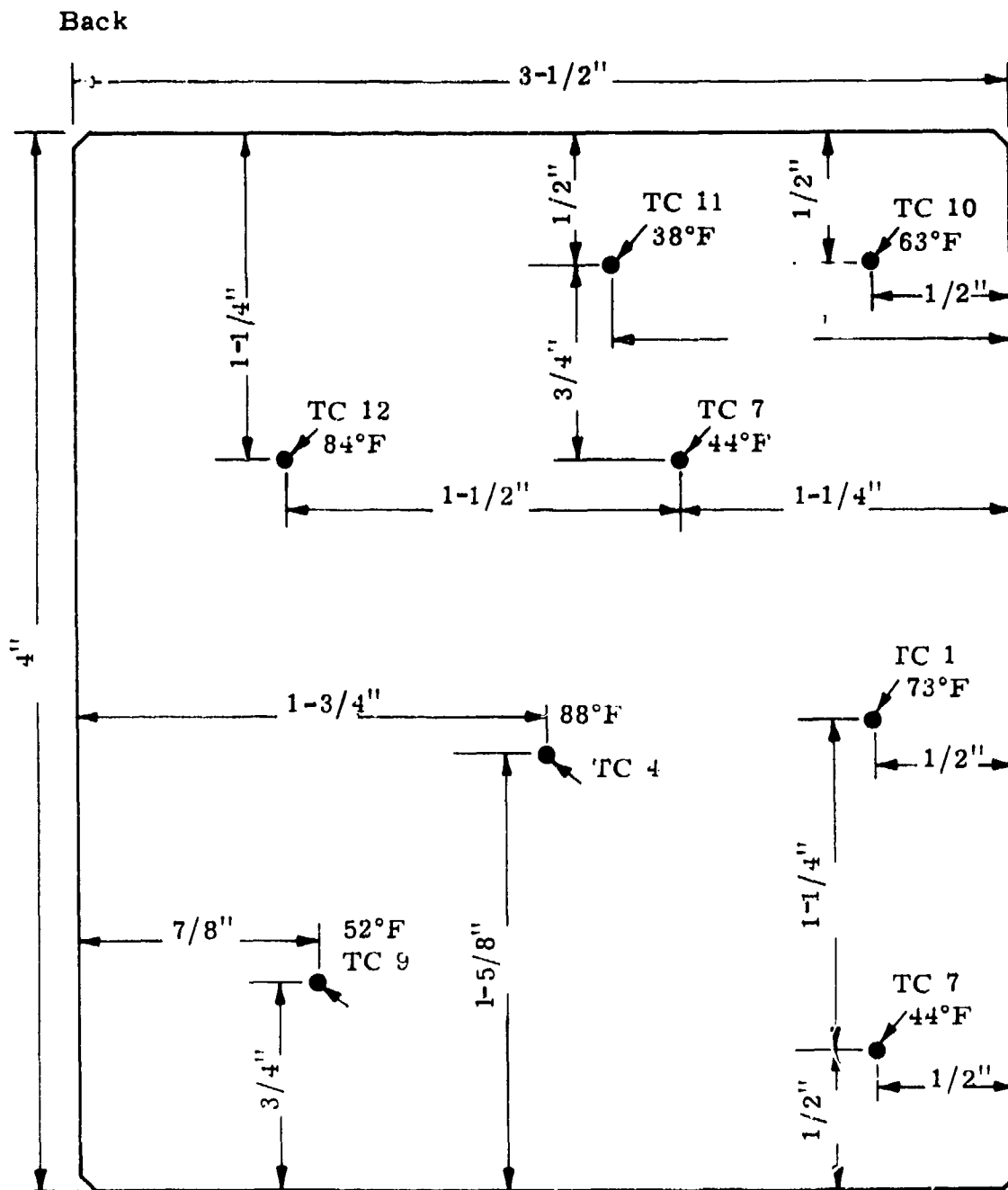


Figure 56. Positions and Recorded Temperatures of Thermocouples on Heated Window Conductive Coating

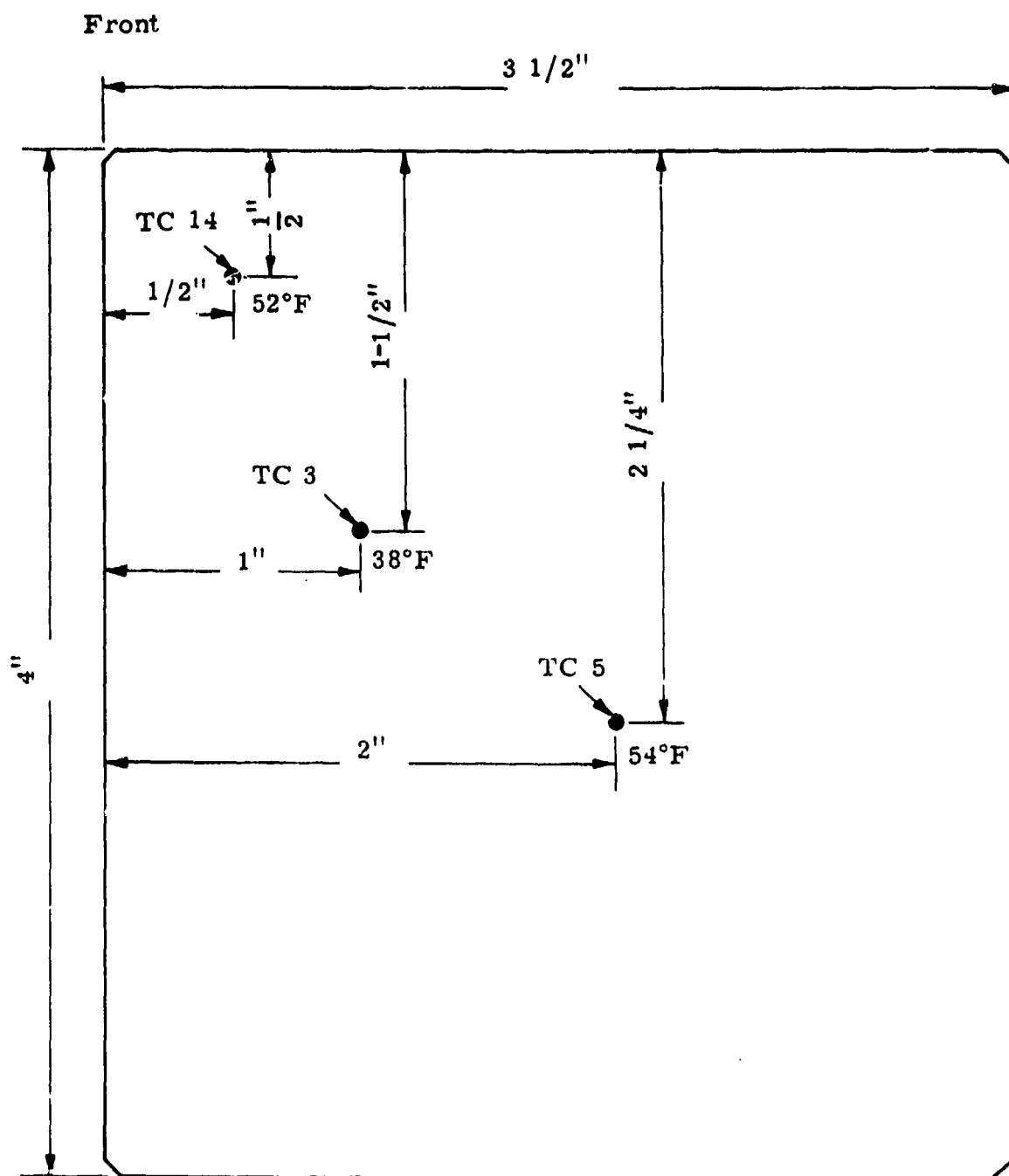


Figure 57. Positions and Recorded Temperatures of Thermocouples on Heated Window Antireflection Coating

- The minimum temperature on the outer surface was 38°F (35°F is the B-1 specification) with a gradient of 16°F
- The inside temperature of the enclosure was 34°F (in use, this temperature will be 70°F)

The results of the thermal profile test indicate that, as expected, special techniques for eliminating edge effects must be incorporated into the mounting design and the power dissipation spec MIL-T-5842A and minimum external temperature can be achieved.

## SECTION 8

### CONCLUSIONS AND RECOMMENDATIONS

#### 8.1 TRANSMISSION VALUES

The work performed under this contract clearly indicates the feasibility of producing transparent, continuous thin-film heaters for the 8 to 11.5  $\mu$  spectral region. While the transmission of 72 percent of the demonstration windows does not compare with the spectacularly high values now achievable at visible frequencies, where the conductive films are essentially nonabsorbing, it is clearly well in excess of any value that might have been expected on a less than detailed examination of the transmission values of the indium-tin-oxide films alone. The value, in fact, falls less than 10 percent short of what used to be considered high for visible region transparent films before these values were increased by the use of multilayer interference filter techniques.

It is unfortunate that it was not possible to realize the slightly higher theoretically predicted values within the scope and funding of the contract; however, we believe that analysis of the experimental work clearly shows in which areas will further experimental work lead to transmission gains. Certainly, the sandwich-type chalcogenide windows currently being considered for FLIR systems would make the film system design problem simple in theory and in practice, as well as increasing the transmission potentially available.

#### 8.2 COATINGS FOR IRREGULAR SHAPED WINDOWS

The degradation of the transmitted wavefront through the test window, following the application of the programmed nonuniform coating and the subsequent correction of that value following the application of the compensating film, clearly indicates that the layers were deposited in the appropriate programmed nonuniform thickness.

The thermal measurements show that the nonuniform coating created a significantly more equal temperature distribution over the window. Special techniques for eliminating edge effects must be incorporated into a mounting design if greater temperatures uniformity is desired.

### 8.3 FOLLOW-ON INVESTIGATIONS

Despite the appearance of some negative results during the course of the investigation, we believe that there were more than sufficient positive results to justify further investigation in certain areas. In particular, a more careful study should be implemented of the relationship between the optical constants  $n$  and  $k$  and the substrate or the film on which they are deposited. Results of this effort should be used to feed a design study to improve transparency of the film system to the values that were theoretically predicted and to incorporate conductive films in designs for common aperture systems. A study of single wavelength designs that might be used for EMI suppression in narrow-band devices would be worthwhile. The nonuniform resistance coating technique for the control of window temperature uniformity should be continued on more complex geometries.

## REFERENCES

- (1) Glacier Program, Perkin-Elmer Report No. 11200.
- (2) Caren, R.P., Funai, A.I. Frye, W.E. and Sklensky, A.F., "Properties of Infrared Sensor Materials", Materials Research and Standards, MTRSA, Volume 11, No. 6, June, 1971, p. 10.
- (3) Technical Report AFAL-TR-73-252, "Chemical Vapor Deposition of Multi-spectral windows", Air Force Avionics Laboratory, Wright Patterson Air Force Base, July, 1973, pp. 29, 30.
- (4) "Raytran ZnSe", Raytheon Data Sheet, Raytheon Research Division, 28 Seyon Street, Waltham, Massachusetts, 02154.
- (5) Telecon, James Pappis, Raytheon with E.A. Strouse, Perkin-Elmer, December 1974, re: Recent CVD ZnSe Data.
- (6) Letter, James Pappis, Raytheon to E.A. Strouse, Perkin-Elmer, June 28, 1973, re: Properties of CVD ZnS, ZnSe and ZnSSe.
- (7) Specification No. L330C2001-1, Rockwell International, B-1 Division, p. 3.
- (8) Military Specification MIL-T-5842A, "Transparent Areas, Anti-Icing, Defrosting and Defogging Systems, General Specification for", September, 1950.
- (9) Timoshenko, S. and Woinowsky-Krieger, S., "Theory of Plates and Shells", McGraw-Hill, 1959.
- (10) Telecon, Phil Mueller and Ron Brigstorke of Boeing to E.A. Strouse, Perkin-Elmer, July 1973, re: B-1 Flight Parameters.
- (11) Rea, S.N. and Wriston, R.S., "Development of Deicing Methods for Chalcogenide Windows for Reconnaissance and Weapon Delivery", Technical Report AFAL-TR-73-340, Air Force Avionics Laboratory, Air Force Systems Command, Wright-Patterson AFB, Ohio, October, 1973, p. 9.
- (12) "Kodak Irtran Infrared Optical Materials", Publication U-72, Eastman Kodak Company, Rochester, New York, 14650, September, 1971, p. 20.

APPENDIX A

OPTICAL TEST DATA FOR UNCOATED ZINC SULFIDE WINDOWS





# TEXAS INSTRUMENTS

INCORPORATED

POST OFFICE BOX 6015 • DALLAS TEXAS 75222

Equipment Group

5 December 1974

In reply refer to:  
230-83-1548  
Mail Station 209

The Perkin-Elmer Corporation  
Electro-Optical Division  
Norwalk, CT 06856

ATTENTION Mr. W. Schilling  
Purchasing

SUBJECT Optical Test Data for  
Uncoated Zinc Sulfide Windows

REFERENCE (a) Perkin-Elmer Purchase  
Order 86028 OS

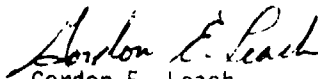
ENCLOSURE (1) Technical Description of  
Optical Test Results of  
Uncoated Zinc Sulfide Windows  
(1 copy)

Gentlemen:

Texas Instruments takes this opportunity to submit enclosure (1) in response to item 1.0 of the reference (a) purchase order. The customer furnished windows were shipped under separate cover on 27 November 1974. Enclosure (1), with its 4 figures and 6 data runs, represents a synopsis of the test data obtained.

If we may be of further assistance or answer your questions on this information, please contact Mr. Bob Crossland at area code 214, 238-4233.

Very truly yours,

  
Gordon E. Leach  
Contract Negotiator

GEL/sr

Enclosure (1) to TI  
Letter 230-83-1548  
Dated 5 December 1974

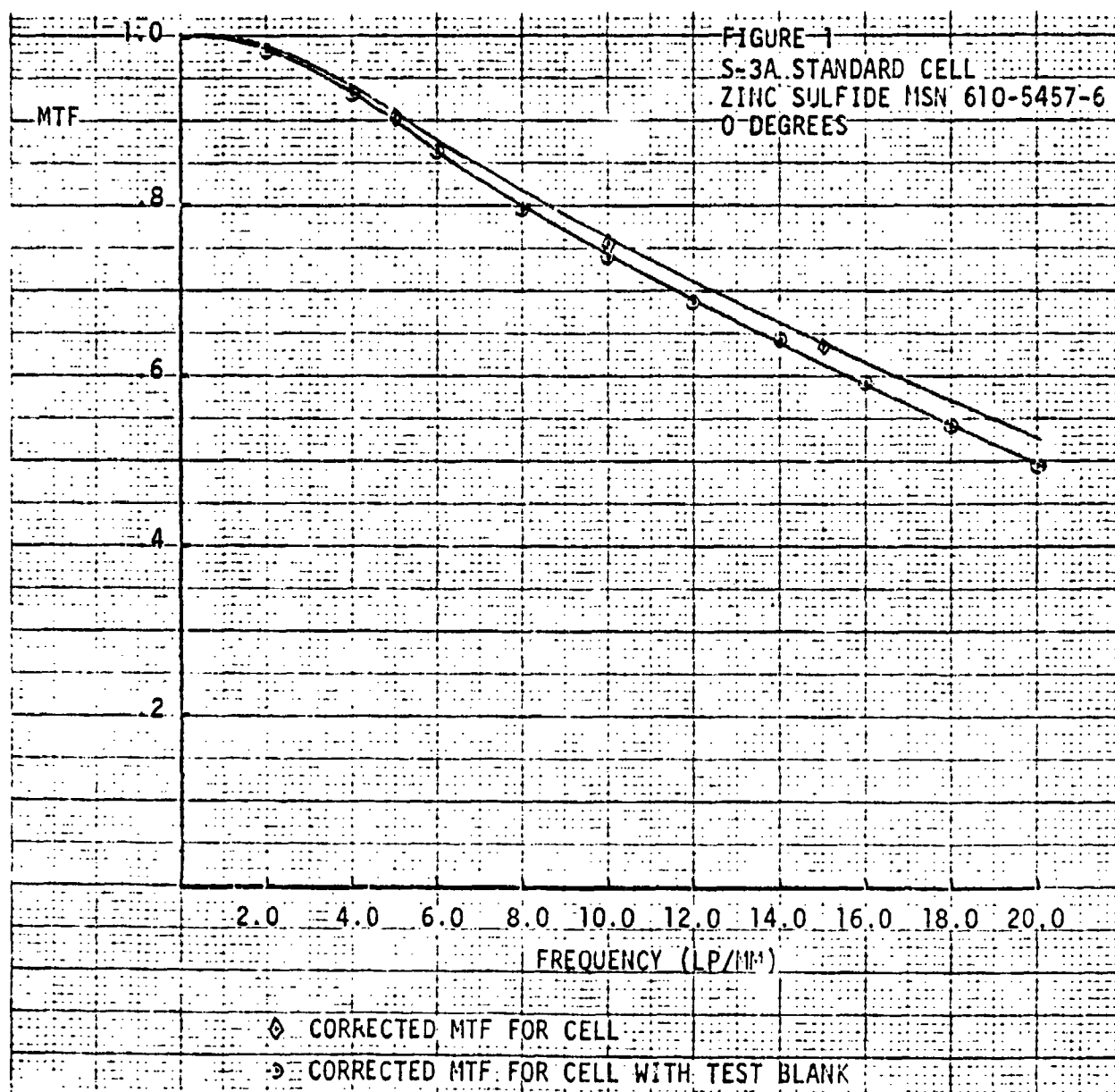
TECHNICAL DESCRIPTION OF OPTICAL  
TEST RESULTS OF UNCOATED ZINC SULFIDE WINDOWS

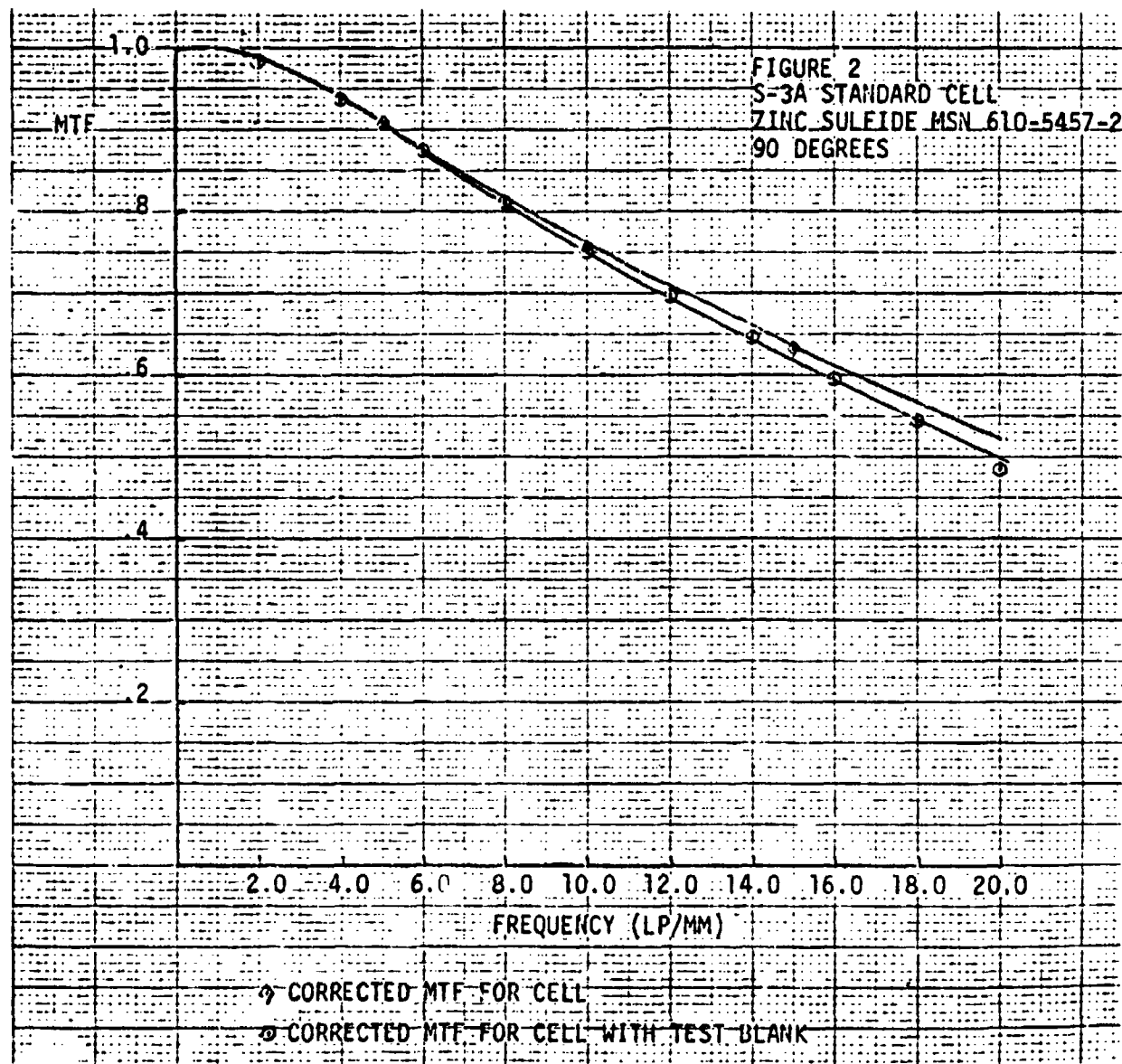
The following is a synopsis of Texas Instruments Image Evaluation Laboratory testing of two Zinc Sulfide optical blanks (Perkin-Elmer serial numbers 610-5457-2 and 610-5457-6). The following aspects are pertinent to the test setup:

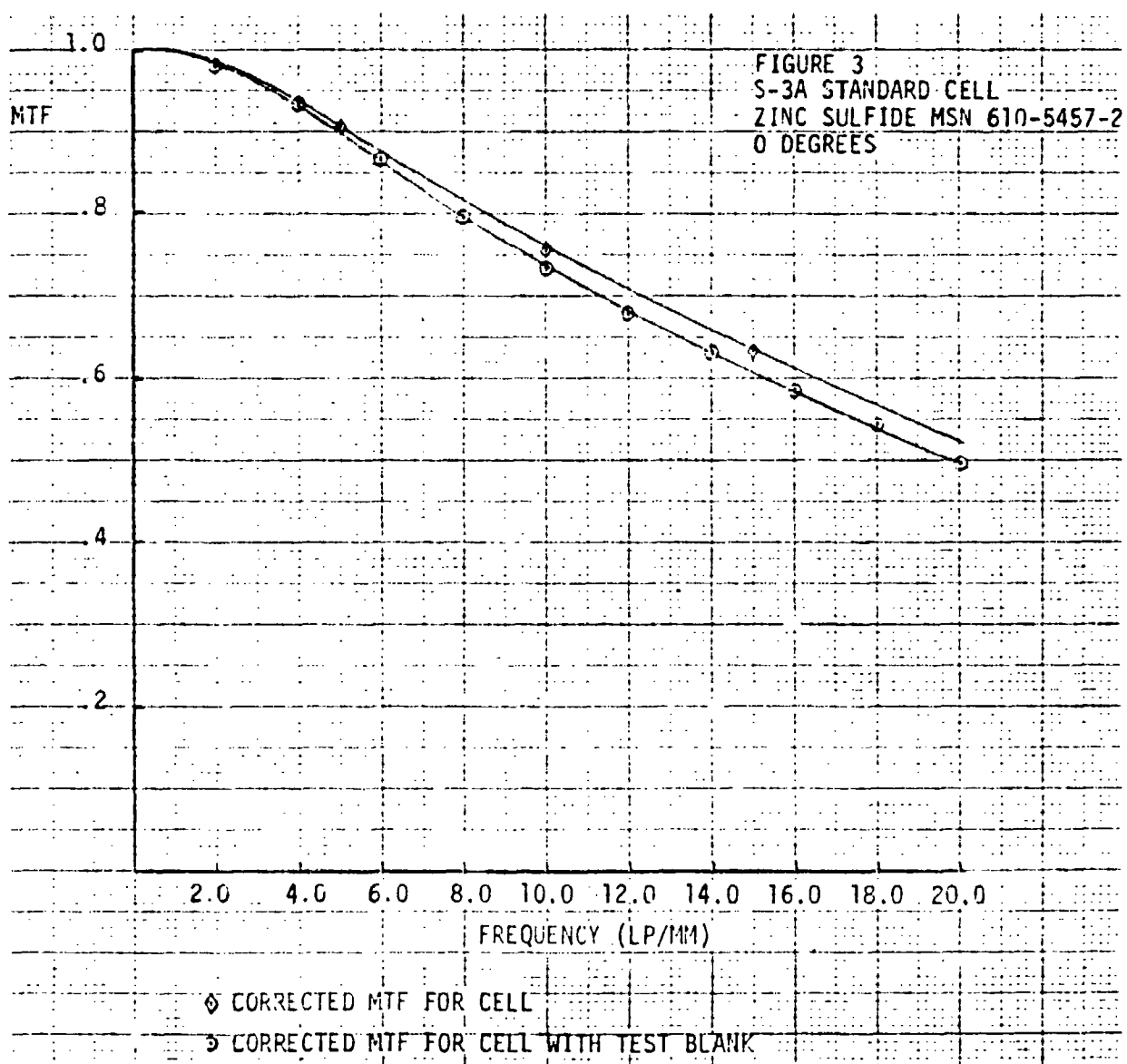
1. The test was conducted with the S-3A standard cell which was designed for 2.0 cycles/milliradian.
2. An aperture of 3.25 inches square was placed over the cell and defined the area tested in each blank.
3. Knife orientation was vertical for all scans.
4. 0° orientation of the blank was defined when the long dimension of the blank was vertical.
5. 90° orientation of the blank was defined when the long dimension of the blank was horizontal.
6. The bandpass filter used for these tests has 50% absolute transmission points located at 7.72 and 11.88 microns which define the in-band transmission region.
7. A focal series was conducted after introducing the blank in front of the standard cell to remove any effects of power or tilt in the surfaces.

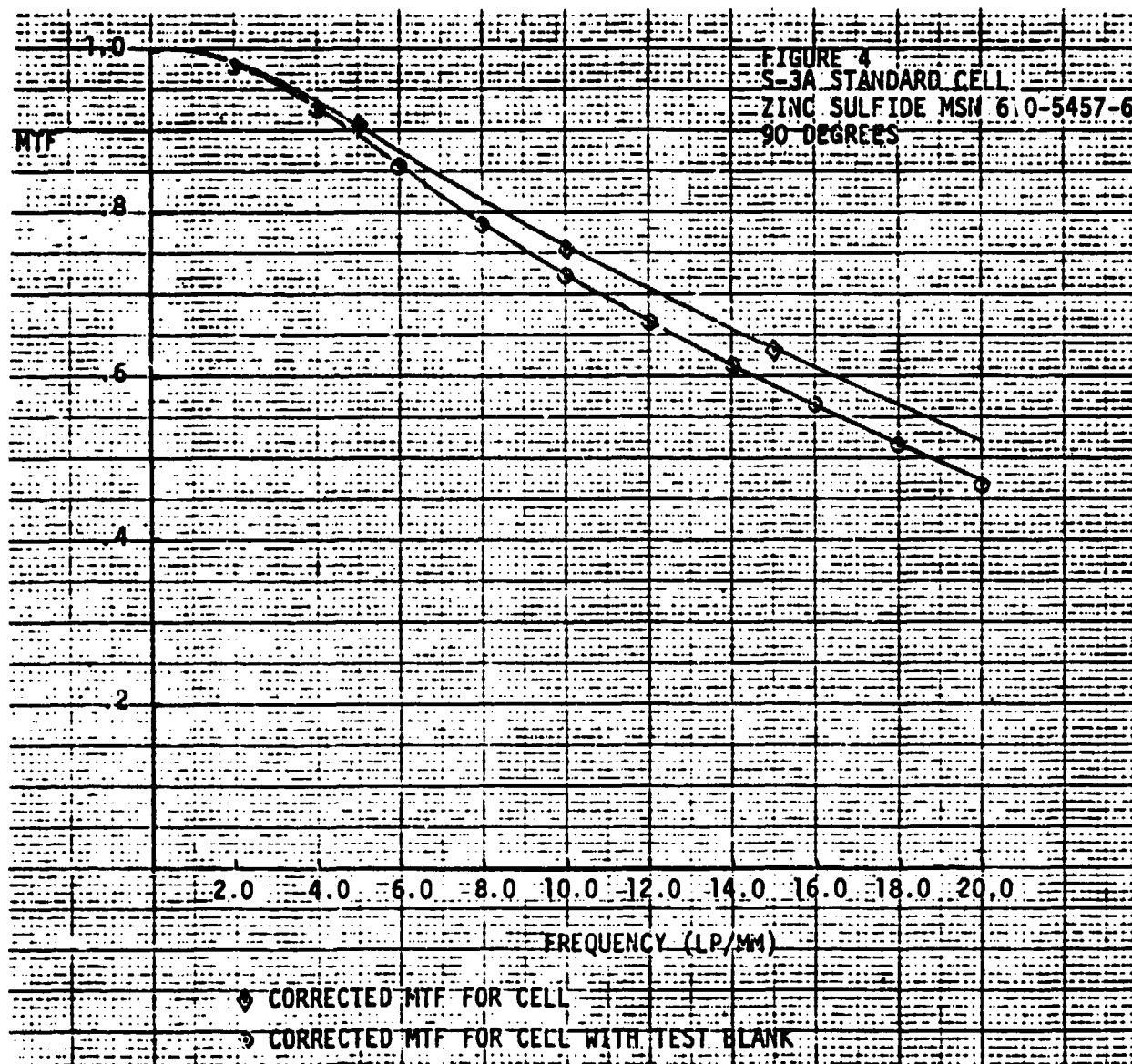
Serial number 610-5457-2 MTF results were 97.7% at 0° and 93.3% at 90° for a frequency of 10 lp/mm. The tabulated data for the standard cell and the respective blank are included as runs 9, 18, and 32. This data is plotted in Figures 1 and 2. The blank transmission in the spectral region previously specified was 63.3%.

Serial number 610-5457-6 MTF results were 97.9% at 0° and 95.5% at 90° for a frequency of 10 lp/mm. The tabulated data for the standard cell and the respective blank are included as runs 9, 49, and 62. This data is plotted in Figures 3 and 4. The blank transmission was 62.8%.









# OPTICAL TRANSFER FUNCTION

RUN NO. 9 FOCAL POSITION= 520.0 MICRONS

J.C. 11-20-74

S-3A STANDARD CELL WITH 4"x3.5" APERTURE

STANDARD CELL CHECK

ON AXIS SA SCAN

FREQ	TR	T1	MTFU	PHASE	MTFC
.0	1.000	.000	1.000	.0	1.000
5.0	.896	-.003	.896	-.2	.909
10.0	.714	-.000	.714	-.0	.756
15.0	.555	-.002	.555	-.2	.632

/★

OPTICAL TRANSFER FUNCTION  
 RUN NO. 18 FOCAL POSITION: 520.0 MICRONS  
 J.C. 11-20-74  
 S-3A STANDARD CELL WITH 4"X3.5" APERTURE  
 ZINC SULFIDE MSN-610-5457-2  
 0 DEGREES ON AXIS SA SCAN  

FREQ	TR	TI	MTFU	PHASE	MTFC
.0	1.000	.000	1.000	.0	1.000
2.0	.980	-.002	.980	-.1	.982
4.0	.926	-.008	.926	-.5	.934
6.0	.851	-.014	.851	-1.0	.869
8.0	.771	-.020	.771	-1.5	.799
10.0	.695	-.020	.695	-1.7	.735
12.0	.626	-.014	.626	-1.3	.680
14.0	.565	-.004	.565	-.4	.632
16.0	.507	.005	.507	.6	.587
18.0	.450	.012	.450	1.0	.543
20.0	.394	.015	.394	2.2	.498



OPTICAL TRANSFER FUNCTION  
 RUN NO. 32 FOCAL POSITION= 524.0 MICRONS  
 J.C. 11-20-74

S-3A STANDARD CELL WITH 4"X3.5" APERTURE  
 ZINC SULFIDE MSN-610-5457-2

90 DEGREES		ON AXIS		SA SCAN	
FREQ	TR	TI	MTFU	PHASE	MTFC
.0	1.000	.000	1.000	.0	1.000
2.0	.981	-.001	.981	-.1	.983
4.0	.931	-.004	.931	-.2	.939
6.0	.860	-.007	.860	-.4	.879
8.0	.783	-.011	.783	-.6	.812
10.0	.709	-.014	.709	-1.1	.751
12.0	.643	-.014	.643	-1.3	.698
14.0	.580	-.009	.580	-.9	.648
16.0	.515	-.000	.515	-.1	.597
18.0	.448	.008	.448	1.1	.541
20.0	.383	.015	.383	2.2	.484

OPTICAL TRANSFER FUNCTION  
 RUN NO. 49 FOCAL POSITION= 540.0 MICRONS  
 J.C. 11-20-74  
 S-3A STANDARD CELL WITH 4"X3.5" APERTURE  
 ZINC SULFIDE MSN-610-5457-6  
 0 DEGREES ON AXIS SA SCAN

FREQ	TR	TI	MTFU	PHASE	MTFC
.0	1.000	.000	1.000	.0	1.000
2.0	.979	-.006	.979	-.3	.981
4.0	.922	-.012	.922	-.7	.931
6.0	.847	-.014	.847	-.9	.865
8.0	.770	-.012	.770	-.9	.798
10.0	.699	-.006	.699	-.5	.740
12.0	.635	.001	.635	.1	.689
14.0	.573	.009	.573	.9	.641
16.0	.510	.014	.510	1.6	.591
18.0	.448	.017	.449	2.2	.541
20.0	.393	.019	.393	2.8	.497

OPTICAL TRANSFER FUNCTION

RUN NO. 62      FOCAL POSITION 540.0 MICRONS  
 J.C.      11-20-74  
 S-3A STANDARD CELL WITH 4"X3.5" APERTURE  
 ZINC SULFIDE MSN-(10-545)-6

FREQ	90 DEGREES	ON AXIS	SA SCAN
TR	TI	MTFU	PHASE
			MTFC
0	1.000	.000	1.000
2.0	.978	.001	.978
4.0	.921	.001	.921
6.0	.842	.000	.842
8.0	.759	.003	.759
10.0	.682	.006	.682
12.0	.614	.008	.614
14.0	.550	.010	.551
16.0	.489	.013	.490
18.0	.429	.015	.429
20.0	.371	.015	.371

APPENDIX B

OPTICAL TEST DATA FOR COATED ZINC SULFIDE WINDOWS



**TEXAS INSTRUMENTS**  
**INCORPORATED**

POST OFFICE BOX 6018 • DALLAS, TEXAS 75222

*Equipment Group*

25 March 1975

In reply, refer to:  
230-83-1681  
Mail Station 209

The Perkin-Elmer Corporation  
Electro-Optical Division  
Norwalk, CT 06856

ATTENTION	Mr. W. Schilling Purchasing, M/S 299
SUBJECT	Optical Test Data for Coated Zinc Sulfide Windows
REFERENCE	(a) Perkin-Elmer Purchase Order 86028 OS
ENCLOSURE	(1) Technical Description of Optical Test Results of Coated Zinc Sulfide Windows (1 copy)

Gentlemen:

Texas Instruments takes this opportunity to submit enclosure (1) in response to item 2.0 of the reference (a) purchase order. Enclosure (1), with its 4 figures and 5 data runs, represents a synopsis of the test data obtained. This submittal completes the contract effort.

If we may be of further assistance or answer your questions on this information, please contact Mr. Bob Crossland at area code 214, 239-4233.

Very truly yours,

*Gordon E. Leach*  
Gordon E. Leach  
Contract Negotiator

GEL:slc

13800 NORTH CENTRAL EXPRESSWAY • DALLAS • 214-239-2011 • TELEX 7-3324 • TWX 910-867-4702 • CABLE: TEXINS

TECHNICAL DESCRIPTION OF OPTICAL  
TEST RESULTS OF COATED ZINC SULFIDE WINDOWS

The following is a synopsis of Texas Instruments Image Evaluation Laboratory testing of two Zinc Sulfide optical blanks (Perkin-Elmer Serial numbers 610-5457-2 and 610-5457-6). The following aspects are pertinent to the test setup:

1. The test was conducted with the S-3A standard cell which was designed for 2.0 cycles/milliradian.
2. An aperture of 2.8 inches square was placed over the cell and defined the area tested in each blank.
3. Knife orientation was vertical for all scans.
4. 0° orientation of the blank was defined when the long dimension of the blank was vertical.
5. 90° orientation of the blank was defined when the long dimension of the blank was horizontal.
6. Initial tests were conducted using the same bandpass filter as the previous tests on the uncoated blanks. However, the results indicated that the coating on the ZnS had a narrower spectral definition. Therefore, for this setup, one blank was placed at the blackbody source in addition to the bandpass filter while the other blank was being tested.
7. A focal series was conducted after introducing the blank in front of the standard cell to remove any effects of power or tilt in the surfaces.

Serial number 610-5457-2 MTF results were 97.3% at 0° and 99.2% at 90° for a frequency of 10 lp/mm. The tabulated data for the standard cell and the respective blank are included as runs 5, 44 and 39. This data is plotted in Figures 7 and 8. The blank transmission in the same spectral region as the previous uncoated test was 59.8%.

Serial number 610-5457-6 MTF results were 97.3% at 0° and 97.5% at 90° for a frequency of 10 lp/mm. The tabulated data for the standard cell and the respective blank are included as runs 5, 16 and 29. This data is plotted in Figures 5 and 6. The blank transmission was 57.3%.

OPTICAL TRANSFER FUNCTION

WAVE NO. 3 FOCAL POSITION 560.0 MICRONS  
I.C. 93-13-75

3-3A STANDARD CELL

WITH 2.4" SQUARE APERTURE

IN AXIS SA SCAN

FREQ	TR	TI	MTFU	PHASE	MTFC
0.0	1.000	.334	1.000	.0	1.000
2.0	.977	.005	.977	.3	.979
4.0	.915	.005	.915	.3	.924
6.0	.836	-.004	.836	-.2	.853
8.0	.753	-.015	.753	-1.2	.780
10.0	.676	-.024	.676	-1.7	.715
12.0	.603	-.014	.604	-1.4	.655
14.0	.532	-.004	.532	-.4	.595
16.0	.461	.001	.461	.2	.534
18.0	.393	-.000	.393	-.1	.474
20.0	.334	-.000	.334	-1.6	.422

Copy available to EDC does not  
permit fully legible reproduction

OPTICAL TRANSFER FUNCTION  
 RUN NO. 18 FOCAL POSITION: 560.0 MICRONS  
 J.C. 03-13-75

ZINC SULFIDE DSN-610-5457-A COATED					
S-3A STANDARD CELL-2.0" SQ. APERTURE					
W DEGREES ON AXIS SA SCAN					
FREQ	TR	TI	MTFU	PHASE	MTFC
0.0	1.000	.000	1.000	.0	1.000
2.0	.971	-.003	.971	-.2	.973
4.0	.897	-.007	.897	-.4	.905
6.0	.807	-.010	.807	-.6	.823
8.0	.725	-.015	.725	-.8	.752
10.0	.657	-.013	.657	-.1	.696
12.0	.593	-.001	.593	.1	.644
14.0	.521	-.009	.521	-1.0	.582
16.0	.439	-.012	.439	-1.6	.509
18.0	.361	-.006	.361	-1.0	.436
20.0	.301	.000	.301	.0	.380



OPTICAL TRANSFER FUNCTION  
 RUN NO. = 20 FOCAL POSITION = 520.0 MICRONS  
 J.C. 03-13-75

ZINC SULFIDE MSN-610-5457-5 COATED  
 S-3A STANDARD CELL-2.8" SQ. APERTURE  
 90 DEGREES ON AXIS SA SCAN

FWFN	TR	TI	MTFU	PHASE	MTFC
.0	1.000	.000	1.000	.0	1.000
2.0	.971	.004	.971	.2	.973
4.0	.899	.009	.899	.4	.907
6.0	.809	-.019	.809	-.6	.826
8.0	.727	-.017	.727	-1.4	.754
10.0	.659	-.017	.659	-1.5	.697
12.0	.595	-.009	.595	-.8	.646
14.0	.524	-.011	.524	-.1	.590
16.0	.456	-.000	.456	-.0	.528
18.0	.386	-.003	.386	-.5	.465
20.0	.325	-.000	.325	-.0	.410

/\*

OPTICAL TRANSFER FUNCTION  
 RUN NO. = 44 FOCAL POSITION = 520.0 MICRONS  
 J.C. 03-13-75

ZINC SULFIDE MSN-610-5457-2 COATED

S-3A STANDARD CELL-2.8" SQ. APERTURE

0 DEGREES ON AXIS SA SCAN

FREQ	TR	TI	MTFU	PHASE	MTFC
.0	1.000	.000	1.000	.0	1.000
2.0	.973	.006	.973	.3	.975
4.0	.904	.007	.904	.4	.912
6.0	.816	.001	.816	.1	.833
8.0	.732	-.002	.732	-.2	.758
10.0	.658	-.000	.658	-.0	.696
12.0	.590	.006	.590	.5	.640
14.0	.520	.007	.520	.8	.581
16.0	.447	-.001	.447	-.2	.517
18.0	.377	-.018	.377	-2.7	.455
20.0	.318	-.028	.319	-5.2	.403

/\*

OPTICAL TRANSFER FUNCTION  
 RUN NO. = 39 FOCAL POSITION = 500.0 MICRONS  
 J.C. 03-13-75

ZINC SULFIDE MSN-610-5457-2 COATED  
 S-3A STANDARD CELL-2.8" SQ. APERTURE  
 90 DEGREES ON AXIS SA SCAN

FREQ	TW	TI	MTFU	PHASE	MTFC
.0	1.000	.000	1.000	.0	1.000
2.0	.973	.006	.973	.3	.975
4.0	.904	.006	.904	.3	.912
6.0	.818	-.000	.818	-.0	.834
8.0	.737	-.008	.737	-.6	.764
10.0	.670	-.000	.670	-.8	.709
12.0	.613	-.004	.613	-.4	.665
14.0	.553	.001	.553	.1	.619
16.0	.486	.002	.486	.2	.563
18.0	.415	-.002	.415	-.3	.500
20.0	.348	-.007	.348	-1.2	.440

FIGURE 5  
S-3A STANDARD CELL  
ZINC SULFIDE MSN 610-5457-6 (COATED)  
0 DEGREES

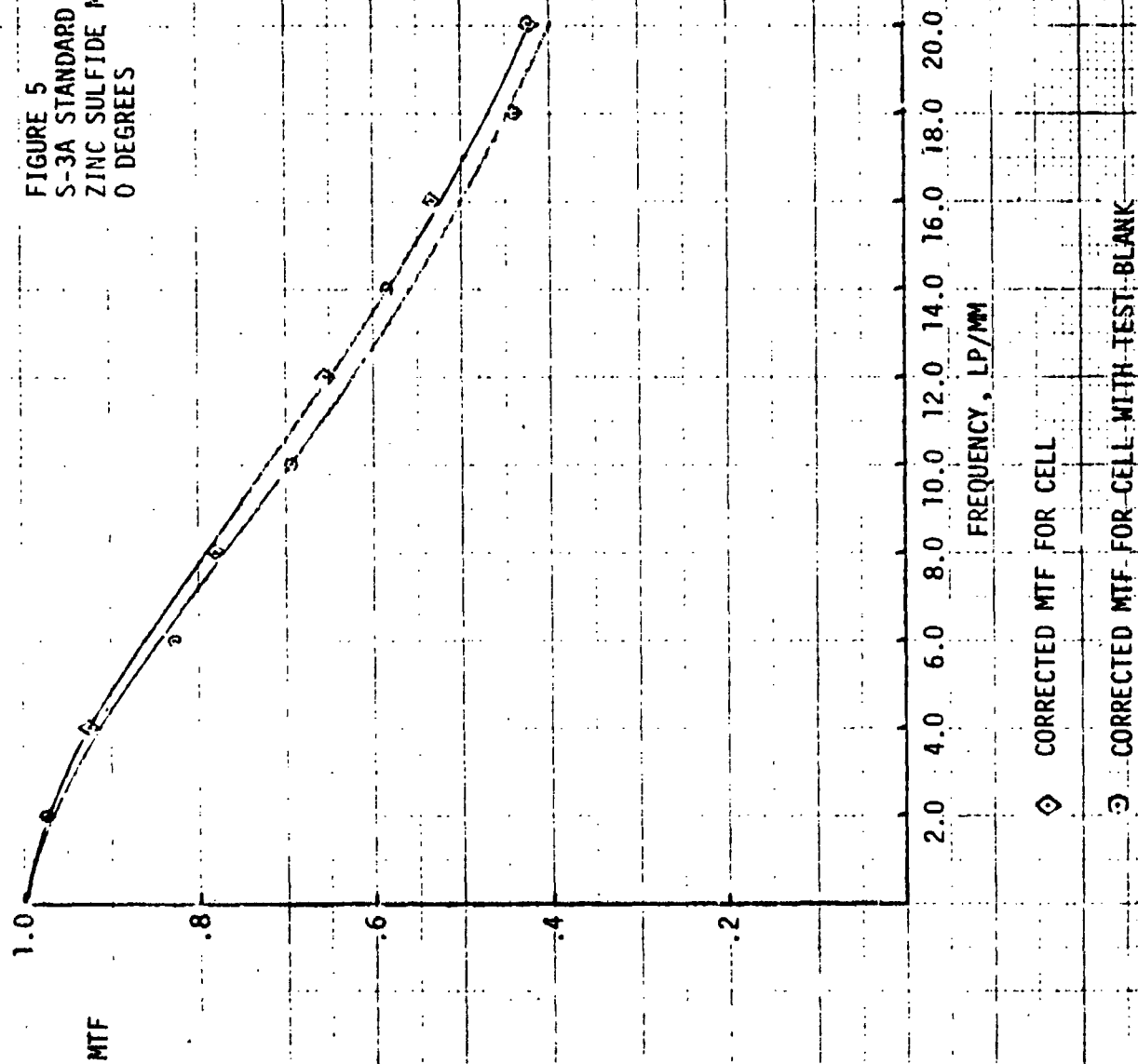


FIGURE 6  
S-3A STANDARD CELL  
ZINC SULFIDE MSN 610-5457-6 (COATED)  
90 DEGREES

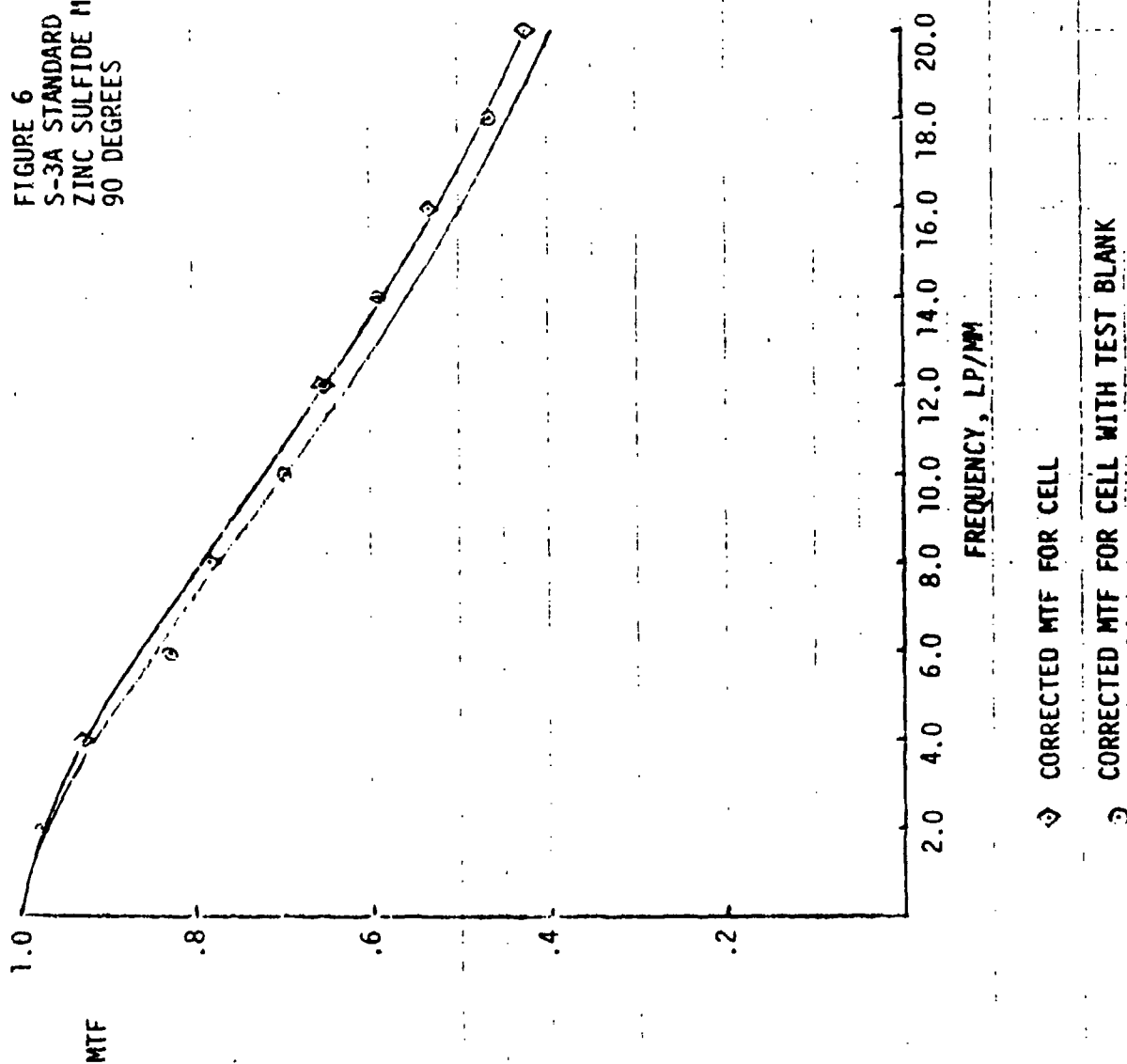


FIGURE 7  
S-3A STANDARD CELL  
ZINC SULFIDE MSN 610-5457-2 (COATED)  
0 DEGREES

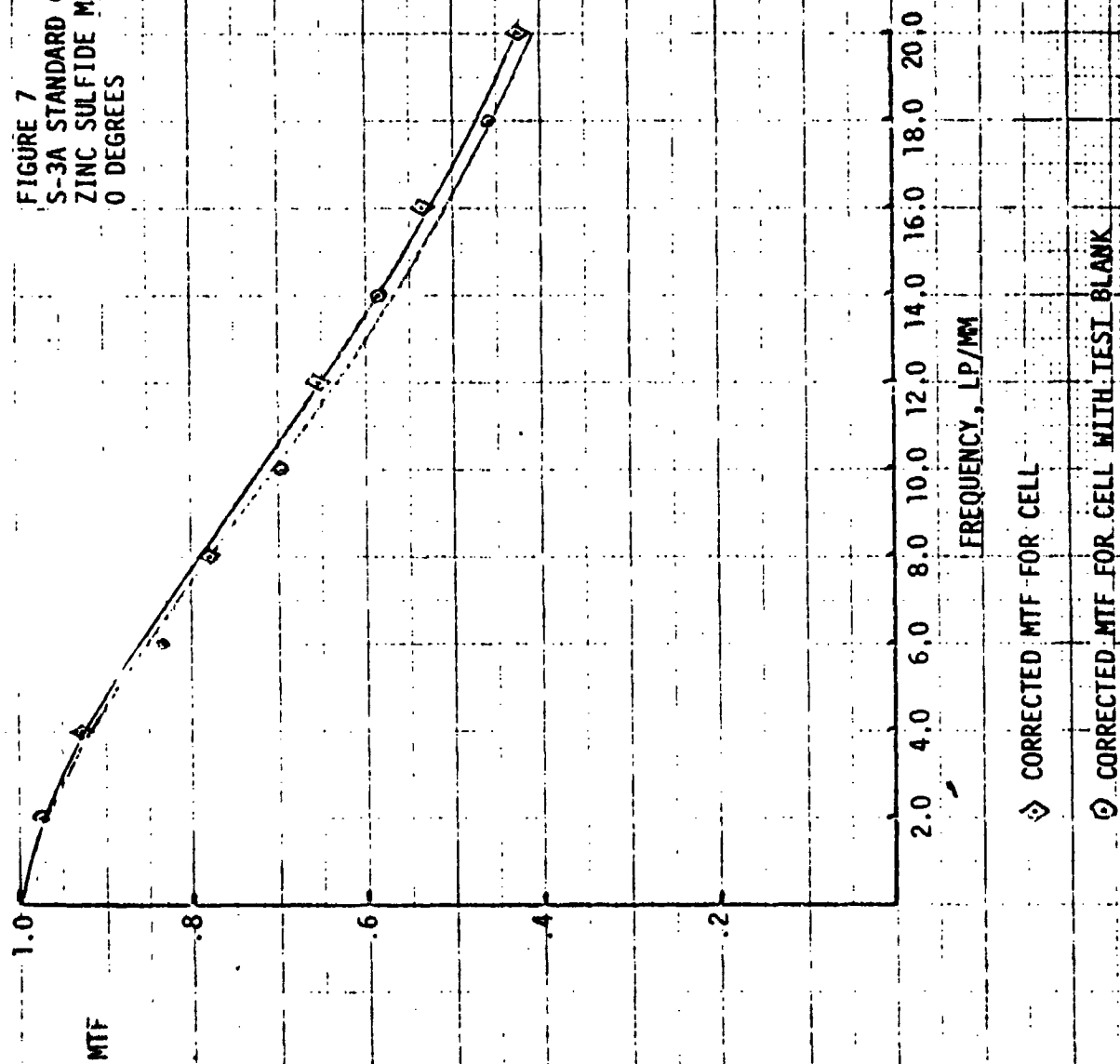


FIGURE 8  
S-3A STANDARD CELL  
ZINC SULFIDE MSN 610-5457-2 (COATED)  
90 DEGREES

